Aus dem Institut für Schlaganfall- und Demenzforschung
Institut der Ludwig-Maximilians-Universität München

Vorstand: Prof. Dr. Martin Dichgans

The role of MIF proteins in ischemic stroke

Dissertation
zum Erwerb des Doktorgrades der Medizin
an der Medizinischen Fakultät der
Ludwig-Maximilians-Universität zu München

vorgelegt von
Sijia Wang

aus
Nei Mongol, P.R.China

Jahr
2021

Mit Genehmigung der Medizinischen Fakultät
der Universität München

Berichterstatter:	Prof. Dr. Jürgen Bernhagen
Mitberichterstatter:	Prof. Dr. Frank A. Wollenweber Prof. Dr. Thomas Pfefferkorn
Mitbetreuung durch den promovierten Mitarbeiter:	Dr. Omar El Bounkari
Dekan:	Prof. Dr. med. dent. Reinhard Hickel
Tag der mündlichen Prüfung:	29.04.2021

Contents

1. INTRODUCTION

1.1 Ischemic stroke

1.1.1 Clinical features

1.1.1.1 Definition and classification

Stroke, also called brain attack, is the rapid development of a focal neurologic deficit. It arises when the blood flow to the brain through critical components of the vasculature is disrupted.

There are two main types of stroke depending on its etiology: ischemic stroke and hemorrhagic stroke. Most strokes result from cerebral ischemia and this contributes for about 85% of all the cases. Ischemic stroke occurs as a result of the occlusion of an artery and leads to oxygen and nutrient deficiency in the brain (Fig. 1). Hemorrhagic stroke, on the other hand, is due to the leaking or rupturing of an artery and constitutes about 15% of all the stroke cases. Dependent on the location of bleeding, hemorrhagic stroke is distinguished into two subtypes: intracerebral hemorrhage and subarachnoid hemorrhage [1].

Ischemic stroke is further divided into five categories based on “The Trial of Org 10172 in Acute Stroke Treatment (TOAST)” [2,3]: (1) Large-artery atherosclerosis, accounts for approximately 30%. This type includes patients who have significant (>50%) occlusion of a large artery, which is usually caused by atherosclerosis of a branch cortical artery or major intracranial vessels. (2) Cardioembolism accounts for 20% to 30%, and this type describes patients with arterial occlusions due to an embolus that originates in the heart. (3) Small-vessel occlusion, also referred to as lacunar stroke, accounts for 25% and includes patients, whose infarct size is less than 20 mm. (4) Stroke of other determined etiology, accounts for about 10% and refers to patients caused by rare reasons, such as non-atherosclerotic vasculopathies, hematologic disorders or hyper-coagulable states. (5) Stroke of undetermined etiology, also called as cryptogenic stroke and accounts for about 6% to 15%. Due to advances in imaging techniques and an improved understanding of stroke pathophysiology, the number of this subtype is now thought to increase in the past several decades [4].

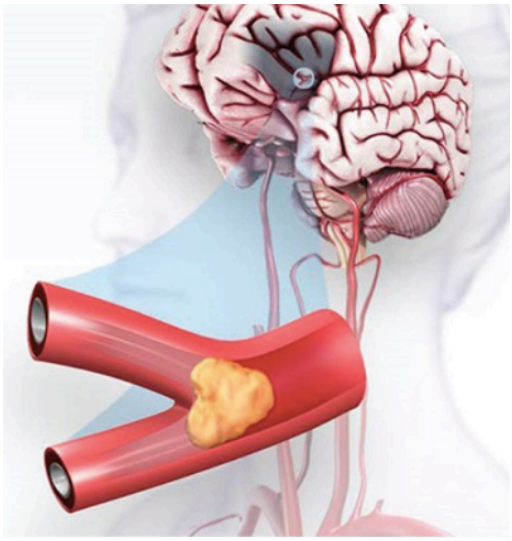

Fig. 1: Ischemic stroke. Ischemic stroke is due to blockage of blood vessels which supply blood to the brain. This figure was taken from https://www.stroke.org/en/about-stroke/types-of-stroke/ischemic-stroke-clots.

1.1.1.2 Epidemiology

As a leading cause of human cerebral damage, annually more than 15 million people suffer from stroke worldwide , almost one third of these people die, and another one third is disabled [5,6]. The incidence of stroke is expected to dramatically increase due to the global increase in an aging population, and is predicted to reach 23 million cases by 2030 [7,8]. In addition to human suffering, stroke also results in a heavy health burden on both patients and the society [9]. It should be pointed out that the incidence of stroke in the young population has increased over the past few decades and this trend also brings enormous burden especially in developing countries [10].

1.1.1.3 Therapy

Although ischemic stroke involves high morbidity and disability, up to now the therapeutic options are still limited and mainly based on thrombolysis or neuroprotection. The only pharmacotherapy approved by the United States Food and Drug Administration (FDA) for ischemic stroke is still recombinant tissue plasminogen activator (rt-PA), which is a thrombolytic therapy that dissolves the fibrin clot and restores blood flow. However, this treatment is only effective for a minority (less than 10%) of people, because of its narrow therapeutic window, which is less than 4.5 hours after symptom onset [11]. There are some other limitations for this treatment. For example, patients must be younger than 80 years old

and haven't had any recent intracranial surgery, cerebrovascular accident or bleeding. The possible adverse effects should also be considered such as the enhanced risk of hemorrhage and cellular damage [12]. Besides the fibrinolytic therapy, multiple trials also showed significant benefits of endovascular thrombectomy in the first six hours of patients who have large vessel occlusion of the anterior circulation, and some trials even extended this window up to 16-24 hours [13,14].

For the majority of ischemic stroke patients, besides the treatment focused on preventing further strokes, the development of safer and more efficacious alternative therapies with broader therapeutic windows therefore is of great importance. For this and other reasons, a lot of neuroprotective therapies to reduce brain injury have been widely evaluated over the years in preclinical research. Unfortunately, although showing convincing success in animal models, almost all the pharmacological neuroprotectants did not show the expected favorable effects in clinical studies and have not been successfully translated for use in ischemic stroke patients in the clinic [15].

However, there are still some potential neuroprotective strategies that may present a promising option. Stem cell-based therapies have made significant progress in the last several years. This includes approach with adipose tissue-derived stem cells and human amnion epithelial cells. One of the involved mechanisms could be the beneficial effects of the paracrine, or extracellular vesicle-mediated restorative effects [16-18]. Several other therapies focused on NADPH oxidase (NOX) inhibitors [19], antibiotics [20], immunomodulators [21] have shown promise in the ischemic stroke treatment. Furthermore, the approaches and new techniques that have been developed to deliver efficient drugs to the specific regions and specific cells of the injured brain could also improve stroke therapy [22,23].

1.1.2 Pathophysiology

Ischemic stroke is characterized by an artery occlusion and reduction in cerebral blood flow (CBF) to a specific brain territory. Brain as an exquisitely sensitive organ to ischemia, receives approximately 20% of cardiac output. Following ischemic stroke, inadequate delivery of oxygen and glucose causes cellular disfunction and death by triggering a complex cascade of pathophysiological processes, which are interlinked and may last hours or even days. In the following, I address several key events in more detail.

1.1.2.1 Infarct core and ischemic penumbra

Because of differential losing of blood supply to different zones, the affected tissue supplied by the occluded artery is divided into the infarct core and the ischemic penumbra, or pre-infarct zone [24]. The infarct core is the central area with blood flow below 20% of baseline, which undergoes immediate and irreversible damage within minutes. The ischemic penumbra is the reversibly injured brain tissue surrounding this core, in which the CBF level is less than the functional threshold but still above the threshold of cell death owing to residual perfusion from collateral vessels. The penumbra as an "at risk" region is functionally impaired. The cells in the penumbra are still salvageable if perfused in time and if cell death occurs less rapidly (within a few hours) [25,26]. Thus, the penumbra always serves as a pharmacological target for therapeutic intervention. The infarct core is not a static parameter but can change in its size over time; the same notion applies to the penumbra. Moreover, it has been demonstrated that the infarct core can expand into the ischemic penumbra over time if without reperfusion [27].

1.1.2.2 Excitotoxicity and ionic imbalance

Oxidative phosphorylation is the predominant way for energy generation in the brain. The depletion of the essential substrates oxygen and glucose caused by vascular occlusion during ischemic stroke creates an energy failure in the affected cells, which then leads to a decrease of total adenosine-5'-triphosphate (ATP) and lactate acidosis [28]. This then quickly affects energy-dependent ion pumps, which further leads to loss of ionic homeostasis in neurons and glial cells. For example, this will influence the Na^+/K^+-ATPase pump and cause an increase in the intracellular sodium level and extracellular potassium level. In addition, this will also cause intracellular accumulation of calcium and chloride [29,30].

This depolarization of the plasma membrane in cells leads to a rapid release of excitatory amino acids to the extracellular matrix and inhibits reuptake [31]. In central nervous system (CNS), glutamate as the most abundant excitatory neurotransmitter acts on around 30% to 40% of synapses. Following ischemic stroke, the presence of excessive amounts of glutamate in the extracellular space causes excitotoxicity as a pathological condition through prolonged stimulation of pre- and post-synaptic glutamate receptors to promote excessive influx of calcium [32]. The high intracellular calcium level is toxic for cells, which initiates catabolic processes by trigging downstream enzymes such as phospholipases, lipases, proteases and nucleases, and leads to further cell destruction [33,34]. Apart from activation of glutamate

receptors, the dysfunction in other channels and ion pumps also participate in calcium accumulation [35,36]. In addition to calcium, sodium and chloride also enter cells *via* the overstimulation of glutamate receptors, which aggravates cell depolarization and causes more glutamate release and calcium influx. The overall result is a massive ionic imbalance, passively followed by an influx of water, which further causes cell swelling, edema (cytotoxic edema) and shrinking of extracellular space [34].

1.1.2.3 Oxidative and nitrosative stress

Oxidative stress and nitrosative stress play essential roles in brain injury after ischemia, particularly after exposure to reperfusion with oxygen supply [37]. These stresses are partly downstream consequences of excitotoxicity, which are caused by an abundant production of reactive oxygen species (ROS) or reactive nitrogen species (RNS), and insufficient activity of endogenous free radical scavenging of cellular antioxidants [38]. Ischemia leads to activation of several ROS-generating enzymatic systems and ROS are massively generated [39-41]. On the other hand, activities of major endogenous antioxidants are low in neurons, including superoxide dismutase, catalase, glutathione and antioxidant vitamins [42,43]. Thus antioxidants are not enough to detoxicate and scavenge the rapid overproduction of free radicals during ischemia [42,43]. ROS are important and could play a beneficial role in normal CNS. However, excessive ROS are powerful mediators of tissue damage, since these free radicals directly attack key cellular components like proteins, nucleic acids and carbohydrates [44,45]. Notably, ROS disrupt the inner mitochondrial membrane and activate the permeability transition pore, which subsequently results in swelling and impeding of ATP generation [46,47]. Oxidative stress is closely related to other pathophysiological processes, such as excitotoxicity, energy loss, necrosis, apoptosis, autophagy, inflammation and blood-brain barrier (BBB) disruption, and all of these events contribute to ischemic cell death [48].

1.1.2.3 Inflammation

The inflammatory response is induced within a few hours after onset of ischemic stroke and is involved in almost all processes of the ischemic stroke sequelae (Fig. 2). It implicates rapid activation of resident glial and endothelial cells, and the infiltration of a wide range of peripheral circulation immune cells and platelets into the ischemic region through the activated endothelium and/or disrupted BBB, which are attracted and activated by cytokines, chemokines and adhesion molecules. Neuroinflammation exacerbates brain damage as well as

composes reperfusion injury. However, it's well accepted that inflammation also conversely plays a beneficial role in ischemic stroke. Therefore, immune responses are also central targets in treatment and rehabilitation under current investigation.

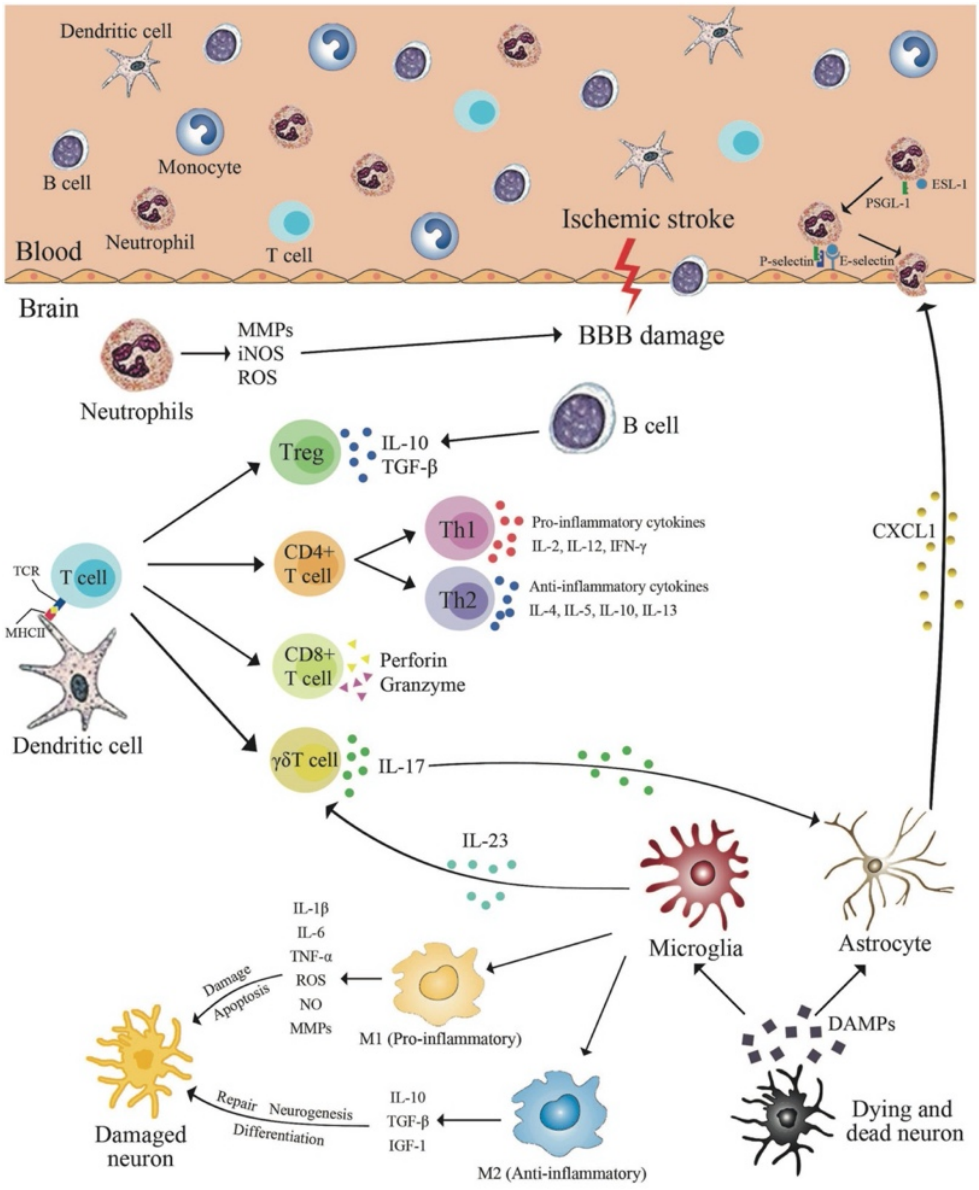

Fig. 2: The inflammatory response and involved immune cells in the ischemic brain. Scheme summarizing of post-stroke neuroinflammation. Following ischemic stroke, resident glial cells (microglia and astrocytes) are rapidly activated, and a wide range of peripheral circulation immune cells are infiltrated into ischemic region in the brain through disrupted BBB, which are attracted and activated by cytokines, chemokines and adhesion molecules. The scheme was taken from reference [50].

1.1.2.3.1 Activation of resident glia cells

Microglia and astrocytes are activated within hours and deeply involved in acute phase of the ischemic process [49]. Microglia as resident immune cells in the brain, are activated within minutes after ischemic onset and work as key immune cells in acute and sub-acute stages [50,51]. After activation, microglia lead to phagocytosis and contribute to post-ischemic inflammation by producing a large amount of pro-inflammatory cytokines [50,51]. Apart from being a pro-inflammatory cell type, microglia produce ROS and proteases such as matrix metalloproteinases (MMP), resulting in aggravated brain damage [52]. However, microglia also generate anti-inflammatory cytokines like interleukin-10 (IL-10), as well as several growth factors which participate in the resolution of inflammation and facilitation of neurogenesis, representing a neuroprotective property [53]. In addition, blood-derived monocytes/macrophages with similar functions as activated microglia, start to get recruit into the ischemic region 3-4 hours after stroke and mainly accumulate in the sub-acute phase [54].

Astrocytes are mainly considered as housekeeping cells, which are chiefly involved in neurotrophic support and homeostasis maintenance of the CNS. However, similar to microglia, activated astrocytes also take part in post-ischemic inflammation by secreting inflammatory mediators like interferon gamma (IFN-γ), interleukin-6 (IL-6), interleukin-1 beta (IL-1β), tumor necrosis factor-alpha (TNF-α) and MMPs [55,56]. Remarkably, astrocytes are also associated with BBB disruption, scar formation, extracellular glutamate release and inhibition of axon function, which are all harmful following ischemia [56,57]. On the other hand, reactive astrocytes are required for angiogenesis and neurogenesis, contributing to BBB rebuilding and neurovascular remodeling [58].

1.1.2.3.2 Leukocyte infiltration

In addition to resident cells in the brain, infiltrated leukocytes also play important roles in neuroinflammation. Following ischemia, leukocytes rapidly infiltrate into the brain parenchyma, where they produce pro-inflammatory factors and contribute to both initiating and aggravating of the ischemic response [59,60]. Notably, infiltration and migration of leukocytes is amplified by increased BBB permeability [61].

Neutrophils are the earliest peripheral leukocytes migrating into the brain in the acute ischemic stage followed by monocytes [62], another prominent infiltrating immune cell type in post-

ischemic inflammatory responses [63]. After migrating through the endothelial cell layer, neutrophils aggravate pathological processes by production of ROS, MMPs and exacerbating inflammation through releasing proinflammatory factors and recruitment of other immune cells [64]. These toxic factors contribute to BBB disruption, tissue damage and post-ischemic edema. Besides the detrimental effects, some evidence also suggests that the infiltrated neutrophils contribute to beneficial regulation processes, like tissue repair and remodeling [65], and clearance of necrotic cell debris [66].

Unlike neutrophils, T lymphocytes migrate into brain parenchyma mainly in the later stages of ischemic injury [67], and show an overall detrimental effect [68]. Dependent on the different glycoprotein expressed on their cell surface, there are two subtypes of T cells, which are CD4+ and CD8+ T cells, and both of them have distinct functions and fates. CD4+ T cells are helper cells (Th) and can be further divided into different subtypes mainly including Th1, Th2 and regulatory T cells (Treg). Although the subtype-specific actions are only partly understood, it was demonstrated that almost all the different T-cell types are recruited into the ischemic brain parenchyma [69-71]. Th1 cells could aggravate brain injury by releasing pro-inflammatory cytokines like TNF-α and IFN-γ [72,73]. Th2 cells promote humoral immunity and may protect the ischemic brain by secreting anti-inflammatory cytokines including IL-10 and so on [72,74]. A number of studies have shown that Tregs play protective roles by downregulating post-ischemic inflammation via transforming growth factor beta (TGF-β) and IL-10 [72,75,76]. On the contrary, CD8+ T cells which have cytotoxic effect can recognize endogenous antigens that present MHC class I molecules, resulting in neuronal cell death by secretion of perforin and granzyme upon antigen-dependent activation [77].

The influence of B cells on ischemic brain pathogenesis remains unclear and controversial [78-80], but emerging evidence suggests B cells have a probable protective function which could limit infarct volume and neurological deficits and promote post-stroke recovery [81,82]. Dendritic cells (DCs) are also found to present in ischemic brain in animal models, although their role in ischemic pathophysiology is poorly understood [83]. Similarly, natural killer (NK) cells are also recruited into ischemic lesions and may have a detrimental effect [84]. In addition, NK cells have been shown to influence cellular immune responses and have contact with microglia and astrocytes [85,86].

1.1.2.3.3 Cytokines and chemokines

Cytokines are critical inflammatory mediators and a large family of more than 100 pleiotropic polypeptides that are barely detectable in normal brain [87,88]. The expression of cytokines is upregulated in brain shortly after an ischemic insult, as well as in blood and cerebrospinal fluid (CSF) [89]. Immunocytes and brain resident cells such as glial cells and neurons secrete cytokines and contribute to their overall significant upregulation [89,90]. During ischemic stroke, cytokines work as key regulators to increase cell adhesion molecules expression, which further regulate leukocyte recruitment and BBB disruption, and the infiltrated leukocytes in turn release more cytokines [91]. IL-1β, TNF-α and IL-6 have been demonstrated in various reports to be the first three most important pro-inflammatory cytokines that aggravate post-stroke inflammatory responses and contribute to neuronal damage [92,93]. On the contrary, TGF-β and IL-10 have been found as the most extensively studied anti-inflammatory cytokines that are neuroprotective by inhibiting inflammation during ischemia [94,95]. In addition, other cytokines are also involved in brain damage or protection during ischemia, such as interleukin-17 and interleukin-2 [96-98]. The measurable expression levels and effects of most cytokines are largely dependent on the different stages of stroke, the applied animal model and its severity, and some of the cytokines even have both neurotoxic and neuroprotective effects in the brain [60,94].

Besides cytokines, chemokines, which are small signaling proteins with chemotactic activity for leukocytes, are also key mediators of inflammation in ischemic stroke [99,100]. There are almost 50 classical chemokines classified into four subfamilies based on their structures: C-, CC-, CXC- and CX_3C-type chemokines. Classical chemokines have both unique and overlapping receptors, and individual chemokine receptors bind multiple ligands [101,102]. A number of chemokines have been shown to be involved in ischemic stroke, with prominent examples: CCL2 and its receptor CCR2 [103-105], CXCL12 and its receptor CXCR4 [106], and CX_3CL1 and its receptor CX_3CR1 [107,108]. The role of classical chemokines and their receptors to worsen stroke pathogenesis are primarily linked to their proinflammatory ability to recruit immune cells and activate resident microglia [109]. Besides chemotaxis, chemokines were demonstrated to be directly involved in BBB disruption [110]. However, some chemokines were also shown to have beneficial effects, are involved in clearance of debris and post-stroke recovery [111].

1.1.2.4 Blood–brain barrier (BBB)

Endothelial cells with tight junctions and a vascular basement membrane, pericytes and an astrocyte-based end-foot are the primarily components of BBB [112]. As the interface between the peripheral circulation and the CNS, the BBB has a specific transport system to supply nutrients and the BBB integrity is needed to maintain the specific neuronal microenvironment [113,114]. To better understand BBB functions, a concept of a well-organized structure called neurovascular unit is suggested, which is composed of cerebral microvessels, glial cells (astrocytes, microglia, oligodendroglia), and neurons [115]. BBB permeability is rapidly increased after the onset of ischemia [116], resulting from several mechanisms, such as cell death, detachment or migration of pericytes and astrocytes [117,118], endothelial swelling and microglial activation [119]. In addition, it needs to be noted that MMPs were demonstrated to be a key player in regulating BBB permeability during ischemic stroke [120]. Blood components infiltrate the brain through the disrupted BBB, which causes vasogenic edema and thereby may lead to secondary damage through intracranial hypertension and hemorrhagic transformation [121]. As described above, the increased permeability facilitates infiltration of circulating inflammatory cells and exacerbates post-ischemic inflammatory responses [122], causing an increased production of adhesion molecules and proinflammatory cytokines, in turn aggravating BBB leakage [123].

However, the disruption of BBB also would be essential for drug delivery into the ischemic brain. Moreover, the refluxed information from brain parenchyma into the circulation are useful in biomarker assays to reflect pathophysiological processes after ischemic stroke [124].

1.1.3 Animal models

In order to explore the mechanisms of cerebral ischemia and develop new treatment, various animal stroke models have been established over the last several decades. Here, I describe the most commonly used models in rodents, with a focus on the middle cerebral artery occlusion (MCAO) model.

In vivo animal ischemic stroke models mainly include two classes: global and focal ischemia [125,126]. Although global models are not as common as focal models, they are useful to mimic clinical cardiac arrest and asphyxia [127]. The most widely used global model in rodents

is induced by ligating bilateral common carotid arteries with systemic hypotension, and some of them also combine with permanent ligation of bilateral vertebral arteries [127,128].

As the most often affected artery in human ischemic stroke is the middle cerebral artery (MCA), in focal ischemia models, the MCAO model was developed to mimic this clinical situation, with either transient or permanent occlusion [129,130]. Although the operative process is more complex than global models, the MCAO model is widely used, as this model can better mimic post-ischemia pathophysiology processes in human stroke. Dependent on different sub-methods, the transient MCAO model can be further divided into the intraluminal suture/filament MCAO model, the craniotomy model/direct distal MCAO model (branches of the MCA are occluded by surgical clip, ligation or cauterization) [131], the photothrombosis distal MCA model, the endothelin-1-induced model and the embolic stroke model [132,133]. The first two models can be also performed as permanent vessel blockade. Among these models, the intraluminal suture/filament MCAO model is one of the most common model in rodents accounting for approximately 40% [130]. The character of this model is that there is no need of craniectomy, and reperfusion can be performed by withdrawal of the filament.

However, there are still some differences between animal models and human stroke, such as brain and vascular anatomy, functional organization and the nature of the immune system [134]. Nevertheless, animal MCAO models provide a useful tool for stroke research although there are no animal models that can entirely mimic the complexity of human ischemic stroke perfectly. The choice of using which model should relate to the research aim and carefully consider the limitations to increase the translational potential between animal and clinical work in both pathophysiological concepts and efficacious therapies [15,135].

Besides the *in vivo* models, *in vitro* ischemia models are also well developed with the purpose of exploring the post-ischemia mechanisms. There are two principal ways to induce *in vitro* ischemia: either the oxygen and glucose deprivation (OGD) or the chemical/enzymatic blockade like via $Na_2S_2O_4$ and $CoCl_2$ [133]. OGD as the most widely used *in vitro* model, is induced by the replacement of the normal O_2/CO_2 atmosphere by a N_2/CO_2 condition, combined with a glucose deprivation medium. Following OGD, the reperfusion can be mimicked by replacing to normal culture conditions. Brain slices and cultured primary neuronal/glial cells from cortex, hippocampus of embryonic or perinatal rats and mice have been widely used as powerful access to understanding molecular mechanisms of ischemic

injury and neuroprotection [136,137]. However, the limitations are still obvious like the lack of intact blood vessels and recruitment of leukocytes.

1.2 Macrophage migration inhibitory factor (MIF)

1.2.1 MIF

Macrophage migration inhibitory factor (MIF) is a highly conserved protein mediator with an approximate molecular size of 37 kDa. The MIF monomer is 12.5 kDa and contains 114 amino acids [138]. In 1966, MIF was initially described to be secreted by lymphocytes, which was involved in depressing the random migration of macrophages [139]. Afterwards, the functions of MIF have been widely expanded. As an evolutionarily conserved protein, MIF has been revealed to broadly express in immune cells like macrophages [140], B and T lymphocytes [141], as well as in various other cell types [142], such as endothelial cells, fibroblasts, neurons, glial cells, and tumor cells [143-146].

It has been demonstrated that MIF is a multi-faceted proinflammatory cytokine with chemokine-like functions over the years, and therefore termed as atypical chemokine (ACK) [147,148]. ACKs have functional similarities to classical chemokines but different structural properties. ACKs interact with classical chemokine receptors and regulate chemotaxis, but some of them also have additional intracellular functions [149]. MIF as a prototypical member of the ACK superfamily is known as a key mediator of the host immune and inflammatory response.

1.2.2 MIF receptors

MIF's effects are mediated by binding to its receptors (Fig. 3). MIF engages 4 receptors - 3 of them are chemokine receptors (CXCR2, CXCR4 and CXCR7, a scavenger receptor (also termed ACKR3)); the other receptor is cluster of differentiation 74 (CD74), also known as the surface-expressed form of the major histocompatibility complex (MHC) class II chaperone invariant chain (Ii), which is a single transmembrane protein of the type II class. The binding of MIF to these receptors induces several signaling pathways that regulate numerous physiological and pathophysiological processes. Briefly, MIF mediates the activation and migration of immune cells by binding to the receptors CXCR2 and CXCR4 during inflammation processes and cardiovascular pathogenesis [140,150]. It has been indicated that

MIF works as a key mediator in various inflammatory diseases, like sepsis, atherosclerosis and rheumatoid arthritis [151-153]. Moreover, several studies also showed that MIF mediates lymphocyte chemotaxis and platelet apoptosis by binding to CXCR7 [148,154]. In addition to these chemokine receptors, by binding to CD74, MIF modulates myeloid cell survival and polarization, and has a protective effect in the ischemic heart [155-157]. Notably, as the cytoplasmic domain of CD74 is short, it is necessary that CD74 recruits accessory molecules such as CD44 (or CXCR2 and 4) for signal transduction [155,158]. Surprisingly, besides its well-known extracellular activities as a cytokine/chemokine, recent findings revealed an intracellular role of MIF as an apoptosis-inducing factor (AIF)-associated nuclease that is involved in neuronal cell death following ischemic or excitotoxic challenges [159] (Fig. 3).

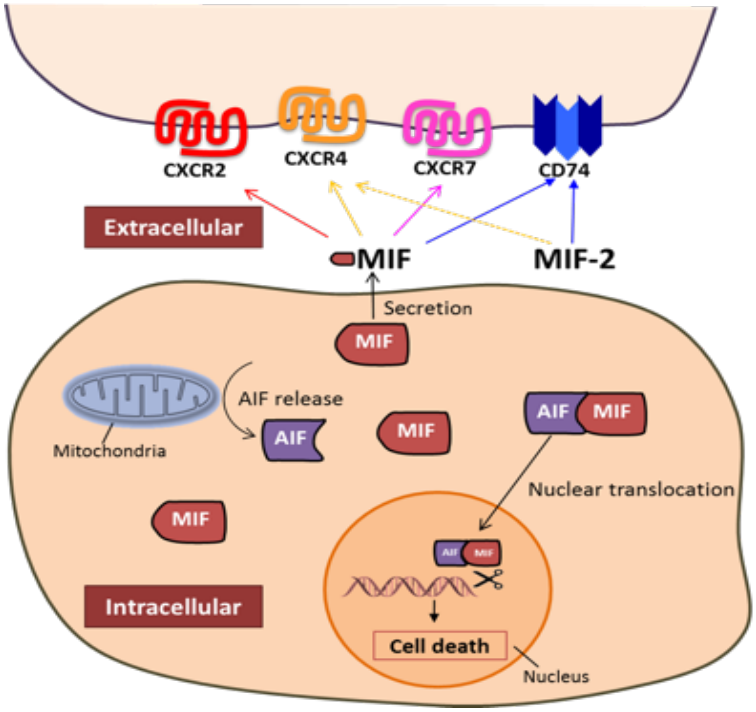

Fig. 3: Extra- and intracellular actions of MIF. MIF mainly functions through binding and signaling via its extracellular receptors CXCR2, CXCR4, CXCR7, and CD74, which then initiate a variety of inflammatory but also some homeostatic cellular effects. Recently, for MIF a novel intracellular function acting as a nuclease was demonstrated. After its nuclear translocation, MIF nuclease activity induces DNA damage to promote neuronal cell death.

1.2.3 Macrophage migration inhibitory factor-2 (MIF-2, D-DT)

MIF-2, a close structural homolog of MIF, also known as D-dopachrome tautomerase (D-DT) is a member of MIF cytokine superfamily [160,161]. The MIF and MIF-2 genes are located

closely proximity on chromosome 22q11.23, with a conserved intron-exon structure and highly homologous coding regions [162]. MIF-2 was shown to interact with CD74, and our lab has unpublished data demonstrating it also binds to CXCR4 (El Bounkari, Zan, and Bernhagen, personal communication). From a clinical point of view, MIF-2 has been reported to be involved in obesity, wound repair [163,164], burn injury [165], myocardial ischemia/reperfusion damage [166,167] and endotoxemia [168]. Interestingly, MIF-2 also plays a beneficial role in myocardial ischemia/reperfusion injury and heart failure [169,170]. However, whether MIF-2 also contributes to the pathogenesis of atherosclerosis remains unknown. Similarly, if MIF-2 also has a nuclease activity like MIF still needs to be further explored.

1.2.4 MIF proteins in atherosclerosis and myocardial infarction

MIF is a well-accepted key mediator in the pathogenesis of cardiovascular diseases. Atherosclerosis is a recognized chronic inflammatory disease and MIF exhibits pro-atherogenic and inflammatory properties through its ability to recruit atherogenic leukocytes and to promote lesional inflammatory processes. MIF has been broadly implicated in atherogenesis in both the *Apoe* $^{-/-}$ and *Ldlr* $^{-/-}$ mouse model, a notion established by *Mif* gene deficiency and antibody blocking [150,171-173]. MIF expression is upregulated in infiltrated leukocytes and platelets as well as in endothelial cells and smooth muscle cells during the development of atherosclerotic lesions in several species including humans, mice, and rabbits [174-177]. As a non-cognate CXCR ligand, MIF's pro-atherogenic functions are mainly due to interactions with CXCR2 and CXCR4 [150,178], respectively, through which MIF mediates monocyte and neutrophil recruitment, and B/T lymphocyte enrichment in aortic lesions [179]. Additionally, atherogenic or inflammatory leukocyte recruitment induced by MIF relies not only on CXCR2 binding, but also involves the MIF-binding protein CD74, which colocalizes with CXCR2 and forms CXCR2/CD74 complexes [142,150,180]. Similarly, functional CXCR4/CD74 complexes have been described for MIF-driven B cell migration [179,180].

In addition to atherosclerosis, a role for MIF in acute myocardial infarction (AMI), as an acute vascular event of CVDs, has been described. MIF exhibits a more complicated role in AMI *via* its phase-specific receptor-mediated cardioprotective effect. According to a wealth of information from experimental mouse models MIF is increased in the early phase of AMI and was found to be initially released by ischemic cardiomyocytes to bind to CD74 promoting a cardioprotective effect *via* activation of AMPK and subsequent increase of glucose uptake and

reduction of apoptosis [157,181]. However, MIF exacerbates the inflammatory responses in the ischemic heart in the late phase *via* binding to CXCR2 and/or CXCR4 to enhance the recruitment of circulating immune cells, including monocytes and neutrophils [182]. Furthermore, *Mif*-deficiency showed a protective effect in ischemic heart through inhibiting the infiltration of neutrophils and monocytes [183].

Thus, ample evidence has shown MIF and its receptors are key regulators in CVDs such as atherosclerosis and myocardial infarction/reperfusion injury. However, its role in ischemic stroke, another vascular disease and pathologic consequence of atherosclerosis and heart failure, as well as normal brain physiology and neuroinflammation in general has remained poorly investigated.

1.3 MIF in central nervous system

1.3.1 MIF expression in normal central nervous system

The expression and location of MIF and its function in normal CNS remain poorly investigated, as well as MIF-2. In the late 1990's, a descriptive study showed MIF was highly expressed in different neurons in the cortex, hippocampus, cerebellum, hypothalamus, pons and hypothalamus in rat brain in both mRNA and protein levels, which may suggest a requirement for this protein in CNS physiology [184]. In addition, MIF protein was also revealed to present in astrocytes in rat brain [185]. On one hand, both mRNA and protein expression of MIF are upregulated in developing rat brain [146], on the other hand after systemic deletion of *Mif*, mice showed higher depression-like behavioral symptoms and poor memory [186], suggesting the role of MIF in physiological brain is related to the growth of brain cells and participates the maintenance of normal brain functions. Furthermore, *in vitro* studies demonstrated MIF could have a growth-promoting effect on particular neuronal cell populations such as neuronal stem/progenitor cells [187].

1.3.2 MIF and its receptors in neurological diseases

As described above, MIF is abundant in the immune system but also expressed in the CNS. Although MIF's physiological function in brain is still poorly explored, MIF and its receptors were reported to be involved in neurological diseases in more and more recent studies.

MIF may have potential beneficial effects in Parkinson´s disease (PD) [188,189]. MIF was shown to be increased in a mouse PD model and may play protective roles via regulating inflammation, inhibiting apoptosis and inducing autophagy [190]. Similar with PD, MIF was also reported to be beneficial in amyotrophic lateral sclerosis (ALS), which mainly results from inhibiting the formation and toxicity of misfolded superoxide dismutase 1 (SOD1) amyloid aggregation [191]. Unlike the potential neuroprotective effect in PD and ALS, it is still controversial about MIF's function in Alzheimer's disease (AD). General agreement about this question is that MIF is a contributing player in the pathogenesis of AD, while the mechanism has remained unknown. MIF is upregulated both in CSF and plasma of AD patients [192]. Some experimental studies revealed that amyloid β protein (Aβ), the main constituent of AD plaques, induced toxicity could be reduced by inhibition of MIF in mouse and human neuronal cell lines [192,193]. In addition, one of MIF receptor-CD74 is also upregulated in neurofibrillary tangles in AD [194]. Furthermore, MIF is upregulated in multiple sclerosis (MS) patients' serum and it is associated with MS disease activity [195,196]. Clinical studies also showed that the serum MIF concentration is enhanced in traumatic brain injury and is related to inflammation, trauma severity and outcomes [197]. Interestingly, MIF was shown to be upregulated specifically and was related to promoting NG2 glia proliferation which was restricted to the gray matter injury but not white matter[198]. In addition to brain injury, MIF was also shown to contribute worse outcome in spinal cord injury in a mouse model *via* promoting neuronal death and inhibiting recovery. [199]. MIF is overexpressed in many tumors, with the function to induce angiogenesis and inhibit cell death [145,200]. Similarly, MIF was also identified to play an essential role in CNS tumors. For example, inhibition of MIF reduces the growth rate of glioma cells [201,202]. *In vivo* data also showed that MIF is increased in glioma cells and neoplastic astrocytes in glioblastoma patients, and that increased MIF may be involved in immune escape of gliomas, which is related to NK and cytotoxic T-cells [203]. Interestingly, studies suggested that glioma cell-derived MIF could work in a paracrine way by binding to its receptor CD74, restricted to glioma-associated microglia/microphage [204]. This binding of MIF to CD74 contributes to a M2 shift of microglia and escaping of pro-inflammatory M1 conversion, thereby facilitates brain tumorigenesis [205].

1.4 MIF in ischemic stroke

MIF is a key regulator in some neurological diseases, especially neurodegenerative diseases, and some mechanisms are known. However, MIF's effect in ischemic stroke as well as its role

in the post-ischemic inflammation are still not studied extensively. Although some studies have addressed this question, it turns out that the data is complex and in part controversial and requires further in-depth elucidation (Fig. 4).

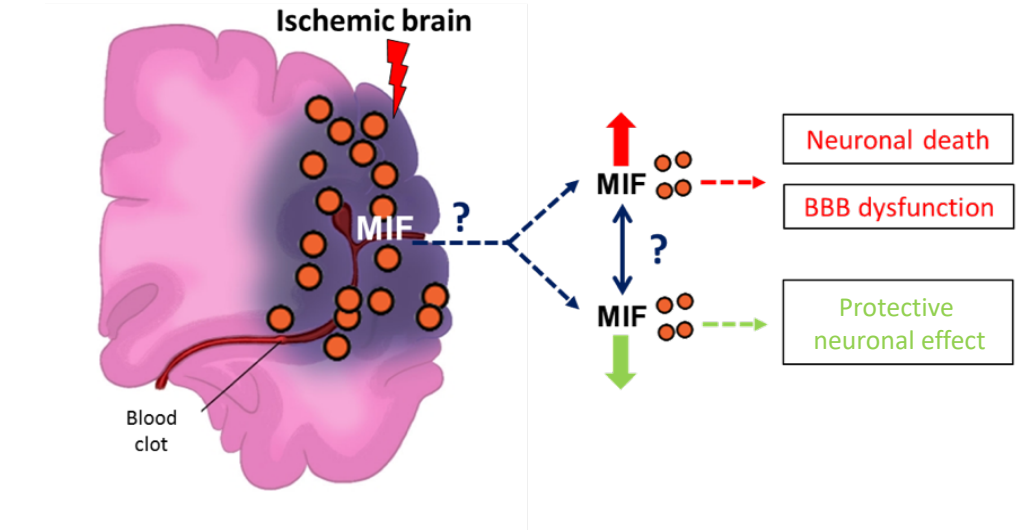

Fig. 4: Complex and controversial effects of MIF in ischemic stroke. Cartoon summarizing the conflicting published data suggesting a complex and in part controversial effect of MIF in ischemic stroke.

1.4.1 Pre-clinical studies in experimental stroke models

Previous animal studies indicate that MIF is transcriptionally and translationally upregulated in the ischemic rat brain with a peak at 24 h after stroke. The increase of MIF was found to correlate with the severity of stroke [206,207]. Inácio et al. [208,209] found that upregulated MIF was elevated in neurons and astrocytes of the ischemic penumbra, as well as in microglia in the infarct core of mouse or rat ischemic brain. In addition, *in vitro* studies suggested that the upregulation of MIF under hypoxic conditions could be related to the hypoxia responsive elements (HREs) present in its promoter, which contributes to an increased activity of the *MIF* gene promotor *via* hypoxia-inducible factor 1-alpha (HIF-1α) [207,210,211]. Furthermore, in male *Mif* $^{-/-}$ mice, Inácio and colleagues also directly revealed that MIF could promote cell death and aggravate neurologic deficits at 7 days after stroke in an MCAO model, which was in line with *in vitro* data using primary neuronal cells under OGD stress [212]. Additionally, Inácio et al. [209] also found that housing rats in an enriched environment after applying a permanent MCAO model, induced a downregulation of MIF protein levels in the penumbra, suggesting that MIF may be involved in brain plasticity and inhibit the sensory-motor function recovery after ischemic stroke. The underlying mechanism involved in upregulated MIF

leading to neuronal death in ischemic stroke is still not clear. Inácio and colleagues [212] showed that after deficiency of *Mif* gene, higher galetin-3 immunoreactivity was found in ischemic brain, which suggested MIF could affect macrophage or microglia responses during ischemic stroke. However, in this study they also showed that deletion of *Mif* did not affect protein expression of IL-1β in brain 7d after MCAO [212]. Moreover, this group also revealed in another report that *Mif* deletion didn't affect the protein level of cytokines like IL-2, IFN-γ, IL-1β, TNF-α and IL-10 in the brain or in the serum during the first week after surgery, suggesting lack of MIF doesn't affect inflammatory/immune responses following ischemic stroke [208]. As discussed above, MIF is an ACK and plays critical roles in various inflammatory conditions, but if MIF regulates neuroinflammation still needs to be clarified. In additional to directly affecting brain parenchyma, MIF also plays an important role in BBB integrity during ischemic stroke. A recent study showed that MIF disrupted tight junctions in adult rat brain endothelial layers but did not affect neural viability in primary neuronal cells under OGD/reoxygenation stress [213]. Consistently, *in vivo* studies showed that administration of MIF following ischemic stroke disrupted BBB tight junctions and increased infarct volume, and this MIF-induced effect can be ameliorated *via* using MIF antagonist [213].

However, controversial data have been reported as well. Deficiency of *Mif* was indicated to aggravate ischemic stroke 72 h after stroke, which seems to be gender dependent and only happened in female mice but did not affect male mice [214]. Interestingly, the larger infarct volume in female $Mif^{-/-}$ mice was associated with higher microglial activation and an increase in the mitochondrial localization of c-Jun activation domain-binding protein 1 (JAB1/CSN5) [214]. Remarkably, the observed effects were fully independent from estrogen levels and pro-inflammatory cytokines profile in both genders. Meanwhile, Zhang and colleagues [215] found that MIF was downregulated in mouse brain after transient MCAO following activation of nuclear factor kappa-light-chain-enhancer of activated B cells (NF-κB) pathway and demonstrated that deletion of the *Mif* gene was associated with caspase-3 activation, resulting in neuronal loss and increasing of infarct volume 24 h after ischemic stroke [215]. Moreover, under *in vitro* OGD stress, MIF reduced caspase-3 activation and protected neurons from ischemia-induced apoptosis; in other words, MIF exerted an apparent neuronal protective effect during stroke in those studies [215]. This protective role of MIF in ischemic brain was consistent with its role in the ischemic heart as mentioned above, although an AMPK activation mechanism has not been explored in brain.

Surprisingly, in addition to the classical extracellular mechanism of MIF, another mechanism has been recently described suggesting a novel intracellular function for MIF in ischemic stroke. Wang et al. [159] described MIF as a novel nuclease which is "poly-ADP-ribose-polymerase-1 (PARP-1)-dependent and AIF-associated" and enhances DNA cleavage *via* the parthanatos route, thereby mediating cell death. PARP-1-related cell death under stress is associated with the release and translocation of apoptosis-inducing factor (AIF) to the nucleus, which leads to chromatolysis. However, AIF is not a nuclease itself. In their study, Wang et al. showed that following oxidative stress, glutamate excitotoxicity, or DNA damage, the nuclease activity of MIF to be strictly dependent on the activation of PARP-1 enzyme, the release of AIF and its translocation together with MIF into the nucleus, where it cleaves genomic DNA. Whether this activity is also involved in other inflammatory and chronic diseases remain to be investigated [159]. Interestingly, AIF itself was also found to be involved in neuronal cell death during ischemic stroke [216,217].

Furthermore, there is initial evidence that MIF's receptors could be involved in ischemic stroke. CD74 was found to be increased in the hippocampal Cornu Ammonis 1 region and colocalized with the M1 microglia subtype 5 days after ischemic stroke [218]. Interestingly, studies also showed that the treatment of partial MHC class II/peptide constructs reduces infarct volume in an MCAO model, partly *via* competitively inhibiting MIF/CD74 signaling pathways [219,220]. CXCR2, CXCR4 and CXCR7 were also implied in ischemic stroke previously, [221-225], but those studies have not determined whether this involved signaling initiated by the cognate ligands CXCL1, CXCL12, or CXCL11/12, respectively, or MIF-triggered signaling.

1.4.2 Clinical studies

Besides experimental stroke studies, several clinical studies point towards a relationship between MIF levels in peripheral blood and the pathological severity or prognosis of stroke patients. Both the protein concentration of MIF in plasma and its mRNA levels in PBMC were indicated to be upregulated in ischemic stroke patients, which is correlated with the severity of ischemic damage based on the NIHSS score [207]. In addition, they also found the increase in MIF expression in blood only occurred during the acute stage (within 3 days), but then decreased to normal levels during later stage (10 to 14 days) [207]. Some other studies also supported this notion [226-228]. Besides confirming the upregulation of serum MIF level and its positive association with short- or long-term outcome, Li et al. [226] also found the serum MIF level and the infarct size have positive correlation in ischemic stroke patients determined

by diffusion-weighted imaging (DWI) at admission. Moreover, they compared MIF levels in different stroke subtypes and demonstrated that despite the etiology and pathophysiology of these subtypes are distinct, MIF levels were upregulated in both subtypes [226]. Interestingly, Xu and colleagues pointed out that increased MIF levels in plasma at admission were related to a higher risk of post-stroke depression [229]. In addition to peripheral levels, MIF immunoreactivity was measured in endothelial cells in the penumbra of human ischemic brain compared to control brain, in which no immunoreactivity was observed [230]. Besides MIF, the level of MIF receptor CD74 in PBMCs was also found to be increased and this peripheral upregulation was related to bigger infarct volume and worse neurological outcome [228].

Although the mechanism(s) of upregulation of peripheral MIF levels in ischemic stroke patients remain unknown, these clinical studies suggested that MIF as a potential biomarker and therapeutic candidate that may evaluate the severity and the outcome of ischemic stroke. Yet, future studies are still needed to clarify the overall role of MIF in clinical diagnosis and treatment of stroke.

Overall, the preclinical and clinical studies made it clear, that it is necessary to perform additional investigations to study the potential role and mechanism of MIF in ischemic stroke, as well as its potential use for clinical diagnosis and therapy. The aim of the present MD thesis therefore was to study the potential role of MIF proteins and the underlying mechanisms in ischemic stroke in more depth, also capitalizing on novel stroke models that avoid the problems, experimental variability, and the lacking robustness of previously applied models.

1.5 Open questions and aims of this thesis

Based on the background and preliminary work of my host institution, I aimed at pursuing the following goals in this thesis:

- Aim 1: Clarify the interaction between MIF/MIF-2 and AIF and explore their novel potential binding partners in brain.
- Aim 2: Study the causal role of MIF in experimental ischemic stroke?
    a) Investigate whether ischemia induces expression and secretion of MIF and MIF-2 from primary neuronal cells.
    b) Examine the role of MIF on the viability of primary neuronal cells under ischemic stress.

c) Clarify the controversial data on exacerbating *versus* protective roles of MIF in experimental models using an MCAO-based ischemic stroke model that was validated in a preclinical randomized multicenter trial (pRCT) as established at my host institution in combination with *Mif*-specific genetic deletion.

- Aim 3: Study the causal involvement and mechanism of MIF receptors CD74, CXCR2 and CXCR4 in MIF-modulated stroke?
    a) Examine the effect of ischemic challenge on MIF receptor expression in neurons and microglia cells *in vitro*.
    b) Test the effect of CD74 on the viability of neurons under ischemic stress.
    c) Determine the stroke phenotype of *Cd74* gene-deficient mice in the pRCT-validated model of ischemic stroke.

2. MATERIALS AND METHODS

2.1 Materials

2.1.1 Equipment and instrument

BD FACSVerse™ flow cytometer	BD Biosciences (Heidelberg, Germany)
Centrifuge 5424	Eppendorf (Heidelberg, Germany)
Cryostat NX70	Thermo Fisher Scientific (Waltham, MA, USA)
DC temperature control system	FHC (Bowdoin, ME, USA)
Decapitation scissors	Fine Scientific Tools (Heidelberg, Germany)
DMi8 fluorescent microscopy	Leica Microsystems (Wetzlar, Germany)
Enspire plate reader	Perkin Elmer (Waltham, MA, USA)
Hardened fine iris scissors	Fine Scientific Tools
Heracell Vios i160 incubator	Thermo Fisher Scientific
Herasafe cell culture hood	Heraeus (Hanau, Germany)
Horizontal gel electrophoresis system	Thermo Fisher Scientific
Hypoxia incubator	Toepffer Lab Systems (Göppingen, Germany)
Iris scissors-tough cut	Fine Scientific Tools
LED light source	Leica Microsystems
Leica M80 Stereomicroscope	Leica Microsystems
Micro adson forceps	Fine Scientific Tools
Mini blot module	Thermo Fisher Scientific
Mini gel tank	Thermo Fisher Scientific
MT B500-0L240 straight microtip (5 pcs)	PERIMED (Järfälla, Sweden)
Nanodrop one spectrophotometer	Thermo Fisher Scientific
Odyssey® Fc imaging system	LICOR Biosciences (Bad Homburg, Germany)
Oslen-Hegar needle holder	Fine Scientific Tools
PCR thermal cycler (Biometra TRIO)	Analytik Jena (Jena, Germany)

PCR workstation pro	PEQLAB Biotechnologie GmbH (Erlangen, Germany)
PeriFlux 5000 laser doppler	PERIMED
PROBE 418-1 master probe	PERIMED
Ring forceps	Fine Scientific Tools
Rotor-gene Q 2 plex HRM-system	QIAGEN (Hilden, Germany)
Safe imager 2.0 blue-light transilluminator	Thermo Fisher Scientific
Stemi 305 EDU dissection microscope	Carl Zeiss AG (Oberkochen, Germany)
TC-20 cell counter	Bio-Rad Laboratories (Hercules, CA, USA)
Thermo shaker lite	VWR International (Radnor, PA, USA)
Vortex shaker, VV 3	VWR International
Zeiss axio imager M2	Carl Zeiss AG

2.1.2 Reagents and consumables

100 mM sodium pyruvate	Thermo Fisher Scientific
2-propanol (isopropyl alcohol)	Carl Roth GmbH (Karlsruhe, Germany)
200 mM L-glutamine	Thermo Fisher Scientific
30% bis acrylamide solution	Bio-Rad Laboratories
6X DNA loading dye	Thermo Fisher Scientific
7-0 fine MCAO suture Re L12 PK5	Doccol (Sharon, MA, USA)
Accelerator insta-set	Drechseln & Mehr (Weiden, Germany)
Agarose neo-ultra quality	Carl Roth GmbH
Albumin fraction V/BSA	Carl Roth GmbH
Albumin standard ampules, 2mg/mL	Thermo Fisher Scientific
B-27 supplement (50X), serum free	Thermo Fisher Scientific
Basal medium eagle (BME)	Thermo Fisher Scientific
Bepanthen® eye and nose ointment	Bayer Vital GmbH (Leverkusen, Germany)

Boric acid	Sigma-Aldrich (St. Louis, MO, USA)
Bovine serum albumin (BSA)	Sigma-Aldrich
Cannula (21G)	Sarstedt (Nümbrecht, Germany)
Carprofen (rimadyl 50mg/ml)	Zoetis (Parsippany-Troy Hills, NJ, USA)
Cell counting kit-8 (CCK8)	Sigma-Aldrich
Cell counting slides	Bio-Rad Laboratories
Chloroform	Sigma-Aldrich
Coomassie brilliant blue R-250 staining solution	Bio-Rad Laboratories
Cover glasses, round, diameter 12 mm	Labmarket (Ludwigshafen, Germany)
CozyHi™ prestained protein ladder	highQu GmbH (Kraichtal, Germany)
D (+)-saccharose (sucrose)	Sigma-Aldrich
DMEM, no glucose	Thermo Fisher Scientific
DMEM/F-12, glutamax supplement	Thermo Fisher Scientific
Dulbecco's phosphate buffered saline	Sigma-Aldrich
EcoRI (10 U / µL)	Thermo Fisher Scientific
EDTA	AppliChem GmbH (Darmstadt, Germany)
Ethanol absolut	Merck Group (Darmstadt, Germany)
Fetal bovine serum (FBS)	Thermo Fisher Scientific
First strand cDNA synthesis kit	Thermo Fisher Scientific
Glucose	Sigma-Aldrich
Glutathione sepharose 4B beads	GE Healthcare (Chicago, IL, USA)
HBSS (no calcium, no magnesium)	Thermo Fisher Scientific
HEPES	Sigma-Aldrich
High pure PCR product purification kit	Roche (Basel, Switzerland)
IPTG (isopropylthio-β-galactoside)	Thermo Fisher Scientific
Isoflurane	CP-Pharma (Burgdorf, Germany)
LB broth (Miller)	Sigma-Aldrich

Maxi-cure super glue cyanoacrylate adhesive gel	PARTS EXPRESS (Springboro, OH, USA)
Medetomidine	Zoetis (Parsippany-Troy Hills, NJ, USA)
Methanol	Carl Roth GmbH
Midazolam	B-Braun (Melsungen, Germany)
Montage gel extraction kit	Sigma-Aldrich
NaCl isotonic solution 0.9%	Fresenius Kabi (Bad Homburg, Germany)
Neurobasal medium	Thermo Fisher Scientific
Nitrocellulose blotting membrane	GE Healthcare
Normal goat serum	Abcam (Cambridge, UK)
Nunc MaxiSorp™ flat bottom plate	Thermo Fisher Scientific
NuPAGE™ LDS sample buffer (4X)	Thermo Fisher Scientific
NuPAGE™ transfer buffer (20X)	Thermo Fisher Scientific
ORA™ SEE qPCR green ROX L mix, 2x	highQu GmbH
Papain, lyophilized	Worthington (Columbus, OH, USA)
Paraformaldehyd (PFA) 4% in PBS, 1000 ml	Morphisto GmbH (Frankfurt, Germany)
Penicillin streptomycin (10,000 U/mL)	Thermo Fisher Scientific
pGEX-4T-1 vector	GE Healthcare
Phusion® high-fidelity DNA polymerase	New England Biolabs (Ipswich, MA, USA)
Pierce protease inhibitor tablets	Thermo Fisher Scientific
Pierce™ IP lysis buffer	Thermo Fisher Scientific
Pierce™ TMB substrate kit	Thermo Fisher Scientific
Poly-L-lysine	Sigma-Aldrich
Poly-L-ornithine	Sigma-Aldrich
Protein assay dye reagent concentrate	Bio-Rad Laboratories
QIAprep spin miniprep kit	QIAGEN
RIPA lysis and extraction buffer	Thermo Fisher Scientific

RPMI 1640 medium, glutamax supplement	Thermo Fisher Scientific
Scalpel (No.11)	Feather (Osaka, Japan)
Streptavidin-POD conjugate	Sigma-Aldrich
Super Signal™ west dura extended duration substrate	Thermo Fisher Scientific
Superfrost plus microscope slides	Thermo Fisher Scientific
T4 DNA ligase	Thermo Fisher Scientific
TEMED	Bio-Rad Laboratories
TRIS PUFFERAN® ≥99,9 %, p.a.	Carl Roth GmbH
Triton X-100 (laboratory grade)	Sigma-Aldrich
TRIzol ™ reagent	Thermo Fisher Scientific
Tween-20	Sigma-Aldrich
VECTASHIELD® antifade mounting medium with DAPI	Vector Laboratories (Burlingame, CA, USA)
XhoI (10 U / µL)	Thermo Fisher Scientific

2.1.3 Buffers and solutions

TBE buffer		
Tris	89 mM	10.8 g
Boric acid	89 mM	5.5 g
EDTA	2 mM	0.74 g

1% Agarose		
Agarose	1%	3 g
TBE		300 ml

LB Media

LB broth (Miller)		25 g
MilliQ-H_2O		500 ml

1 M Tris-HCl

Tris base	1 M	24.228 g
MilliQ-H_2O		200 ml

2.5 M NaCl

NaCl	2.5 M	29.22 g
ddH_2O		200 ml

100 mM PMSF

PMSF	100 mM	0.174 g
Isopropanol		10 ml

GST-lysis buffer

Tris-HCl pH7.5 (1 M)	25 mM	1.25 ml
Triton X-100	0.1%	50 ul
PMSF (100 mM)	1 mM	500 ul
MilliQ-H_2O		To 50 ml

GST-washing buffer

Tris-HCl pH7.5 (1 M)	25 mM	2.5 ml
Triton X-100	0.05%	50 ul
NaCl (2.5 M NaCl)	100 mM	4 ml
PMSF (100 mM)	1 mM	1000 ul
MilliQ-H_2O		To 100 ml

20% glucose

Glucose	20%	20 g
MilliQ-H_2O		100 ml

1 M HEPES, pH 7.3

HEPES	1 M	119.15 g
ddH_2O		500 ml

Phosphate-buffered saline (PBS)

NaCl	137 mM	8 g
KCl	2.7 mM	0.2 g
KH_2PO_4	1.5 mM	0.2 g
$Na_2HPO_4x2H_2O$	8.1 mM	1.44 g
MilliQ-H_2O		1 L

Tris-buffered saline (TBS)

NaCl	150 mM	8.76 g
Tris	20 mM	2.42 g
MilliQ-H_2O		1 L

TBS with 0.1% Tween (TBST)

Tween-20	0.1%	1 mL
TBS		1 L

10% SDS

SDS	10%	10g
ddH_2O		100 ml

10% ammonium persulfate (APS)

APS	10%	1 g
MilliQ-H_2O		10 ml

Resolving gel buffer, pH 8.8

Tris base	1.5 M	90.75 g
MilliQ-H_2O		500 ml

Stacking gel buffer, pH 6.8

Tris base	0.5 M	30.3 g
MilliQ-H_2O		500 ml

1 M DTT

DTT	1 M	2.313 g
ddH_2O		15 ml

LDS-DTT buffer

NuPAGE™ LDS sample buffer (4x)	1x	1 ml
1 M DDT	0.125 M	0.5 ml
ddH_2O		To 4 ml

5xrunning buffer for Western blot

Tris		15.14 g
Glycin		72.05 g
10% SDS	20%	50 ml
MilliQ-H_2O		Add to 1 L

Transfer buffer for Western blot

NuPAGE ™ Transfer Buffer (20X)	1x	12.5 ml

Methanol	10%	25 ml
MilliQ-H_2O		Add to 250 ml

Blocking buffer for Western blot (3% BSA)

Albumin Fraction V/BSA	3%	3g
TBST		100 ml

Washing buffer for ELISA (PBST)

Tween-20	0.05%	0.5 ml
PBS		1 L

Blocking solution for ELISA

BSA	1%	1 g
Sucrose	5%	5 g
PBS		100 ml

Reaction buffer for ELISA

BSA	1%	0.1 g
Tween-20	0.5%	50 ul
TBS		10 ml

FACS buffer (0.5% BSA in PBS)

BSA	0.5%	0.5 g
PBS		100 ml

5% goat serum in PBS

Goat serum	5%	0.5 ml
PBS		10 ml

SDS-PAGE gel (for 4 gels)

11% separating gel

30% Bis acrylamide solution	13,2 ml
Resolving gel buffer, pH 8.8	15 ml
ddH_2O	7.5 ml
10% SDS	360 ul
10% APS	120 ul
TEMED	36 ul

4% stacking gel

30% Bis acrylamide solution	2 ml
Stacking gel buffer, pH 6.8	1.5 ml
ddH_2O	7.8 ml
10% SDS	120 ul
10% APS	60 ul
TEMED	18 ul

2.1.4 Antibodies

Rabbit polyclonal anti-MIF antibody (Ka565)	BernhagenLab (LMU)
Rabbit polyclonal anti-MIF-2 antibody	Kind gift of Prof. R. Bucala, Yale
Mouse monoclonal anti-AIF antibody (E-1) (sc-13116)	Santa Cruz Biotechnology (Dallas, TX, USA)
Mouse monoclonal anti-β-tubulin III antibody (neuronal) (T8578)	Sigma-Aldrich
Goat HRP-conjugated anti-mouse secondary antibody (ab6789)	Abcam
Goat HRP-conjugated anti-rabbit secondary antibody (P0448)	Dako (Santa Clara, CA, USA)
Goat anti-rabbit secondary antibody, Alexa fluor 555 (A-21428)	Thermo Fisher Scientific

Mouse anti-mouse MIF antibody (capture antibody for ELISA) (XIV.14.3)	Kind gift of Prof. R. Bucala, Yale
Human MIF biotinylated antibody (detection antibody for ELISA) (BAF289)	R&D Systems (Minneapolis, MN, USA)
Mouse anti-mouse MIF-2 antibody (capture antibody for ELISA)	Kind gift of Prof. R. Bucala, Yale
Detection anti-mouse MIF-2 antibody (detection antibody for ELISA)	Kind gift of Prof. R. Bucala, Yale
FITC rat anti-mouse CD74 (555318)	BD Biosciences (Heidelberg, Germany)
APC/Cyanine7 anti-mouse CD182 (CXCR2) antibody (149314)	BioLegend (San Diego, CA, USA)
PE rat anti-mouse CD184 (551966)	BD Biosciences
APC anti-human/mouse CXCR7 antibody (331114)	BioLegend

2.1.5 Primer sequences

Target gene	Forward primer (5'-3')	Reverse primer (5'-3')
Mouse MIF	ACAGCATCGGCAAGATCG	AGGCCACACAGCAGCTTAC
Mouse MIF-2	CCAGCTTCTTCAAGTTCCTCA	GGGAAGAAGCGGATAACGAT
Mouse CD74	CCCCATTTCTGACCCATTAGT	TGTCCAGCCTAGGTTAAGGGT
Mouse CXCR2	CAGGACCAGGAATGGGAGTA	TCCCCTCCAAATATCCCCTA
Mouse CXCR4	TGGAACCGATCAGTGTGAGT	GGGCAGGAAGATCCTATTGA
Mouse CXCR7	CAGCCACATGTCCATCAGAC	CACAGCTCGCTGACACCTAA
Mouse TNF-α	CATCTTCTCAAAATTCGAGTGACAA	TGGGAGTAGACAAGGTACAACCC
Mouse IL-1β	GAAATGCCACCTTTTGACAGTG	TGGATGCTCTCATCAGGACAG
Mouse IL-6	ATGGATGCTACCAAACTGGAT	TGAAGGACTCTGGCTTTGTCT
Mouse IL-10	CAGAGCCACATGCTCCTAGA	TGTCCAGCTGGTCCTTTGTT
Mouse TGF-β1	CAACCCAGGTCCTTCCTAAA	GGAGAGCCCTGGATACCAAC
Mouse βactin	GGAGGGGGTTGAGGTGTT	GTGTGCACTTTTATTGGTCTCAA

2.1.6 Software

SnapGene viewer (version 5.1.2)

BD FACS Diva software (version 1.0.6.5230)

Carl Zeiss ZEN 2010

FlowJo software (version 10)

GraphPad Prism 8 software

Image Studio™ software (version 5.2.5)

ImageJ 2 software

Leica application suite X (version 3.0.1.15878)

Rotor-Gene Q software (version 2.3.1)

2.2 Methods

2.2.1 Animals

All the mice that used in thesis were housed under standardized light-dark cycles in an air-conditioned environment with a temperature-controlled system at the Center for Stroke and Dementia Research (CSD), Munich, Germany. Mice used in this study were between 8-12 weeks of age, weighing 18 to 22 g and were on pure C57BL/6-J background. *Mif* $^{-/-}$ mice which have been established in the Bernhagen lab [231,232] and the respective *Mif* $^{+/+}$ (wild type (WT)) littermates were used for experimental ischemic stroke studies, namely for the MCAO model. Similarly, *Cd74* $^{-/-}$ mice, which are also routinely used in the Bernhagen lab [232] and respective *Cd74* $^{+/-}$, *Cd74*$^{+/+}$ mice were used in the experimental ischemic stroke studies to explore the function of CD74 in ischemic stroke. Littermate mice in two genders were utilized in this study. All mouse experiments were approved under approval number 02-17-41 by the Animal Care and Use Committee of the local authorities and performed under the supervision of animal welfare officer at CSD.

2.2.2 Transient middle cerebral artery occlusion (MCAO) model

A 60 min occlusion of the left MCA was performed to induce cerebral ischemia with intraluminal filament [233-235] (Fig. 5). In brief, isoflurane was used to anesthetize mice, which was initialized with a mixture of 4% isoflurane, 30% O_2 and 70% N_2O in an induction chamber for 60-90 s and anesthesia maintained with isoflurane (1.8-2%) by face mask. A feedback-controlled heating pad was used to keep mouse body temperature during the surgery. Eye ointment was applied during the experimental procedure to protect the eyes from dryness. A laser doppler probe was used to continuously monitor the regional cerebral blood flow (CBF), which was affixed over the MCA branches after exposing the left parietal skull. In the supine position, after making a neck midline incision, the left common carotid artery (CCA) and bifurcations -external and internal carotid artery (ECA and ICA) were exposed. After ligating the CCA and ECA, a 2-mm silicone rubber-coated monofilament was induced *via* the cut CCA, passed into ICA, and went forward to the root of the MCA until occlusion occurred (monitored by laser doppler). Generally, an immediate cerebral blood flow reduction of more than 80% of baseline was to be achieved. All surgery procedures were performed within 20 min. After suturing wounds, a recovery chamber at 32°C was used to place mice temporarily. Mice were shortly re-anesthetized after 60 min of MCAO to withdraw the monofilament, meanwhile reperfusion was to be observed. After surgery, to maintain the body temperature, mice were placed for 2 h in the 32°C chamber and then transferred into a cage in a temperature-controlled locker (24°C). Mice were killed 24 h after reperfusion. The mice that did not exhibit a rapid reduction in CBF following induction of MCA occlusion, or died during the reperfusion time as well as the mice that did not develop sufficient infarct volume were excluded from the study.

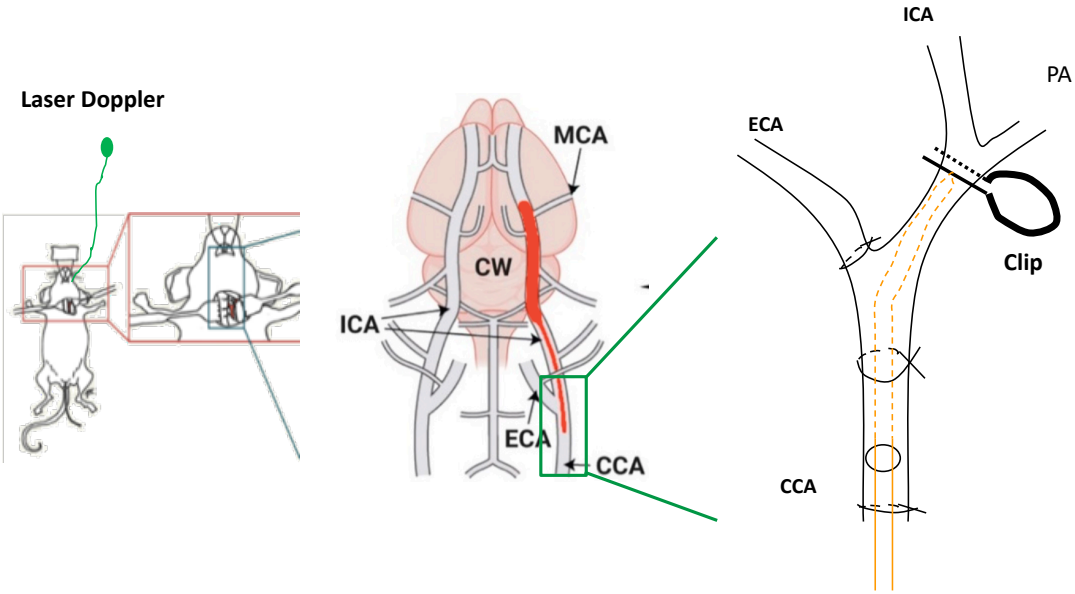

Fig. 5: **Scheme of the *in vivo* MCAO model in mice.** Modified after Lunardi Baccetto S et al. 2019 [236]. CCA, common carotid artery; ICA, internal carotid artery; ECA, external carotid artery; MCA, middle cerebral artery; PA, pterygopalatine artery.

2.2.3 Behavior test

At one hour after MCAO induction as well as 24 h after reperfusion, neurological deficits of all the animals were tested using a rough behavior test (Neuroscore/Modified Bedersen score, 0 to 4) like described before [233,237]:

0 = No deficit;

1 = Weakness of the contralateral forepaw or flexion of contralateral forelimb during tail suspension;

2 = Circling;

3 = Leaning to contralateral side;

4 = No motor activity.

2.2.4 Tissue and organ harvesting from mice

For termination, animals were intraperitoneally injected with medetomidine (0.5 mg/kg), midazolam (5 mg/kg) and fentanyl (0.05 mg/kg) until the deep anesthesia was achieved. To

remove the circulation blood, perfusion was performed by injecting 30 ml of physiological saline (0.9% NaCl) via a 21G cannula fixed in the left ventricle which then went through the body and come out from the cut right atrial appendage. After that, brain was carefully removed and placed immediately on powdered dry ice for quick-freezing and kept in -80°C for further analyzing.

2.2.5 Evaluation of infarct volume

After 24 h reperfusion, all the *Mif* $^{-/-}$, *Mif* $^{+/+}$, *Cd74* $^{-/-}$, *Cd74* $^{+/-}$ and *Cd74* $^{+/+}$ mice that were subjected to the MCAO model were killed and the infarct volume was analyzed as described before [237,238]. Briefly, 10 mm thick coronal brain sections were cut on a cryostat at 750 mm intervals, in a total of 12 sequential sections for each brain and applied to one glass slide, which was kept at -80 °C for further analysis. Infarct volume was estimated by using cresyl violet/Nissl staining. In brief, 70% ethanol was used to fix sections for 2 min and then the sections were stained in cresyl violet for 15 min. After two rinses in water, the slides were put in 70% ethanol, 96% ethanol, 100% ethanol, isopropanol, rotihistol I and rotihistol II for 2 min successively, following by lidding with a coverslip. The sectioned images were digitally photographed by a Zeiss Axio Imager M2 microscope and analyzed with imaging software. The whole area of contralateral hemisphere (Contra) and ipsilateral hemisphere (Ipsi) and the infarct area (IA) were measured in 12 sequential sections. The infarct volume (IV) of each hemisphere was quantified as the following formula: IV = (IA1 + IA2 + IA3… + IA12) * 0.75 (0.75 um, which is the distance between two sections). Infarct volume was corrected for brain edema by following the equation: $IV_{corrected} = IV_{Ipsi} – (V_{Ipsi} - V_{Contra})$.

2.2.6 Vessel anatomy

WT and *Mif* $^{-/-}$ mice were sacrificed and perfused with physiological saline (0.9%) followed by stamp ink solution. The brain was harvested, placed in saline solution and pictures were subsequently taken immediately with Leica dissection microscope. ImageJ software was used to analyze the bilateral posterior communicating artery (PcomA) and MCA-territory of two different mice. PcomA anatomy was characterized with the following scores [239]: 0, absent; 1, capillary, but not well developed; 2, well formed with clear vascular trunk; 3, robust vessel collateralization. MCA-territory was determined as percentage of MCA-territory area compared to the corresponding hemisphere area.

2.2.7 Primary neuronal cell cultures

Primary cortex neuronal cell cultures were prepared as previously described [240], with some modifications. Briefly, early postnatal WT, *Mif* $^{-/-}$ or *Cd74* $^{-/-}$ pups at P0-P1 were used to dissect cerebral cortices, which were then placed in cold dissection medium (Hank's Balanced Salt Solution (HBSS) containing 0.1% glucose, 1 mM sodium pyruvate and 10 mM HEPES) and cut into small pieces. After two rinses with dissection medium, cortices were incubated for 15 min in 2 mg/ml papain (freshly prepared from lyophilized enzyme) in dissection medium at 37°C. Papain was aspirated and ice cold plating medium, which was prepared in advance using Basal Medium Eagle (BME) supplemented with 2 mM glutamine, 10% FBS, 1 mM sodium pyruvate, 0.45% glucose and 100 U/ml penicillin/streptomycin, was used to wash cortices two times. Tissue was dissociated in pre-warmed plating medium with a fire-polished glass pipette by pipetting up and down gently, followed by filtering through a 70 μm cell strainer. Cells were plated on multi-well plates or coverslips which were pre-coated using poly-L-lysine hydrobromide (0.1 mg/mL) overnight at +4°C. Cells were cultured in the standard condition with 5% CO_2 in a humidified incubator at 37°C. Four to eight hours after initial plating, maintenance medium (Neurobasal medium supplied with 10% B-27 supplement, 2 mM glutamine and 100 U/ml penicillin/streptomycin) was used to change plating medium, and the maintenance medium was changed (half) twice per week. All the experiments were performed after 10-13 days of incubation. Neurons should represent 70% to 90% of the mature final cultures.

2.2.8 Cell cultures of BV-2 cell and N2a cell

BV-2 cell culture

BV-2 cell is a commonly used mouse cell line of microglial cells [241], which were purchased from ATCC and is usually served as an alternative model for primary cultured microglia. Roswell Park Memorial Institute (RPMI) 1640 medium which contains glutamax supplement and supplemented with 10% FBS as well as 100 U/ml penicillin/streptomycin was used to culture BV-2 cells. Cells were plated on plates or flasks (coated with 0.01% poly-L-ornithine) and maintained in the standard incubator at 37 °C with 5% CO_2. The cells that reached 75% to 80% confluence and less than 20 passages were used to perform experiments.

Neuro-2a cell culture

Neuro-2a cells (N2a) which are mouse neuroblast cells were initially purchased from DSMZ. The culture medium of N2a cells was prepared using Dulbecco's Modified Eagle Medium (DMEM) which contained 10% FBS 100 U/ml and penicillin/streptomycin, and cells were maintained in the standard cell culture incubator as mentioned above. All experiments were performed, when cells reach 75% to 80% confluence and less than 20 passages.

2.2.9 Oxygen-glucose deprivation (OGD) treatment

Mouse primary cortical neurons were subjected to ischemia-reperfusion (IR) injury *in vitro* using an OGD-reoxygenation cell culture model. Under OGD conditions, the maintains medium was replaced by the basal DMEM without glucose and cells were cultured in a hypoxia chamber (hypoxic glove box HGB-090-1, Toepffer lab systems) at 37°C with 1% O_2 and 5% CO_2 which was achieved by complement with N_2 for several hours. In addition, the oxygen was fully removed from the medium by leaving the medium in the hypoxia chamber overnight prior to use. In the control condition, the cell cultures were changed to fresh maintenance medium and incubated in normal incubator (95% air and 5% CO_2). After OGD treatment, medium was changed again to maintenance medium and transferred to the normal incubator for another 24 h to mimic reperfusion/reoxygenation phase. After treatment, cell viability of primary neuronal cells was assessed using CCK-8 kit, conditioned medium was collected and subsequently cell was lysed and messenger RNA (mRNA) was purified for further analysis. After 24 h OGD treatment, the influence of the hypoxia on MIF receptors cell surface expression of BV-2 cells was assessed using flow cytometry.

2.2.10 Cell viability

The cell counting Kit-8 (CCK-8) assay was used to analyze cell viability (relative cytotoxicity) according to the manufacturer's instruction. The working principle of CCK-8 is to measure the ability of dehydrogenases in cells to reduce WST-8 (2-(2-methoxy-4-nitrophenyl)-3-(4-nitrophenyl)-5-(2,4-disulfophenyl)-2H-tetrazolium, monosodium salt) into yellow colored formazan dye which is water-soluble. The amount of living cells is positively proportional to the amount of formazan directly. Briefly, primary cortical neuronal cells isolated from WT, *Mif* $^{-/-}$ *or Cd74* $^{-/-}$ mice were plated in 96-well plates and cultured for 10-13 d as described before. After 4 or 8 h of OGD treatment, cells were incubated during the reoxygenation phase

for another 24 h in culture medium (100 µl/well). After incubation, the CCK-8 solution was added (10 µl/well) and placed for 2 h in the normal incubator. After incubation, EnSpire Multimode Plate Reader (Perkin Elmer) was used to measure the absorbance of each well at 450 nm. Background control was achieved by adding maintenance medium in the well without cells. Each time experiment was performed as technical triplicates. Cell viability of all these three different genotype cells was analyzed by normalizing the absorbance of OGD treated cells to the absorbance of untreated (control) cells and expressed as a relative survival ratio.

2.2.11 Cloning of recombinant GST-MIF and GSF-MIF-2

To clarify the interaction between MIF proteins (MIF, MIF-2) with AIF, as well as potential new binding partners for MIF/MIF-2 in brain, recombinant GST-MIF and GST-MIF-2 was generated to perform glutathione S-transferase (GST)-pulldown assay. For this purpose, mouse MIF and MIF-2 were cloned into pGEX-4T1 vector (Fig. 6) using the restriction enzymes EcoRI and XhoI using the following corresponding primer pairs: mouse MIF forward 5'-GCGAATTC-ATGCCTATGTTCATCGTG-3' and reverse 5'-GCCTCGAG-AGCGAAGGTGGAACCGTT-3'; mouse MIF-2 forward 5'-GCGAATTC-ATGCCATTCGTTGAGTTG-3', reverse 5'-GCCTCGAG-CAGAAATGTCATGACAGT-3'. High pure PCR product purification kit was used to purify PCR products from agarose following the manufacturer's protocol. After that, MIF and MIF-2 PCR fragments were ligated into the vector. After ligation, the generated plasmids were transformed into competent Escherichia coli (*E. coli*) DH5α and the positive clones were selected *via* plasmid miniprepation and subsequent colony PCR. The successfully cloned plasmids were then confirmed by sequencing and transformed into competent *E. coli* BL21 (DE3) for the recombinant protein expression.

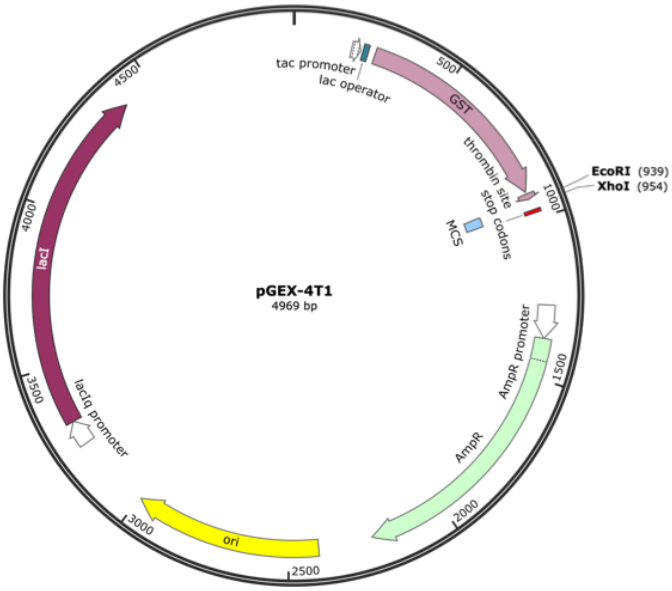

Fig. 6: Plasmid map of the pGEX-4T1 vector. pGEX-4T1 is one of the pGEX-series vectors with GST (N terminal) tag, tac promotor, thrombin protease cleavage site and ampicillin bacterial resistance.

2.2.12 GST-tagged protein expression and purification

After transformation with pGEX-4T1-GST-MIF, pGEX-4T1-GST-MIF-2 or pGEX-4T1 plasmid, Luria Bertani (LB) broth media with the ampicillin antibiotic were used to culture the *E. coli* (BL21) until OD_{600}=0.6-0.8 at 37°C. After that, 1 mM isopropyl-1-thio-β-D-galactopyranoside (IPTG) was added into LB media to induce protein expression for 3 h at 37 °C. Bacterial pellets were collected after centrifuging and lysed with ice-cold GST-lysis buffer. After centrifugation, the supernatant with recombinant proteins were incubated with glutathione sepharose 4B beads overnight at 4°C to purify GST-tagged proteins, following the manufacturer's protocol. After three times rinses with GST-washing buffer, the bead-bound GST-tagged proteins were analyzed in a sodium dodecyl sulfate-polyacrylamide gel electrophoresis (SDS-PAGE) with Coomassie blue staining or Western blotting using specific anti-MIF or anti-MIF-2 antibodies. After purification, recombinant proteins were stored at 4°C in order to perform further GST pulldown assay experiments. GST protein expressed by the empty pGEX-4T1 vector was used as a control.

2.2.13 GST pulldown assay

For the GST pulldown assay, beads-bound recombinant proteins (GST-MIF and GST-MIF-2) were incubated with the lysates of primary neuronal cells, BV-2 cells, or N2a cells. GST alone was used as a control. Briefly, cells used for this pulldown assay were lysed with cold Pierce™

IP lysis buffer (1% NP-40, 1 mM EDTA, 25 mM Tris-HCl, 150 mM NaCl and 5% glycerol) supplemented with protease inhibitor cocktail and 1mM PMSF, and subsequently incubated with GST-tagged proteins or GST overnight at 4°C. After incubation, the probes were washed for 5 times and afterwards mixed with NuPAGE™ lithium dodecyl sulphate (LDS) buffer supplemented with 1 mM dithio-threitol (DTT). The proteins were separated by 11% SDS-PAGE following by analyzing *via* Coomassie staining or Western blot using anti-AIF antibody.

2.2.14 Protein extraction and Western blot analysis

Primary neuronal cells or mouse brain tissue were lysed in cold RIPA lysis buffer which was supplemented with protease inhibitors. Bradford assay according to the manufacturer's protocol were used to measure protein concentration of the whole cell lysates. Cells or tissue lysates were then mixed with LDS/DTT sample buffer and boiled at 95°C for 15 min. The same amounts of protein were added into an 11% or 15% SDS-PAGE gel and followed by analyzing with Coomassie blue staining and/or Western blot analysis. For Western blot, the proteins were transferred on nitrocellulose membranes which were then blocked with 3% BSA in TBST, followed by incubating with the primary antibodies including anti-MIF, anti-MIF-2, anti-AIF or anti-β-actin at a dilution of 1:1000 in TBST containing 1% BSA overnight at 4°C. After washing, a secondary antibody conjugated with horseradish peroxidase (HRP) at a dilution of 1:10,000 were incubated for 1 h at room temperature. After rinse, Super Signal™ West Dura Extended Duration Substrate was used for detection, which was visualized and analyzed on the Odyssey® Fc Imaging System with Image Studio™ software, respectively. After densitometry analysis, the expression of target proteins is normalized to expression of β-Actin.

2.2.15 RNA extraction and qPCR

Trizol reagent was used to extract total RNA from primary neuronal cells or brain tissues. The RNA concentration was determined on Nanodrop Spectrophotometer. 1000 ng of RNA per reaction was used to perform reverse transcription with a first strand cDNA synthesis kit. The cDNA is diluted 1:5 for qPCR analysis, which is performed with sequence-specific primers for MIF, MIF-2, MIF receptors, inflammatory cytokines and β-actin on a Rotor-Gene Q 2 plex HRM using ORA™ SEE qPCR Green ROX L Mix. The qPCR results were analyzed by Rotor-Gene Q software. The expression of the housekeeping gene β-actin was used to normalize the expression of these target genes by calculating the comparative cycle time (CT) difference between tested gene and housekeeping gene (ΔCT) and the relative quantification of gene

expression were calculated via ΔΔCT by quantifying difference between control and treatment conditions [242]. Each time qPCR reactions were performed in duplicates.

2.2.16 Sandwich enzyme-linked immunosorbent assay (ELISA)

The concentration of MIF and MIF-2 protein in the supernatants of treated primary neuronal cells were measured *via* ELISA. MIF ELISA was performed as described previously [243,244]. Briefly, 96-well microplates (Nunc MaxiSorp™ flat bottom plate) were coated with 15 µg/ml capture antibody XIV.14.3(diluted in PBS) which is a monoclonal mouse anti-mouse MIF antibody, and incubated on a soft shaker overnight at 4°C. After 3 times rinses using TBST, plates were treated by blocking buffer under soft shaking for 2 h at room temperature, and standard (recombinant mouse MIF range from 0 to 200 ng/ml diluted in reaction buffer) and supernatant samples were applied for another 2 h incubation under the same condition. After three rinses, biotinylated anti-MIF antibody (detection antibody BAF289, 200 ng/ml in reaction buffer) was added and incubated for 2 h. After washing and incubation with streptavidin-POD conjugate (1:10 000 in TBS) for 20 min, the color reaction was determined by Pierce™ TMB substrate kit following the manufacture's introductions (1:1 mixture of H_2O_2 and tetramethylbenzidine (TMB)). After 20 min incubation, 2 M H_2SO_4 was added to stop the reaction and the plates were subjected to detection at 450 nm on the microplate reader Enspire. Similarly, MIF-2 levels were measured by ELISA with homemade capture and detection anti-mouse MIF-2 antibodies respectively. All the measurements were performed in duplicates.

2.2.17 Flow cytometry

The expression levels of MIF receptors on the cell surface of BV-2 cells were verified *via* flow cytometry. Briefly, BV-2 cells were detached gently with cell scraper after washing with cold PBS. After centrifuging, the cells were washed with cold flow cytometry buffer (0.5% BSA in PBS). After that, an antibody cocktail comprising FITC-conjugated anti-CD74, APC-Cy7-conjugated anti-CXCR2, PE-conjugated anti-CXCR4 and APC-conjugated anti-CXCR7 was added to the cells and stained in the dark for 1 h at 4°C. After rinsing with cold flow cytometry buffer, the probes were analyzed on the flow cytometer (BD FACSVerse™) and quantified using FlowJo software.

2.2.18 Immunofluorescence

To conform the efficiency of primary neuronal cells isolation, a neuronal marker anti-β-Tubulin III antibody was used to stain the cells. Briefly, primary neuronal cells were cultured on 12-mm glass coverslips for 10-13 days. After aspirating the culture medium and washing with PBS, PBS containing 4% paraformaldehyde was used for fixation and incubated for 20 min. After washing, PBS containing 0.1% Triton X-100 were used to permeabilize cells for 15 min. After that, the cells were washed with PBS and blocked with 5% goat serum for 1 h at room temperature. Subsequently, the cells were incubated with the primary antibody mouse anti-β-tubulin III (neuronal) overnight at 4°C, with a dilution of 1:200 in PBS containing 3% goat serum. After washing, Alexa Fluor 555 goat anti-rabbit IgG secondary antibody (1:500 in 3% goat serum) was added to the cells and incubated for 1 h. Nuclear counterstain was performed *via* using mounting medium containing DAPI (4'- diamidino-2-phenylindole) (VECTASHIELD® Antifade). To exclude unspecific signal generated by secondary antibody and check the specificity of the primary antibodies, control samples were stained as mentioned above but without the primary antibody. Samples were imaged on the fluorescence microscope Leica DMi8 and Leica Application Suite X software was used to analyze the acquired images.

2.2.19 Statistical analysis

Statistical analysis was performed using Student's t-test or one-way ANOVA with Tukey's multiple comparisons test as post-test. All the data are expressed as the mean ± standard deviation (SD) from more than three independent experiments. P values < 0.05 are considered statistically significant. Statistically significant differences are indicated by asterisks: *P<0.05; **P<0.01; ***P<0.001; ****P<0.0001.

3. RESULTS

3.1 Characterization of new binding partner of MIF and MIF-2 in the brain

3.1.1 Cloning and purification of GST-tagged proteins GST-MIF and GST-MIF-2

As mentioned in the introduction, the interaction between MIF and AIF was recently identified to initiate the nuclease activity of MIF which is required for cell death [159]. To date, the function and the binding partner(s) of MIF in brain have been poorly investigated. Therefore, I first aimed to confirm the binding between MIF and AIF, asked whether MIF-2 would also interact with AIF, and searched for new binding partners of MIF or MIF-2 in brain.

To answer this question, I used GST pulldown assay with recombinant GST fusion proteins of MIF and MIF-2. Fig. 7A shows the schematic overview of the cloning, expression and purification of these GST-tagged proteins. I first generated pGEX-4T1-GST-MIF and pGEX-4T1-GST-MIF-2 plasmids through cloning of the mouse MIF/MIF-2 cDNA insert into the pGEX-4T1 vector (Fig. 7A, B, and C). To check the expression of the related recombinant proteins, these plasmids were transformed into competent *E. coli* BL21 (DE3) after DNA sequencing, using empty vector (pGEX-4T1 vector) as a negative control. After IPTG-mediated induction, the bacteria were lysed, and protein expression analyzed by SDS-PAGE gel electrophoresis followed by Coomassie blue staining. As expected, both GST-tagged MIF and MIF-2 as well as GST alone were highly expressed after 3 h stimulation (Fig. 7D). After successful expression, Glutathione Sepharose 4B beads were used to purify GST-tagged proteins and enrichment confirmed by both SDS-PAGE/Coomassie blue staining and Western blot using specific anti-MIF or anti-MIF-2 antibody (Fig. 7E, F, and G). To conclude, GST-MIF and GST-MIF-2 were successfully cloned and purified.

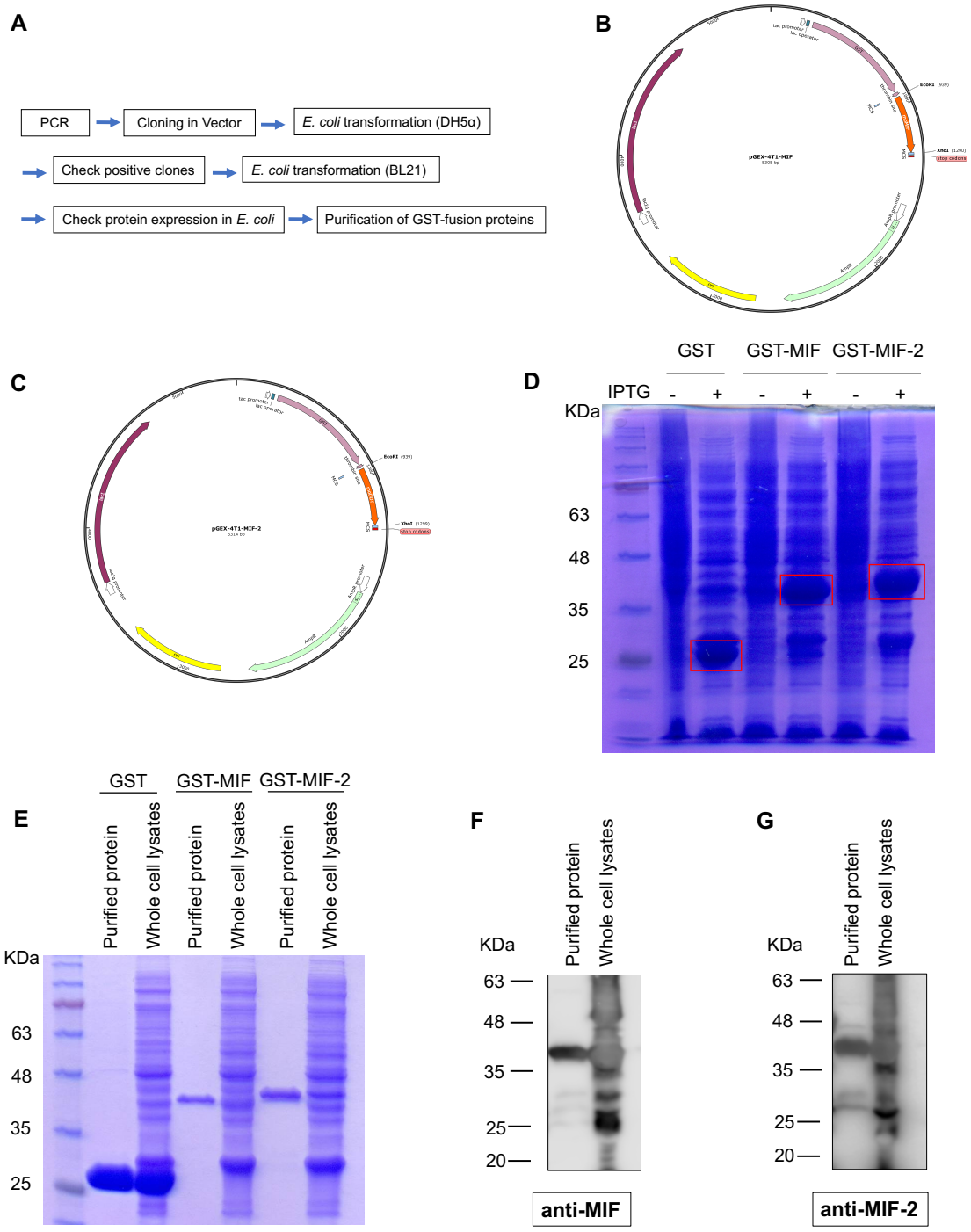

Fig. 7: Cloning and purification of GST-tagged proteins GST-MIF and GST-MIF-2. A, Schematic overview of cloning strategy, expression and purification of GST-tagged proteins GST, GST-MIF and GST-MIF-2. **B-C,** Plasmid map of the generated plasmids pGEX-4T1-GST-MIF and pGEX-4T1-GST-MIF-2. **D,** Coomassie staining of expressed GST-tagged proteins in *E. coli* (BL21) after induction with IPTG. **E,** Purification of GST-tagged proteins with Glutathione Sepharose beads using the whole bacteria cell lysates as control. **F-G**, Confirmation of purified GST-MIF and GST-MIF-2 on Coomassie blue (**E**) and Western blot using anti-MIF (**F**) as well as anti-MIF-2 antibody (**G**). The experiments shown in **D-G** are representative of 9-10 experiments performed.

3.1.2 Analysis of the MIF/AIF interaction and novel potential MIF partners in brain

After successful expression and purification of recombinant GST-tagged proteins, I set out to search for novel binding partners of both MIF and MIF-2 in neuronal cells and microglia cells.

To address this question, first the isolation of primary neuronal cells from the early postnatal (P0-P1) mouse cortex was established. Fig. 8A shows the overview of this technique. After isolation and cultured for 10 days, the cortical neurons were incubated with anti-β-tubulin III antibody (a neuronal marker) followed by a fluorescence-labeled secondary antibody to confirm the efficiency of primary neurons isolation. As illustrated in Fig. 8B, more than 80% of the cultured cells were neuronal cells, which is also in line with previous publications [245,246].

Therefore, after establishing the primary neuron isolation procedure, GST pulldown assay was performed with purified GST-MIF, GST-MIF-2 and cell lysates of primary neuronal cells isolated from C57BL/6 mice, the mouse neuronal cell line N2a, and the mouse microglia cell line BV-2. GST was used to be the negative control. After incubation and subsequent intensive bead washing, bound protein fractions were loaded to SDS-PAGE and analyzed by Coomassie staining. Interestingly, a band of ~ 54 kDa was observed in pulldowns of both GST-MIF and GST-MIF-2 but not in the GST alone control in lysates from primary neuronal cells, N2a lysates, and BV-2 lysates, indicating a potentially novel and common interacting partner protein of both MIF and MIF-2 in neurons and microglial cells (Fig. 8C). The identification of this band as well as other novel MIF- or MIF-2-binding proteins by mass spectroscopy was pending at the time this thesis was completed. Notably, this ~ 54 kDa band cannot be AIF, because of the molecular weight of AIF is 67 kDa.

Although AIF was apparently not pulled down as a MIF- or MIF-2- interacting protein in the above unbiased GST pulldown approach, I next used a specific GST-pulldown approach to examine whether AIF binds to MIF or to MIF-2 in my employed cell systems. After pulldown, bound protein fractions were again separated by SDS-PAGE, but this time detected by immunoblotting with an established anti-AIF antibody. However, contrary to the previously reported interaction between MIF and AIF, no anti-AIF-immunoreactive band was observed, neither in primary neurons nor the N2a cell line. (Fig. 8D).

To conclude, although the interaction of MIF and AIF was not observed, my GST pulldown experiments indicate that there is at least one potentially novel binding partner of MIF and MIF-2 with a size of ~ 54 kDa, which deserves in-depth follow up studies including mass spectrometry sequencing and functional follow up analysis.

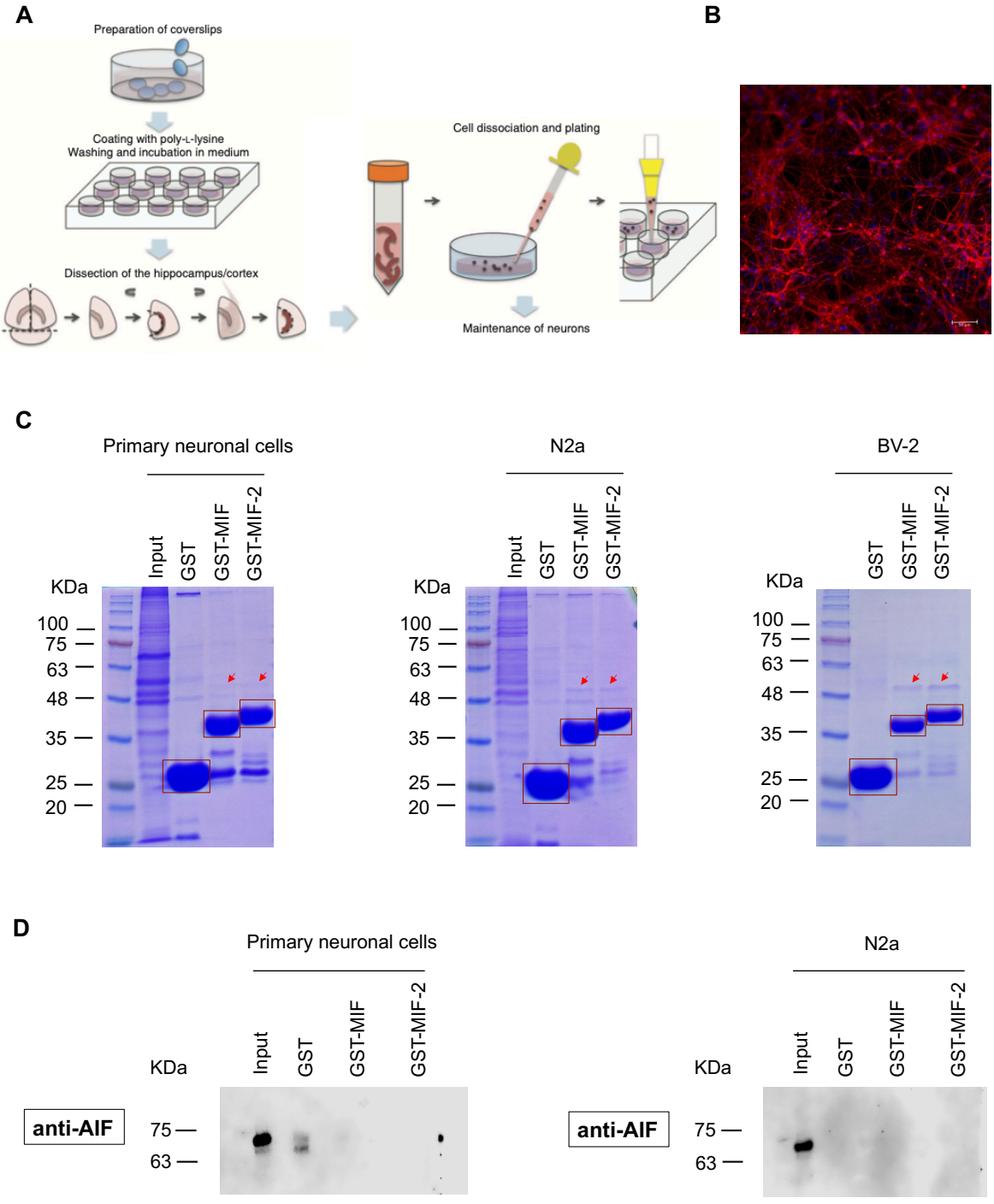

Fig. 8: Investigation of novel binding partner of MIF and MIF-2 in brain using GST-Pulldown assay. **A,** Scheme of primary neuronal cell isolation [240]. **B,** After cultured for 10 days, primary cortical neurons were stained with anti-β-tubulin III antibody and fluorescence-labeled secondary antibody (red). Nucleus

were presented as blue by staining with DAPI. The images were acquired with fluorescence microscopy and scale bar is 50 μm. **C,** To perform GST pulldown, purified fusion proteins GST, GST-MIF and GST-MIF-2 were incubated with cell lysates of primary neuronal cells, neuronal N2a cell line, and microglia cell line BV-2 cells. After subsequent beads washing, bound proteins were separated by SDS-PAGE and detected by Coomassie staining. Red arrows indicate a novel band observed in GST-MIF and GST-MIF-2 pulldown. **D,** GST pulldown assay were performed as described in (**B**) using cells lysates of primary neuronal cells and N2a cells respectively, and the probes were analyzed by Western blot with anti-AIF antibody.

3.2 The MIF/CD74 axis is involved in cell death of primary neuronal cells under OGD

3.2.1 MIF is upregulated in primary neuronal cells after OGD treatment

Previous studies have shown the controversial data on exacerbating *versus* protective roles of MIF in experimental ischemic stroke models [212,214,215]. To clarify the causal role of MIF proteins in ischemic stroke as well as the underlying mechanisms, I started out performing *in vitro* studies and asked, what is the effect of MIF on neuronal cell fate under ischemic stress? Fig. 9A shows a schematic overview of the experimental design.

To address this question, I first sought to investigate whether the expression and secretion of MIF proteins could be altered by hypoxic stress. Therefore, primary cortical neuronal cells isolated from C57BL/6 mice as described above were subjected to an "*in vitro* ischemia/reperfusion" treatment regimen, which using the oxygen glucose deprivation (OGD) model. Briefly, after 4 or 8 h OGD treatment followed by an additional 24 h of normoxic incubation, protein expression of MIF in these cells were analyzed by Western blot using anti-MIF antibody. Primary neuronal cells that were not subjected to OGD treatment were used to be control group. As shown in Fig. 9B and C, a significant upregulation of MIF protein expression in primary neurons after OGD treatment was observed, with an increase of 2.29 ± 0.40-fold ($P<0.01$) after 4 h and 3.19 ± 0.42-fold ($P<0.001$) after 8 h in comparison to the control group. Intriguingly, there was a second MIF-reactive band of a slightly higher molecular weight appearing in the Western blot result of lysates from cells under OGD stress (Fig. 9B), indicating that MIF may be post-translationally modified under hypoxic conditions.

After observing that the protein expression of MIF was upregulated in primary neurons under hypoxia stress, I next analyzed the transcriptional levels of MIF. Therefore, primary neuronal cells were treated with OGD stress as described above and mRNA expression of MIF analyzed

by qPCR. Cells that were not subjected to OGD treatment were used to be control group. As shown in Fig. 9D, OGD stress caused a significant upregulation of MIF mRNA expression in primary neurons, as indicated by an increase of 1.97 ± 0.51-fold ($P<0.05$) at OGD 4 h treatment and 2.32 ± 0.80-fold ($P<0.01$) at 8 h treatment, respectively. These results indicate that both protein and mRNA expression of MIF are enhanced after OGD treatment (Fig. 9B, C and D).

Up to now, the role of MIF-2 in ischemic stroke has not been studied yet. Therefore, in addition to MIF, the mRNA expression of MIF-2 in primary neuronal cells after OGD stress was also examined. Interestingly, a decreasing tendency was observed for MIF-2 mRNA level at both 4 h (0.7 ± 0.36-fold) and 8 h (0.7 ± 0.31-fold) OGD treatment compared to the control group (Fig. 9E). This could be an initial hint that MIF and MIF-2 may have different functions in this model.

As shown above, OGD treatment increased both protein and mRNA expression of MIF in primary neuronal cells. To further explore whether hypoxia stress could alter the secretion of MIF proteins, primary neuronal cells were treated with OGD stress as described above, and the conditioned media were collected to analyze the concentration of MIF using ELISA. Cells that were not subjected to OGD treatment were used to be control group. As illustrated in Fig. 9F, the increase of MIF protein expression triggered by OGD stress also coincided with the pattern of MIF protein secretion, while no obvious difference was observed in MIF concentration in the conditioned supernatants after reperfusion. Besides MIF, the secretion of MIF-2 in primary neurons after OGD stress was also examined and showed an increasing tendency both after OGD treatment and after reperfusion (Fig 9.G).

To conclude, these results suggest that OGD stress increases both mRNA and protein expression of MIF in primary neuronal cells, while MIF-2 mRNA expression seems to be decreased. In addition, the secretion of both MIF and MIF-2 was found to be upregulated by OGD stress.

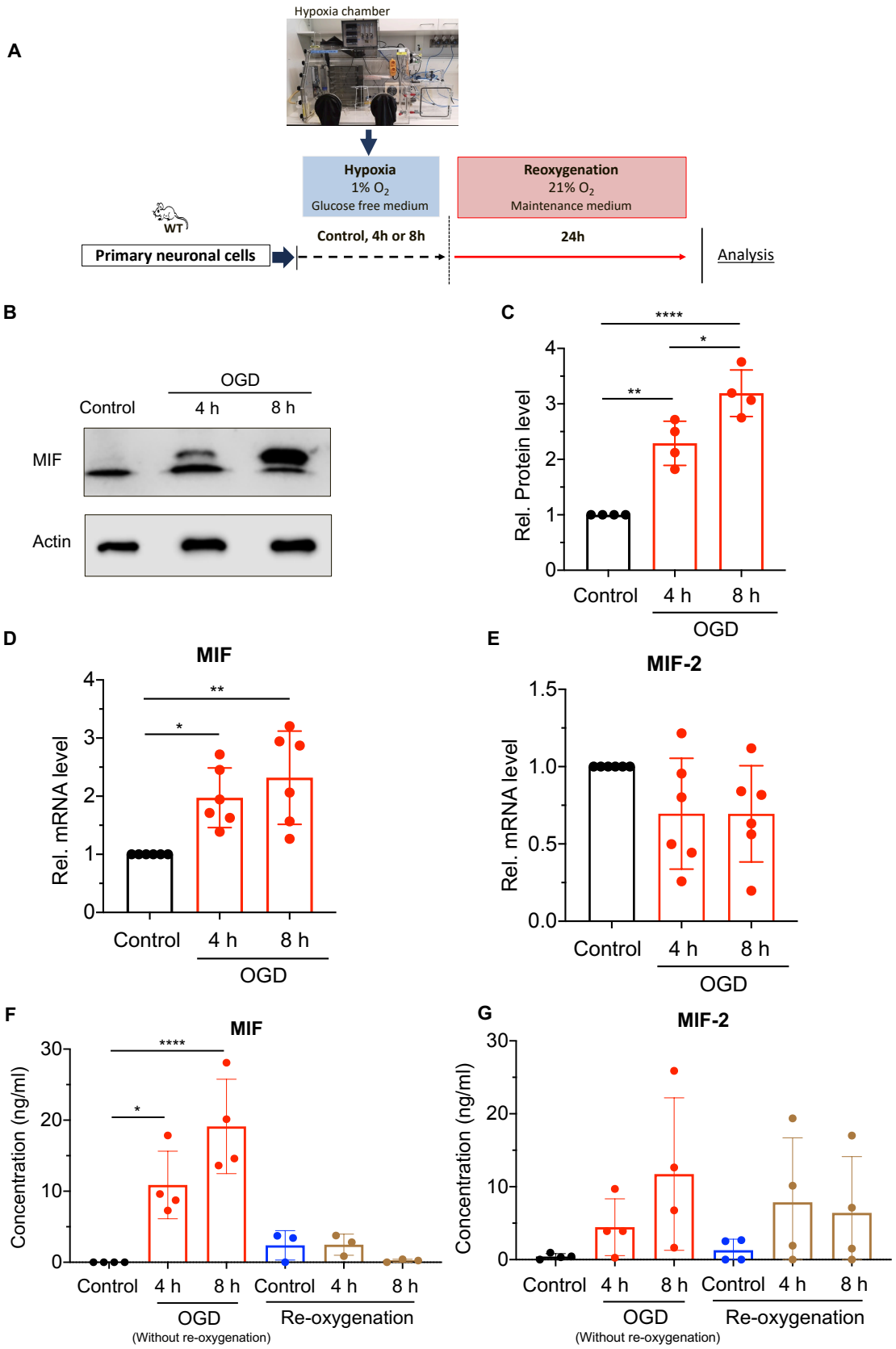

Fig. 9: OGD stress increases the expression and secretion of MIF in primary neuronal cells. Primary neuronal cells isolated from C57BL/6 mice were treated in an *in vitro* hypoxic environment, which was

created by OGD stress. Neuronal cells without hypoxia treatment were used as control. **A**, Schematic overview of the experimental design. **B**, Cells were lysed after treatment and analyzed with SDS-PAGE followed by Western blot with anti-MIF and anti-β-actin antibody. **C**, The graphs show the quantified results from (**B**). The intensity of target protein was normalized to β-actin and the resultant value was plotted as relative protein level. **D-E**, After OGD treatment, mRNA expression of MIF and MIF-2 in primary neuronal cells were analyzed by qPCR. Relative mRNA levels were obtained by normalizing to β-actin. **F-G**, Media were collected from OGD-treated neuronal cells and the concentration of MIF (**F**) and MIF-2 (**G**) were quantified with ELISA. Data are reported as means ± SD of (n=4 (**C**); n=6 (**D**); n=6 (**E**); n=3-4 (**F**); and n=4 (**G**)) independent experiments. Statistical analysis was performed with one-way ANOVA with Tukey's multiple comparisons test (*P<0.05, **P<0.01, ****P<0.0001).

3.2.2 Hypoxia regulates the expression of MIF receptors in primary neuronal cells

Previous experiments suggested that hypoxia altered the expression and secretion of MIF proteins in primary neuronal cells. I next checked whether hypoxic stress would modulate the expression of MIF receptors. To address this question, neuronal cells isolated from C57BL/6 mice were subjected to 4 or 8 h OGD treatment as described above and the mRNA expression of the MIF receptors were analyzed by qPCR using respective specific primers. Neuronal cells without hypoxia treatment were used as control.

Although no significant difference was achieved for the mRNA level of CD74 in cells under OGD stress, as shown in Fig. 10A, a trend towards an upregulation was noted after 4 h of OGD treatment (to 1.58 ± 1.12-fold, P=ns). For the receptor CXCR2, as illustrated in Fig. 10B, OGD stress led to a time-dependent upregulation of its mRNA level in primary neuronal cells, which was significant at 8 h (4 h OGD: 1.69 ± 1.11-fold; 8 h OGD: 16.11 ± 18.56-fold, P<0.05), compared to control. Interestingly, unlike CD74 and CXCR2, the mRNA level of CXCR4 was found to be downregulated after 4 h (to 0.62 ± 0.56-fold) and 8 h (to 0.48 ± 0.22-fold, P<0.05) of OGD stress (Fig. 10C).

These data indicated that hypoxia stress regulates the expression of MIF receptors in primary neurons; it upregulates the expression of CXCR2 (with a trend for CD74), but downregulates CXCR4 expression, indicating a differential regulatory role of the MIF/CXCR2 and MIF/CXCR4 axes under those conditions.

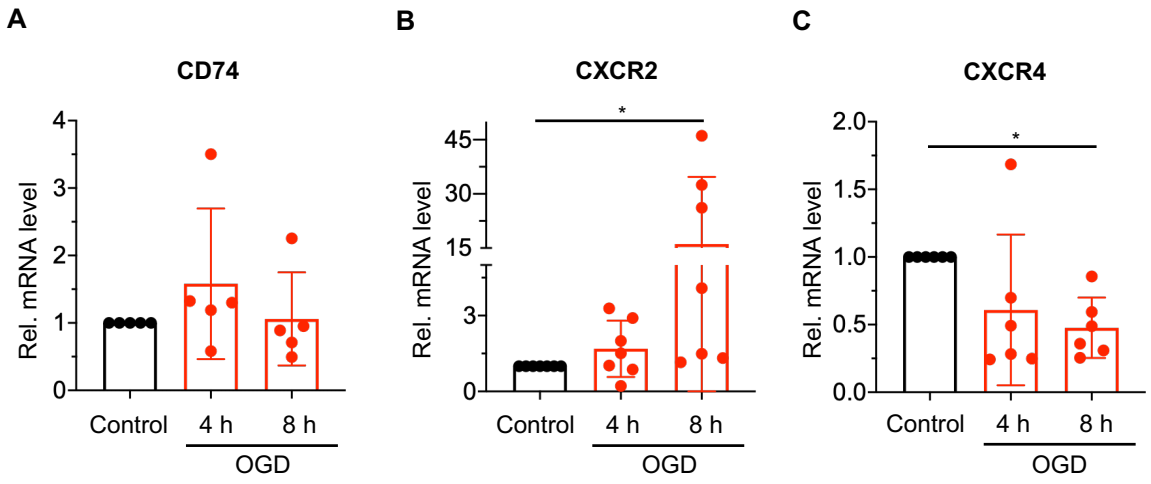

Fig. 10: **OGD stress dysregulates the expression of MIF receptors in primary neuronal cells.** Primary neuronal cells isolated from C57BL/6 mice were treated by OGD stress. Neuronal cells without hypoxia treatment were used as control. **A-C**, After OGD treatment, mRNA expression of MIF receptors-CD74 (**A**), CXCR2 (**B**) and CXCR4 (**C**) in primary neuronal cells were analyzed by qPCR. Relative mRNA levels were acquired by normalizing the values with mRNA level of β-actin. Data are reported as means ± SD of (n=5 (**A**); n=7 (**B**); n=6 (**C**)) independent experiments. Statistical analysis was performed with one-way ANOVA with Tukey's multiple comparisons test (*P<0.05).

3.2.3 *Mif* or *Cd74* deficiency protects primary neuronal cells under OGD treatment

As shown above, hypoxia stress affects both the expression and secretion of MIF as well as the expression of the MIF chemokine receptors in primary neuronal cells. To further examine the functional impact of dysregulated MIF on neuronal cells under hypoxia stress, I tested the cell viability of the primary neurons in the presence or absence of MIF after OGD treatment. Therefore, primary neuronal cells were isolated from *Mif* $^{-/-}$ *mice* and subjected to OGD treatment as before, and the cell viability was analyzed by comparing to cells isolated from C57BL/6 WT mice using the CCK-8 cell viability assay. As shown in Fig.11, OGD stress affected cell viability of cells isolated from WT mice in a time-dependent manner. Depletion of *Mif* showed a protective effect after 4 h of OGD treatment when compared to WT cells (69.30 ± 17.36%-vs. 49.59 ± 13.56%, P<0.05).

As mentioned in the introduction, it was recently reported that the treatment with the partial MHC class II/peptide construct RTL1000 reduces infarct volume in an MCAO model, partly via competitively inhibiting the MIF/CD74 signaling pathway [219,220]. However, the direct involvement of CD74 in cerebral infarction has been not examined. After showing that

deficiency of *Mif* protected neuronal death from hypoxia stress, I next investigated whether the depletion of *Cd74* is involved in neuronal cell viability. To address this question, neuronal cells isolated from *Cd74* $^{-/-}$ mice were subjected to OGD treatment, and the cell viability was analyzed by comparing to cells isolated from WT mice as before. Interestingly, deficiency of *Cd74* also significantly increased the cell viability under OGD stress, which is increased to 85.54 ± 29.40% compared to 49.59 ± 13.56% in WT cells ($P<0.01$) after 4 h and to 32.04 ± 21.79% -vs. 13.29 ± 6.86% in WT cells ($P<0.05$) after 8 h OGD treatment (Fig. 11).

Taken together, these data indicated that the MIF/CD74 axis may work as a key regulator in the survival of neuronal cells under OGD stress.

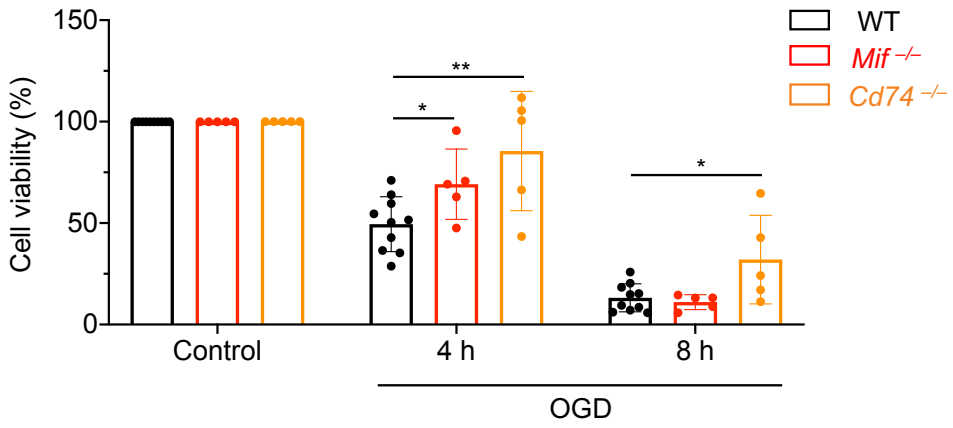

Fig. 11: *Mif* or *Cd74* deficiency has a protective effect on primary neuronal cells under OGD treatment. Primary neuronal cells isolated from WT, *Mif* $^{-/-}$ and *Cd74* $^{-/-}$ mice were subjected to OGD treatment and the cell viability were analyzed by using CCK-8 kit. The cell viability of neurons from these three different genotypes was reported as percentage of control condition respectively and analyzed by comparing cells isolated from *Mif* $^{-/-}$ and *Cd74* $^{-/-}$ mice to cells isolated from WT mice after 4 or 8 h OGD treatment. Data are reported as means ± SD of independent experiments (n=5-10). Statistical analysis was performed with unpaired T-test (*$P<0.05$, **$P<0.01$).

3.3 Hypoxia regulates the expression of MIF receptors in BV-2 microglial cells

After revealing the role of MIF proteins in primary neuronal cells under hypoxia stress demonstrating an increase of MIF secretion and dysregulation of MIF receptors expression, I next sought to explore whether hypoxia stress regulates the expression of MIF receptors in

microglial cells, which work as key mediators in the pathophysiological process of neuroinflammation in ischemic stroke.

To answer this question, mouse BV-2 microglial cell line was subjected to OGD stress over 24 h and the expression of MIF receptors analyzed *via* flow cytometry. Cells which were not subjected to hypoxia stress were used as control.

As illustrated in Fig. 12 A and E, no significant difference in CD74 cell surface expression was observed under OGD treatment compared to the control. Interestingly, OGD stress increased the expression of CXCR2 (Fig. 12B and F) and a significant difference was seen *via* analyzing the mean fluorescence intensity (MFI) between control and OGD group (903.70 ± 494.90-vs. 53975.00 ± 29208.00, $P<0.01$) (Fig. 12F). In addition, CXCR7 was also significantly upregulated under OGD stress (Fig. 12D and H), with MFI 251.50 ± 8.90 in control group -vs. 610.50 ± 123.80 in OGD group ($P<0.0001$). Noteworthy, an opposite effect was seen for CXCR4 expression, which was reduced by ODG stress (Fig. 12C, G), with an MFI 1304.00 ± 94.00 of control group -vs. 737.50 ± 146.80 of OGD group ($P<0.0001$). The changes of MIF receptor expression in BV-2 microglia cells under hypoxia treatment are overall consistent with the findings seen in primary neuronal cells (Fig. 10).

To conclude, these data demonstrated that OGD stress regulates MIF receptors expression in BV-2 microglial cells. No difference was observed for CD74 cell surface expression, while CXCR2 and CXCR4 were significantly enhanced and reduced, respectively, showing an opposite expression pattern in BV-2 cells. While mRNA expression levels were not measured in BV-2 cells, these results are overall in line with the hypoxia-induced dysregulation of MIF receptors in primary neuronal cells.

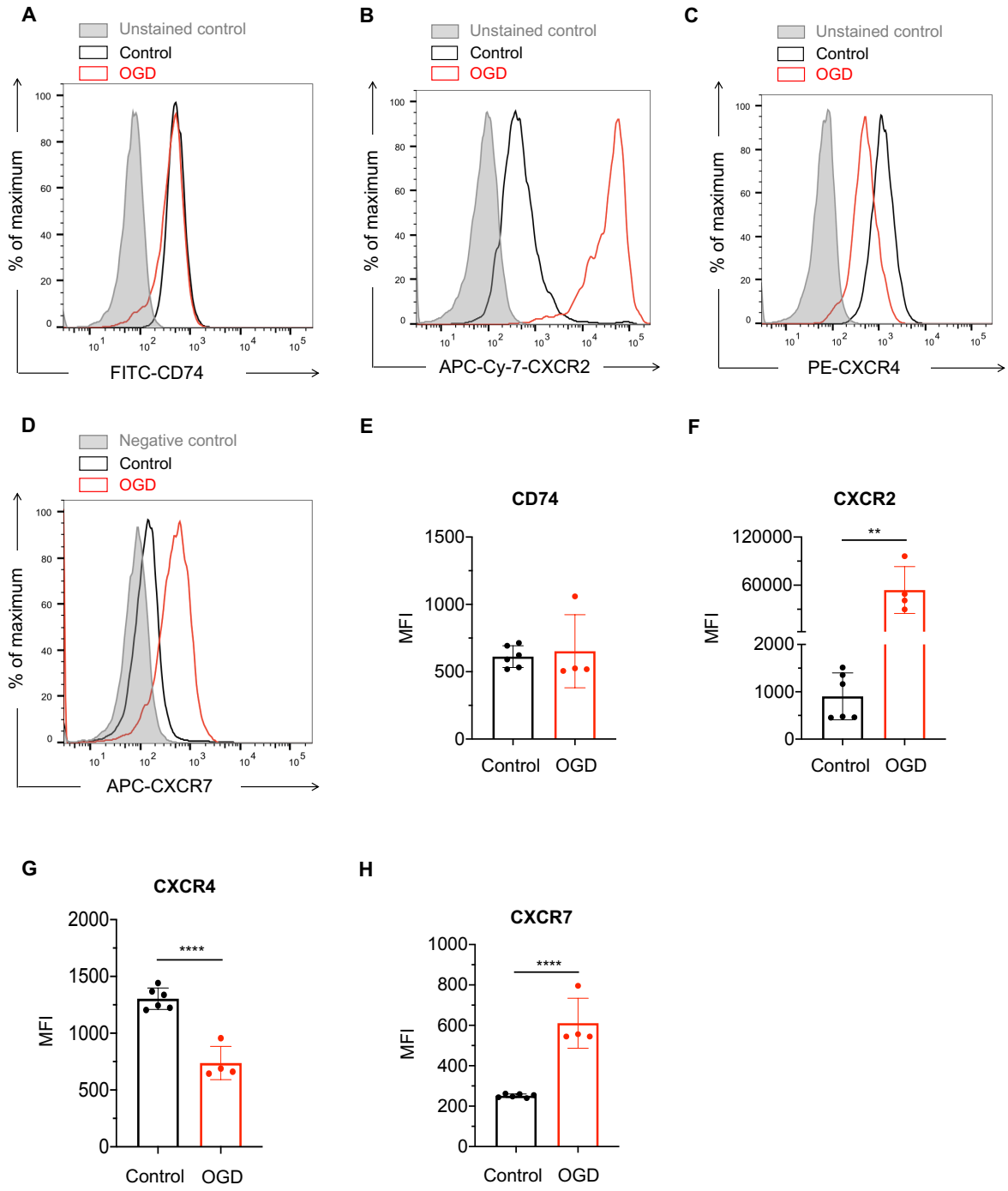

Fig. 12: OGD stress regulates MIF receptors cell surface expression in BV-2 microglial cells. BV-2 cells were subjected to 24 h OGD treatment, and the cells without hypoxia treatment were used as control. **A-D**, MIF receptors-CD74 (**A**), CXCR2 (**B**), CXCR4 (**C**) and CXCR7 (**D**) cell surface expression were analyzed *via* flow cytometry. Gray shaded area represents unstained control. **E-F**, Analysis of median fluorescence intensity (MFI) of each receptor between OGD stress and control condition. Data are reported as means ± SD of (n=4-6 (**B-F**)) independent experiments. Statistical analysis was performed with unpaired T-test (**P<0.01, ****P<0.0001).

3.4 Effect of *Mif* deficiency in a mouse model of experimental ischemic stroke

As shown above, our *in vitro* studies demonstrated that *Mif* depletion showed a protective effect in neurons and the MIF/CD74 axis may drive its regulation under hypoxic stress. Additionally, hypoxia regulates MIF receptor expression in both neuronal cells and microglial cells. To further explore the *in vivo* relevance of those findings, I investigated if genetic ablation of *Mif* in mice is protective in an experimental ischemic stroke model.

To address this question, *Mif*$^{-/-}$ mice with WT littermates as controls were used in an ischemic stroke model, which was induced by 1 h MCA occlusion followed by 24 h reperfusion. As previous studies had reported that the effect of MIF in ischemic stroke may be gender-dependent [212,214], mice in both gender were used in this thesis. Fig. 13A shows a schematic overview of the *in vivo* MCAO experimental design.

Firstly, CBF parameters were measured by laser doppler during the operation to confirm MCA occlusion efficiency. As expected essentially all mice exhibited a reduction in CBF to less than 20% of the baseline value (Fig. 13B). Mice were sacrificed after MCA occlusion followed by reperfusion, and infarct volume analyzed by Nissl staining. As shown in Fig. 13C, a clear difference in infarct volume was seen between WT littermate and *Mif*$^{-/-}$ mice. Furthermore, the quantification revealed a tendency that *Mif* depletion is protective in both male mice (66.92 ± 29.58 mm^3 of *Mif*$^{+/+}$ group-vs. 57.68 ± 28.95 mm^3 of *Mif*$^{-/-}$ group) and female mice (68.51 ± 20.04 mm^3 of *Mif*$^{+/+}$ group-vs. 50.47 ± 22.93 mm^3 in *Mif*$^{-/-}$ group), and this effect is even clearer when both genders were analyzed together (67.56 ± 25.78 mm^3 in *Mif*$^{+/+}$ control group vs. 54.97 ± 26.29 mm^3 in *Mif*$^{-/-}$ mice (Fig. 13D). Although these observed differences failed to reach statistical significance (P=0.54 (male); P=0.14 (female); P=0.13 (both genders)), these results suggested that *Mif* deficiency is protective in both genders of mice in ischemic stroke.

In addition to infarct volumes, a rough behavior test called “Neuroscore” was performed to evaluate neurological deficits after 1 h MCA occlusion as well as 24 h reperfusion. As shown in Fig. 13E, F and G, after 1 h occlusion, no difference was seen in neurological score in *Mif*$^{-/-}$ mice in comparison to WT mice in both male (Fig. 13E) and female (Fig. 13F) mice as well as in the cumulative analysis (Fig. 13G), arguing that the MCAO model in these mice actually works reliably. However, after 24 h reperfusion, the results showed all mice improved and *Mif*

$^{-/-}$ mice showed a clear trend towards a protective impact in both male and female mice (Fig 13E and F), likewise in the cumulative analysis (Fig. 13G).

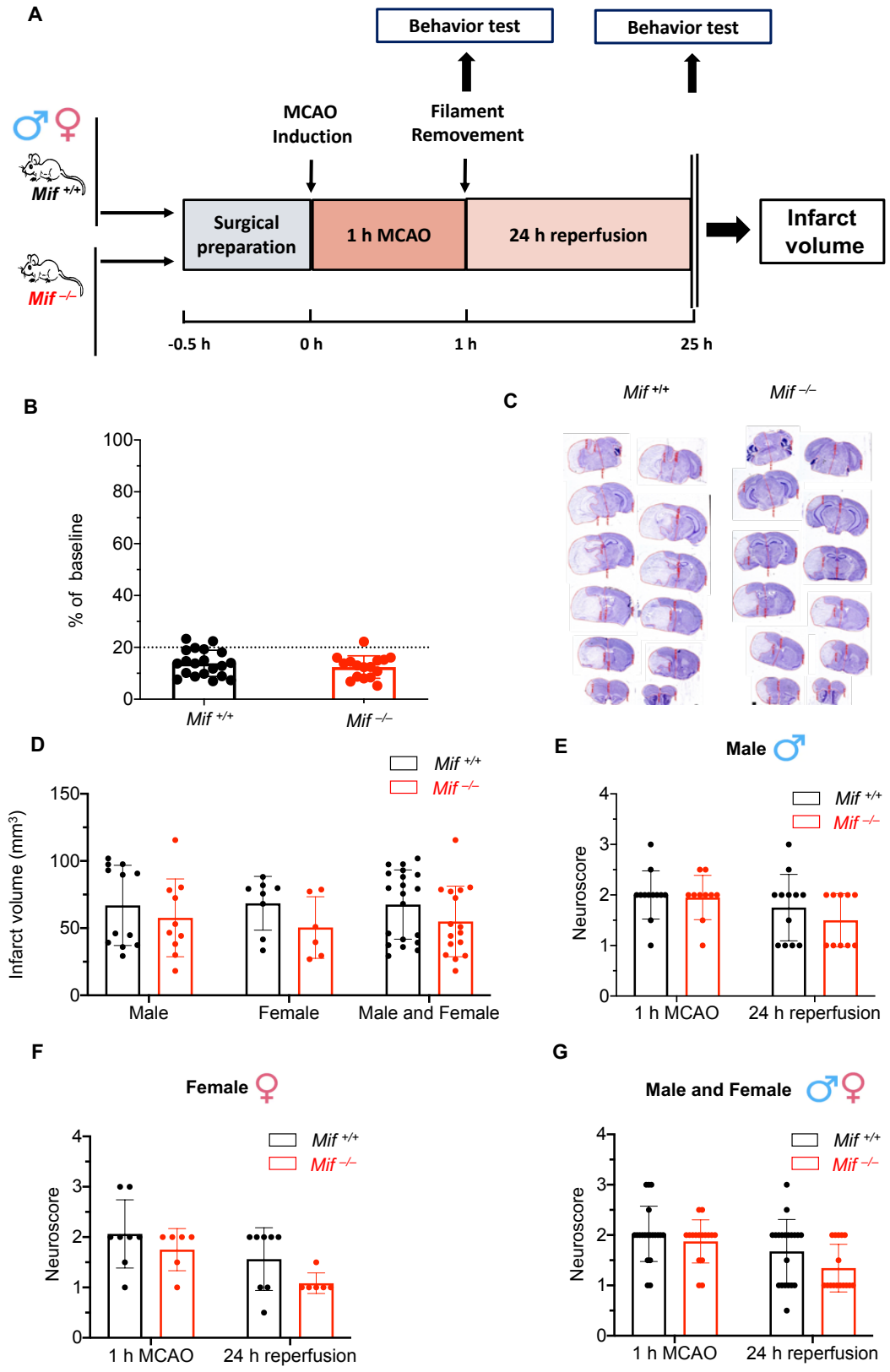

Fig. 13: MIF deficiency reduces the infarct volume and post-stroke neurological deficits after transient MCAO (*trend*). **A,** Ischemic stroke was induced in an *in vivo* model by MCAO for 1 h and 24 h reperfusion using *Mif* $^{-/-}$ mice and WT littermates as control. **B,** CBF parameters were measured by laser doppler during the operation to confirm sufficient MCA occlusion efficiency. **C**, After MCAO model, the infarct volume was analyzed by Nissl staining. **D,** The graph shows the quantification of corrected infarct volume in male (n=10-12), female (n=6-8) and cumulative analysis (n=16-20). **E-F,** Neurological deficits of the mice were evaluated by Neuroscore after 1h MCAO and after 24h reperfusion in male (**E**), female (**F**) and cumulative analysis (**G**). Data are reported as means ± SD of (n=16-20 (**B**); n=6-20 (**D**); n=10-12 (**E**); n=6-8 (**F**); n=16-20 (**G**)) independent experiments. Statistical analysis was performed with unpaired T-test and/or Mann Whitney test as appropriate.

With the aim of checking whether the *Mif*-KO genotype alters the cerebral vascular anatomy that may influence the infarct volume after ischemic stroke, I visualized the whole vessel system via ink perfusion analysis in both *Mif* $^{-/-}$ and *Mif* $^{+/+}$ mice, and subsequently characterized the plasticity of the bilateral posterior communicating artery (PcomA) (Fig. 14A and B) and MCA-territory (Fig. 14B). As shown in Fig. 14B, *Mif* $^{-/-}$ mice had better formed PcomAs on the right side (contralateral side) compared to WT mice (1.43 ± 0.38 of *Mif* $^{+/+}$ group-vs. 2.43 ± 0.53 of *Mif* $^{-/-}$ group, P<0.001). Of note, no differences were seen in the left PcomAs of the same mice (ipsilateral side) (1.50 ± 0.87 of *Mif* $^{+/+}$ group-vs. 1.21 ± 0.53 of *Mif* $^{-/-}$ group, P=0.54). Interestingly, the comparison of bilateral MCA-territory in both genotypes showed no changes (right: 40.56 ± 3.48% of *Mif* $^{+/+}$ group-vs. 40.77 ± 2.73 of *Mif* $^{-/-}$ group, P=0.91; left: 44.99 ± 2.71% of *Mif* $^{+/+}$ group-vs. 45.84 ± 2.17 of *Mif* $^{-/-}$ group, P=0.54, Fig. 14C).

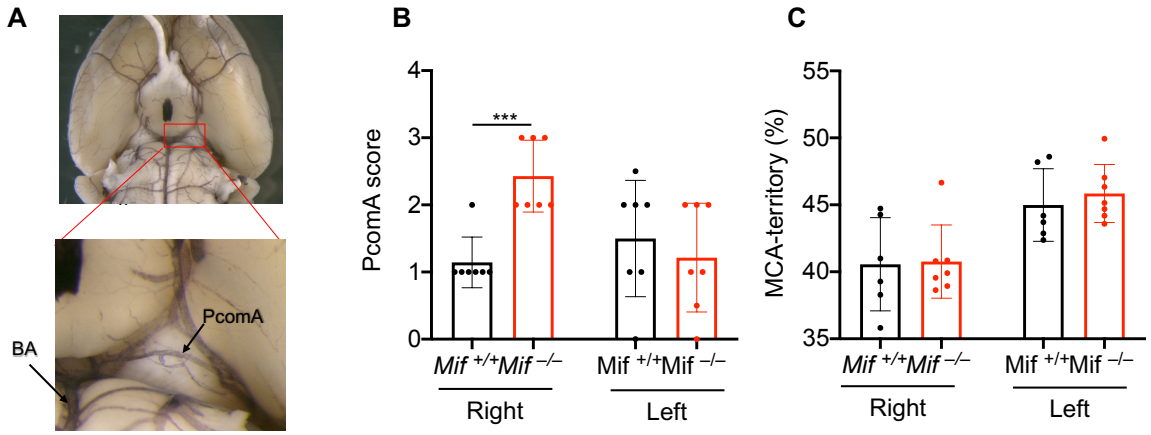

Fig. 14: Posterior communicating artery anatomy and MCA-territory in WT versus *Mif* $^{-/-}$ mice. A, Circle of Willis and the position of PcomA labeled with ink solution. Arrows: BA, basilar artery; PcomA,

posterior communicating artery. **B,** Right and left PcomA scores between WT and *Mif*$^{-/-}$ mice. **C**, Right and left MCA-territory between WT and *Mif*$^{-/-}$ mice. The data was reported as percentage of MCA-territory area compared to the corresponding hemisphere area. Data are reported as means ± SD of (n=6-7 (**B**); n=6-7 (**C**)) independent experiments. Statistical analysis was performed with unpaired T-test (***P<0.001).

Taken together, *Mif* deficiency was associated with a protective effect in the MCAO model in both genders (trend), which is in line with the *in vitro* OGD-stressed primary neuronal cells data shown above, while confounding effects of an altered plasticity of the vessel anatomy cannot currently be excluded. Further data points need to be obtained to exclude such potential effects as indicated by the uneven distribution of data points in the *Mif*$^{-/-}$ group.

3.5 Expression of MIF and MIF-2 are downregulated in the ipsilateral hemisphere after MCAO

Although only trends, the above results indicated that *Mif*-deficient mice would have a protective phenotype in both male and female mice in an MCAO model of ischemic stroke. To better understand the mechanisms by which *Mif* deficiency is protective after MCAO, the protein expression of MIF and MIF-2 was analyzed in the ipsi- and contralateral hemispheres of *Mif*$^{+/+}$ (WT) mice after MCAO applying Western blot. As shown in Fig. 15A-D, there were no obvious differences between two hemispheres for either MIF (Fig. 15A and C) or MIF-2 (Fig. 15B and D) protein expression. In addition to protein expression, I also analyzed the transcription levels of MIF and MIF-2 in both hemispheres of WT and *Mif*$^{-/-}$ mice after MCAO. Surprisingly, mRNA expression of MIF was significantly downregulated to 0.71 ± 0.17-fold in the ipsilateral hemisphere in comparison to contralateral (P<0.0001, Fig. 15E). In addition, the mRNA expression of MIF-2 was significantly downregulated in the ipsilateral hemisphere after ischemic stroke in both WT (0.63 ± 0.21-fold, P<0.0001) and *Mif*$^{-/-}$ (0.67 ± 0.25-fold, P<0.05) mice (Fig. 15F).

These data indicated the mRNA expression of MIF proteins is downregulated in the ipsilateral hemisphere after ischemic stroke, which is different from the results obtained in the OGD-stressed neuronal cultures, indicating that this may be an effect related to whole tissue that comprises a pool of other cells including glial cells that may regulate MIF differently.

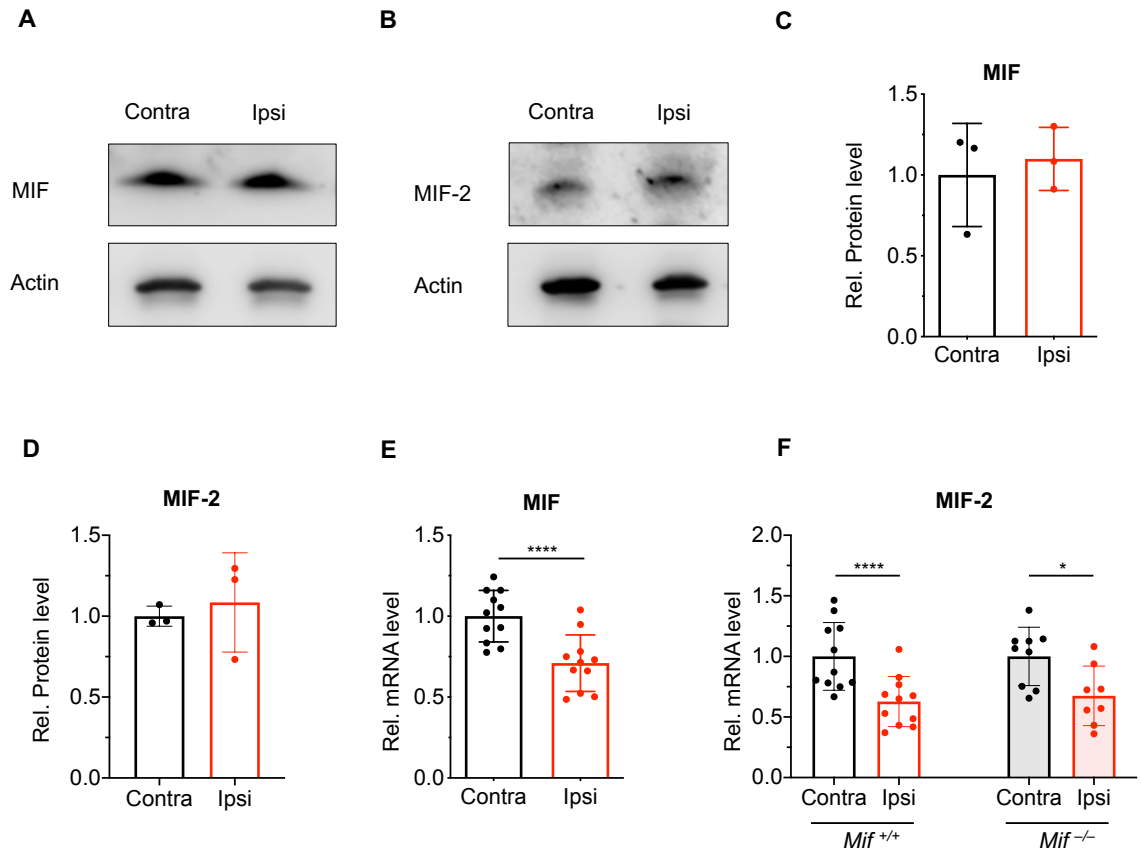

Fig. 15: The gene expression of MIF and MIF-2 is downregulated in the ipsilateral hemisphere after MCAO. A-B, After 1 h MCAO followed by 24 h reperfusion, both ipsi- (Ipsi) and contralateral (Contra) hemispheres of mice were lysed and analyzed by SDS-PAGE followed by Western blot with anti-MIF (**A**) and anti-MIF-2 (**B**) antibodies. **C-D,** The graphs show the quantified results from (**A**) and (**B**). The intensity of each protein was normalized using β-actin and the resultant value was presented as relative protein level. **E-F**, MCAO was performed as described in (**A**) and mRNA expression levels of MIF (**E**) or MIF-2 (**F**) in the ipsi- or contralateral hemisphere determined by qPCR. Relative mRNA expression was obtained by normalization to β-actin. Data are reported as means ± SD of (n=3 (**C**); n=3 (**D**); n=11 (**E**); n=9-11 (**F**)) independent experiments. Statistical analysis was performed with Paired T-test (*P<0.05, ****P<0.001).

3.6 CD74 is enhanced in ipsilateral hemisphere

As shown above, mRNA expression of MIF proteins was found downregulated in the ipsilateral hemisphere after ischemic stroke and hypoxic stress induced dysregulation of MIF receptors expression in both neuronal and microglial cells *in vitro*. Therefore, I next checked the expression of the MIF receptors in the ipsi- and contralateral hemisphere after MCAO using qPCR.

As illustrated in Fig. 16A, mRNA level of CD74 was significantly upregulated to 2.60 ± 0.78-fold in the ipsilateral hemisphere in comparison to contralateral side in WT mice (P<0.0001) and to 2.01 ± 1.48-fold in *Mif* $^{-/-}$ mice (P<0.05). An increasing trend was also seen for CXCR4, which was upregulated to 1.61 ± 0.70-fold in the ipsilateral hemisphere in WT mice and to 1.20 ± 0.57-fold in *Mif* $^{-/-}$ mice (Fig. 16C; P=0.07 and P=0.20, respectively). There were no changes observed for the level of CXCR2 in both genotypes (Fig. 16B). These results are different from the *in vitro* data in the OGD-stressed neuronal and microglial cultures, and the reason of this could be the presence of infiltrated inflammatory cells after MCAO having different expression patterns of MIF receptors and influencing thereby the obtained results.

Overall, these data indicated that the gene expression of CD74 was enhanced in the ipsilateral hemisphere after experimental ischemic stroke.

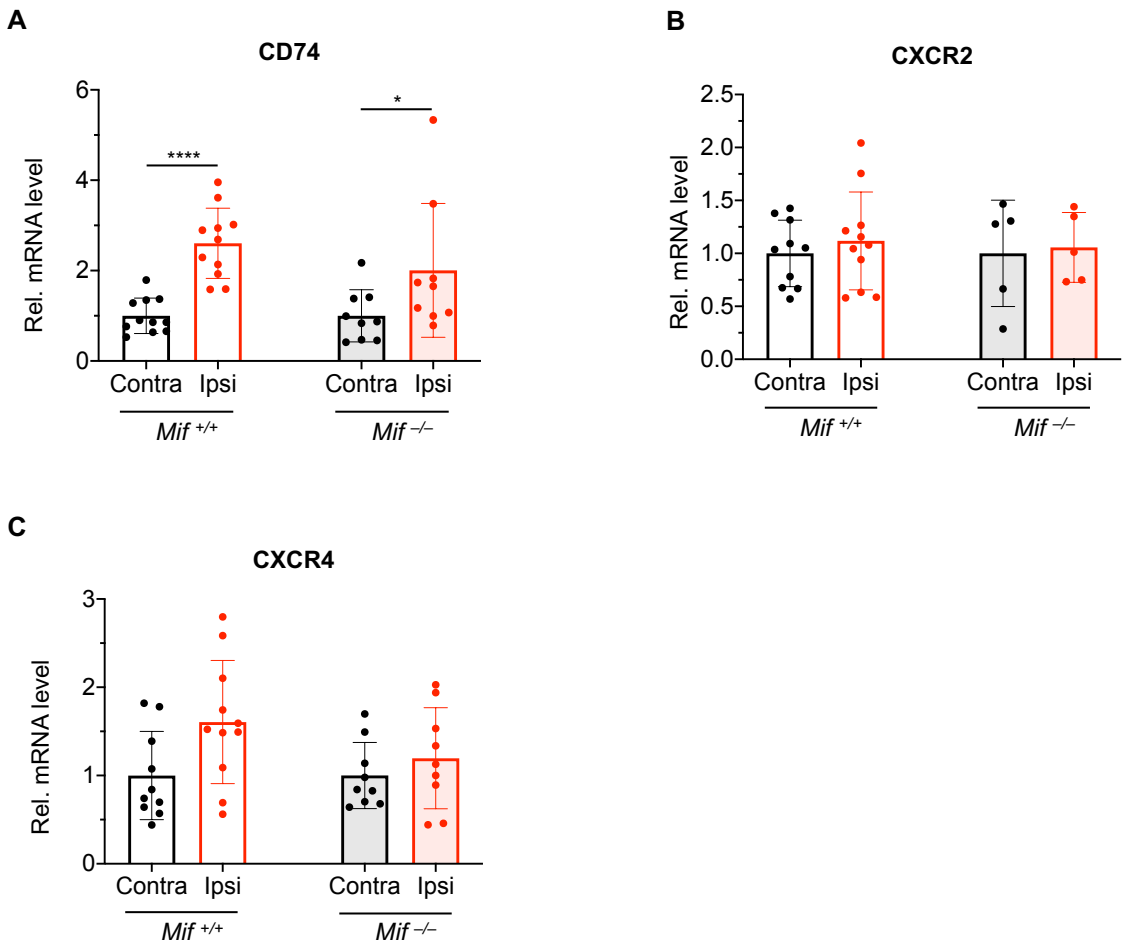

Fig. 16: Ischemic stress leads to an upregulation of CD74 gene expression in ipsilateral hemisphere. **A-C,** After 1 h MCAO and 24 h reperfusion, mRNA was isolated from ipsi- (Ipsi) and contralateral (Contra) hemispheres of *Mif* $^{-/-}$ and *Mif* $^{+/+}$ (WT) mice. The mRNA levels of MIF receptors CD74 (**A**), CXCR2 (**B**)

and CXCR4 (**C**) were analyzed by qPCR using respective primers. Relative mRNA levels were obtained by normalizing to β-actin. Data are reported as means ± SD of (n=9-11 (**A**); n=5-11 (**B**) n=9-11 (**C**)) independent experiments. Statistical analysis was performed with paired T-test (*P<0.05, ****P<0.0001).

3.7 *Mif* deficiency affects the levels of major inflammatory cytokines in the ipsilateral hemisphere after MCAO

It is well accepted that inflammation is a major driver of ischemic stroke pathology. To further explore the mechanism of MIF-mediated effects and its correlation with the inflammatory process in ischemic stroke, I asked whether *Mif* depletion could affect post-stroke neuroinflammation by checking the mRNA expression of the typical pro-inflammatory cytokines TNF-α, IL-1β, and IL-6, and the anti-inflammatory cytokines IL-10 and TGF-β1 in the ipsilateral hemisphere of *Mif*$^{-/-}$ *versus* WT mice after MCAO.

Surprisingly, the mRNA expression level of all five cytokines was found to be increased in the ipsilateral hemisphere of *Mif*-deficient mice compared to the control (Fig. 17). Briefly, the expression of TNF-α was markedly increased (9.58 ± 3.41-fold, P<0.01) in *Mif* $^{-/-}$ mice compared to WT littermates (Fig. 17A). A significant increase for IL-1β (2.45 ± 0.33-fold, P<0.001) and IL-6 (1.83 ± 0.37-fold, P<0.05) was also detected (Fig. 17B and C). In addition to the pro-inflammatory cytokines, *Mif* deficiency also upregulated the mRNA expression of the anti-inflammatory cytokines IL-10 (3.02 ± 0.25-fold, P<0.0001) and TGF-β1 (2.95 ± 0.43-fold, P<0.001) (Fig. 17D and E). While no multiplex or cytokine array analysis was performed, these data suggested that MIF may affect major pro- and anti-inflammatory cytokines in the ipsilateral hemisphere following MCAO.

Taken together, these *in vivo* data indicated that *Mif* deficiency in mice is protective during ischemic stroke even though the difference did not accomplish statistical significance. Interestingly, both pro- and anti-inflammatory cytokines were upregulated in the ipsilateral hemisphere of *Mif* deficiency mice compared to WT mice, indicating a more general role of MIF in cytokine gene regulation in this disease. Additional studies will be needed to explore the mechanism (e.g. NF-κB-mediated?) and the effect on other pro- and anti-inflammatory cytokines. Moreover, the data will have to be confirmed by ipsilateral protein expression data and data on corresponding circulating cytokine levels.

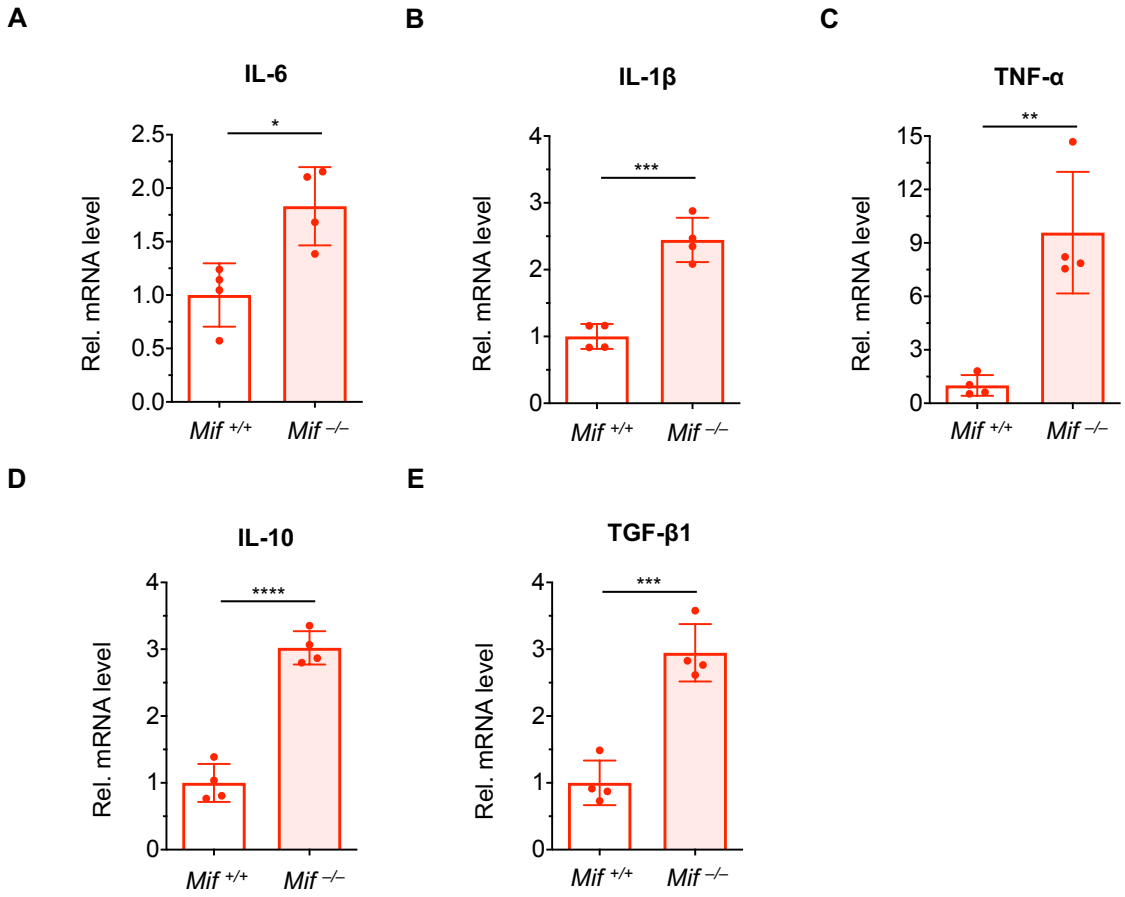

Fig. 17: *Mif* deficiency affects inflammatory cytokine levels in the ipsilateral hemisphere after ischemic stroke. A-E, After 1 h MCAO and 24 h reperfusion, the mRNA levels of major inflammatory cytokines in ipsilateral hemispheres of *Mif* $^{-/-}$ and WT mice were acquired from qPCR with specific primers of TNF-α (**A**), IL-1β (**B**), IL-6 (**C**), IL-10 (**D**) and TGF-β1 (**E**). Relative mRNA levels were obtained by normalizing to β-actin. Data are reported as means ± SD of n=4 independent experiments. Statistical analysis was performed with unpaired T-test (*P<0.05, **P<0.01, ***P<0.001, ****P<0.0001).

3.8 The role of *Cd74* deficiency in ischemic stroke

Based on the *in vitro* OGD stress data using *Cd74*-deficient neuronal cells and on the upregulation of CD74 in the ipsilateral hemisphere of *Mif* $^{-/-}$ mice after ischemic stroke combined with the effects of MIF in the MCAO model, I hypothesized that CD74 may have an exacerbating effect *in vivo*. To this end, experimental ischemic stroke was performed on *Cd74* $^{+/+}$, *Cd74* $^{+/-}$ and *Cd74* $^{-/-}$ mice by 1 h MCAO and 24 h reperfusion, and the infarct volumes and behavior were analyzed as monitored above.

CBF parameters were firstly measured by laser doppler during the operation to confirm MCA occlusion efficiency, and as expected the results showed that essentially all mice underwent a reduction in blood flow to less than 20% of the baseline value (Fig. 18A). After MCA occlusion followed by reperfusion, mice were sacrificed, and infarct volume was analyzed *via* Nissl staining. As shown in Fig. 18B, a promising trend towards protection of *Cd74* deficiency in infarct volume was seen between *Cd74* $^{+/+}$, *Cd74* $^{+/-}$ and *Cd74* $^{-/-}$ mice. Furthermore, the quantification revealed a tendency that *Cd74* depletion is protective in both male mice (81.32 ± 12.08 mm^3 in *Cd74* $^{+/+}$ group-vs. 74.58 ± 26.70 mm^3 in *Cd74* $^{+/-}$ group-vs. 69.35 ± 27.22 mm^3 in *Cd74* $^{-/-}$ group) and female mice (85.80 ± 13.51 mm^3 in *Cd74* $^{+/+}$ group-vs. 67.08 ± 29.28 mm^3 in *Cd74* $^{+/-}$ group-vs. 57.57 ± 31.17 mm^3 in *Cd74* $^{-/-}$ group), and this effect was clearer when both genders were analyzed together with infarct volume 83.81 ± 12.31 mm^3 in *Cd74* $^{+/+}$ mice-vs. 72.70 ± 26.19 mm^3 in *Cd74* $^{+/-}$ mice-vs. 66.44 ± 28.19 mm^3 in *Cd74* $^{-/-}$ mice (Fig. 18C). These results suggested that *Cd74* deficiency may be protective in both genders of mice in ischemic stroke, a trend that will have to be confirmed with a larger number of mice per cohort.

In addition to infarct volumes, “Neuroscore” was performed to evaluate neurological deficits after 1 h MCA occlusion and reperfusion in these mice. As shown in Fig. 18D, E and F, after 1 h occlusion, no difference was seen in the neurological score in *Cd74* $^{+/+}$, *Cd74* $^{+/-}$ and *Cd74* $^{-/-}$ mice in male (Fig. 18D) and female (Fig. 18E) mice, and in the cumulative analysis (Fig. 18F), arguing that the MCAO model in these mice actually works reliably. However, after 24 h reperfusion, the results showed the same protective trend consistent with infarct volume both in male and female mice (Fig. 18D and E), and in the cumulative analysis (Fig. 18F).

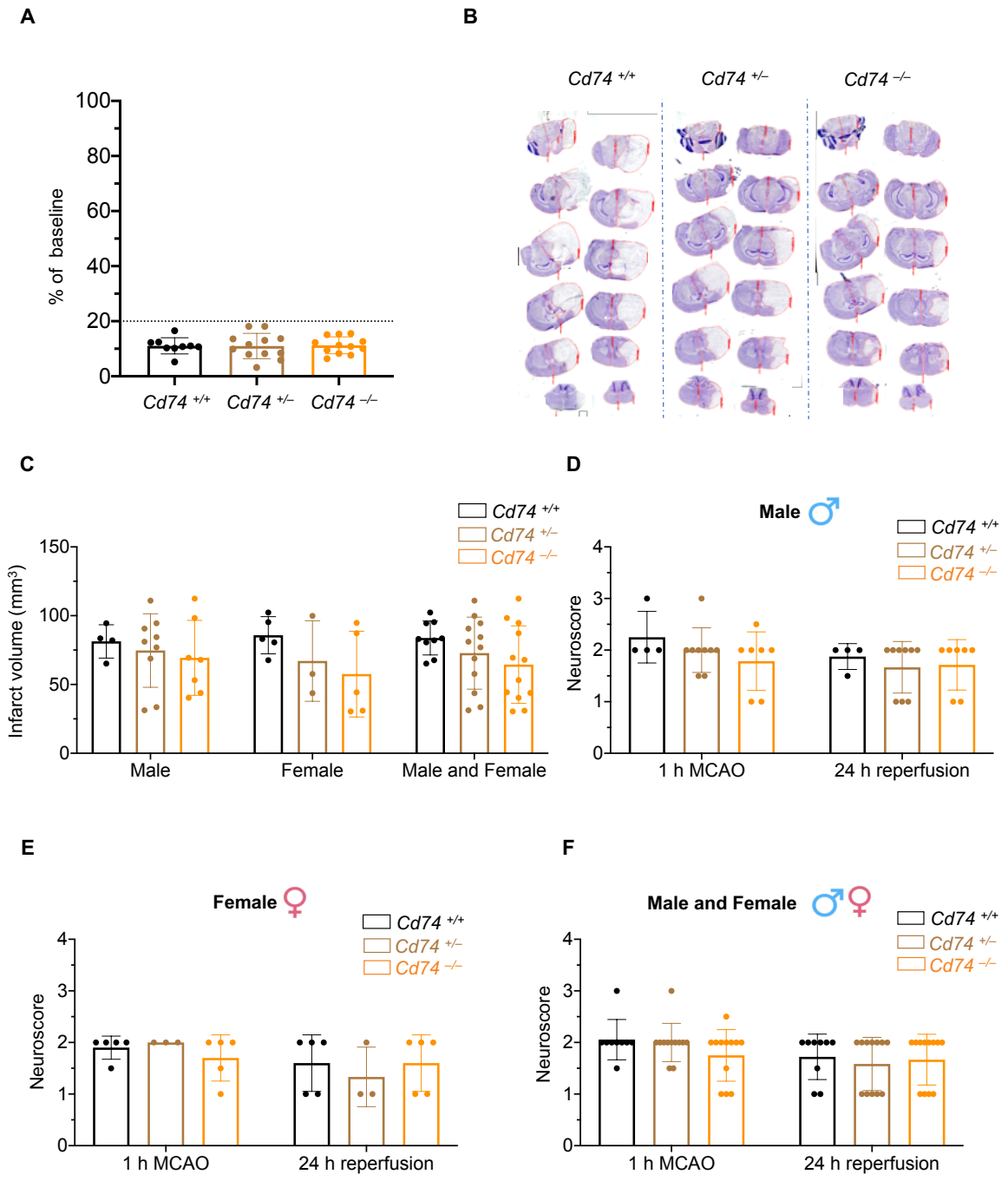

Fig. 18: Effect of CD74-deficiency on infarct size and neurological deficits in ischemic stroke. *In vivo* ischemic stroke was performed on *Cd74* $^{+/+}$, *Cd74* $^{+/-}$ and *Cd74* $^{-/-}$ mice by 1 h MCAO with 24 h reperfusion. **A**, CBF parameters were measured by laser doppler during the operation to confirm sufficient MCA occlusion efficiency. **B**, After MCAO model, the infarct volume was analyzed by Nissl staining. **C,** The graph shows the quantification of corrected infarct volume in male (n=4-9), female (n=3-5) and cumulative analysis (n=9-12). **D-E**, Neurological deficits of these mice were evaluated by Neuroscore after 1 h MCAO and after 24 h reperfusion in male (**D**), female (**E**) and cumulative analysis (**F**). Data are reported as means ± SD of (n=9-12 (**A**); n=3-12 (**C**); n=4-9 (**D**); n=3-5 (**E**); n=9-12 (**F**)) independent experiments. Statistical analysis is performed by one-way ANOVA with Tukey's multiple comparisons test.

In conclusion, *Cd74* depletion is indicative of a protective effect in the MCAO model in both genders, and taken together with the results showed above, suggested MIF/CD74 axis could be involved in neuronal death in ischemic stroke.

4. DISCUSSION

MIF is a proinflammatory cytokine with chemokine-like functions and has been well characterized in cardiovascular diseases like atherosclerosis and myocardial infarction. However, its role in the brain has remained rather poorly investigated and its role in ischemic stroke is still unclear. A few studies have addressed MIF's impact in ischemic stroke. However, the reported data turn out to be complex and in part controversial and require further elucidation. In this study, I found that MIF exacerbates neuronal cell death in ischemic stroke through the MIF/CD74 axis and by regulating neuroinflammation. Below, I discuss the key findings of this thesis, and potential approaches for further investigations.

4.1 Interaction between MIF/MIF-2 and AIF and search for new binding partners of MIF proteins

As mentioned in the introduction, Wang *et al* [159] demonstrated that MIF was recently identified as a neuronal nuclease, which is involved in cell death under stress. According to this study, the nuclease activity of MIF is related to the interaction with AIF that mediates its nuclear translocation [159]. To confirm this interaction and to study in microglia as well, a GST pulldown assay was performed using the recombinant GST-tagged proteins GST-MIF and GST-MIF-2 in combination with cell lysates of neuronal or microglial cells. However, no interaction was observed neither between MIF and AIF nor between MIF-2 and AIF in neither cell type.

One possible explanation for these results could be that in the study of Wang *et al* cell lysates of human HeLa cells were used to perform the GST pulldown assay. Conversely, cells lysates of primary mouse neuronal cells, the mouse neuronal N2a cells, as well as the mouse microglia BV-2 cells were used in this thesis, and the affinity of one protein for another could be cell type-dependent. In addition, a change in buffer conditions such as salt concentration, temperature and pH can all affect protein binding. Another possible explanation is that Wang *et al* used recombinant human MIF to perform all the experiments, but we used mouse MIF protein and mouse cells in this thesis, and the protein-protein interactions could be different in distinct species. Yet, Wang *et al* also performed *in vivo* experiments in mice and linked their MIF/AIF data to observed phenotypes in the mouse model. However, in my thesis multiple independent GST pulldown assays with cell lysates were performed and I was unable to

confirm the supposed interaction between MIF and AIF in the cell lysates used. Therefore, further experiments with purified AIF protein could be performed to simplify the reaction conditions and/or human cell lines could be tried.

Interestingly in my pulldowns, a band which was ~54 kDa was detected *via* Coomassie staining, suggesting a novel potential binding partner of MIF proteins in brain. Remarkably, previous studies have shown that MIF interacts with high temperature requirement serine protease A1 (HTRA1) which the molecular weight is 51 kDa and it is expressed in the brain [247,248]. In addition, it has been reported to be involved in neurological diseases including AS [249]. Whether HTRA1 serves as a common binding partner of both MIF and MIF-2 needs to be evaluated via mass spectrometry.

4.2 Upregulation of MIF and MIF-2 expression in neuronal cells under hypoxic conditions

As a pleiotropic and multi-functional protein MIF is pointed out to be existed in several organs, which also include the brain, particularly in neurons [184]. In addition to physiological conditions, MIF is upregulated in many diseases, such as in atherosclerosis [175,177], glial tumors [250], and some neurodegenerative diseases [190,251].

In the present work, both mRNA and protein expression of MIF was demonstrated to be increased in primary neuronal cells under hypoxia (OGD) stress. These findings are consistent with previous studies [206,207,212]. Indeed, several *in vivo* studies pointed out the expression of MIF is upregulated in the ischemic boundary zone or in the peri-infarct areas of ischemic rat brain with a peak at 24 h after stroke [206,207]. MIF was also shown to be accumulated in neurons in the peri-infarct cortex early after MCAO in mice [212]. Furthermore, a study with human brain sections found that MIF expression was increased in the peri-infarct region, specifically in the blood vessel-lining endothelial cells [215]. However, in this work I did not see any appreciable upregulation of MIF protein expression in the ipsilateral hemispheres compared to contralateral after experimental stroke. Contrary, my results showed a downregulation of MIF in the whole ipsilateral hemisphere after MCAO. The whole hemisphere was analyzed without discriminating between specific brain regions including infarct core or penumbra or different cell types in the brain. Also, the observation time point after MCAO in this study is 24 h. This could be a factor that affects the obtained results,

suggesting the necessity of additional kinetic studies that may reveal the cellular distribution of MIF in different brain regions and its regulation after ischemic stroke.

Although MIF was shown to be dysregulated, the mechanisms involved in MIF overexpression during different diseases, especially under ischemic stress are not well understood. One possibility is under hypoxia stress, the activity of the MIF gene promoter is upregulated through HIF-1α/hypoxia-responsive elements (HRE) [207,210,211]. Additionally, microRNA-493 which was recently demonstrated to regulate angiogenesis under ischemia conditions via directly targeting the expression of MIF [206], could be an involved mechanism. However, the involvement of HIF-1α or miR-493 mediated MIF upregulation was not considered in this study.

Remarkably, OGD stress treatment of the neuronal cells and anti-MIF Western blot showed a second higher molecular weight band at approximately 15 kDa in addition to the expected MIF band at 12.5 kDa. This band increased in density across the OGD kinetics, whereas the signal of the 12.5 kDa MIF band decreased. This could indicate that MIF may be post-translationally modified under hypoxic conditions. Indeed, nitric oxide generated during ischemia plays crucial roles in the pathophysiology of both ischemic stroke and myocardial infarction [252,253]. It has been shown that Cys-81 was selectively modified by S-nitros(yl)ation both *in vitro* and *in vivo* in myocardial inshemia/reperfusion injury, leading to a protective phenotype of MIF (SNO-MIF) in the ischemic heart [156,254]. Previous studies also identified other different modifications which occur at different sites of MIF and revealed distinct biological consequences of these modifications. For example, proline-2-oxidized MIF (proxMIF) is specifically generated by certain reactive oxygen species (ROS) [255]. Still, the second upper band observed in our study and the related potential modification remains to be identified.

Similarly, MIF-2, which also bind to the CD74 receptor [161,162] exerts a cardioprotective effect in myocardial ischemia *via* the CD74/AMPK pathway [105]. Contrary to the expression pattern of MIF, I noticed in this study decreasing levels of MIF-2 mRNA expression in primary neuronal cells under OGD stress. However, a similar downregulation of MIF-2 mRNA expression was found in the ipsilateral hemisphere of both *Mif* gene deficient mice and WT mice under experimental ischemic stroke. These results suggested that MIF and MIF-2 may have different functions in ischemic stroke. Whether the MIF-2/CD74 signaling pathways is involved in the ischemic brain still need to be further elucidated. To be noted, the use of *Mif-*

2-KO and *Cd74*-KO mice combined with selective inhibitors of MIF-2, e.g. 4-CPPC [256,257] under ischemic conditions will certainly help answer this question.

4.3 Hypoxia dysregulates the expression of MIF receptors

It's known that the functions of MIF mainly depend on its binding to receptors, i.e. CD74, CXCR2, CXCR4, and CXCR7. Briefly, the interaction between MIF and CD74 modulates cell survival, cell polarization, and protects cardiomyocytes in the ischemic heart [155-157]. Whereas, *via* interaction with CXCR2 or CXCR4, MIF mediates the activation and migration of immune cells during inflammation in cardiovascular pathogenesis [150,178]. MIF/CXCR7 signaling pathway hasn't been studied extensively, however previous studies also showed that CXCR7 mediates MIF-induced platelet apoptosis and lymphocyte chemotaxis [148,154].

In this thesis, expression of CD74 mRNA was strongly upregulated in the ipsilateral hemisphere of both WT and *Mif*-KO mice after ischemic stroke, which was showed for the first time. In addition, in *vitro* data also showed a slight upregulation of CD74 at mRNA levels in primary neuronal cells under OGD stress. Of note, Yang and colleagues [228] indicated that CD74 positive cells and CD74 expression in PBMC are upregulated in ischemic stroke patients. Interestingly, CD74 has been found to be upregulated in some neurological diseases, such as in the neurons and microglia of Alzheimer disease [194,258]. CD74 was also recruited to microvesicles derived from dendritic cells and enhanced the activation of NF-κB signaling pathway in microglia, which may regulate the process of MS [259].

Although the mechanism of CD74 upregulation in ischemic stroke or in the other neurological diseases is still poorly understood, the upregulation of CD74 and the increasing secretion of MIF may induce higher activity of MIF/CD74 signaling pathways under hypoxia stress, the same as MIF-2/CD74 axis. Upon its ligand binding, CD74 was shown to activate intracellular pathways, which include the phosphorylation of extracellular signal regulated kinase (ERK1/2)/mitogen-activated protein kinase (MAPK) pathway, phosphatidylinositol-4,5-bisphosphate 3-kinase (PI3K)/protein kinase B (AKT) pathway and AMPK pathway, and these corresponding downstream signaling pathways regulate important development and functions including cell proliferation, migration, inhibition of apoptosis and inflammatory activation in different cell types like lymphocytes, macrophages and cardiomyocytes [155,157,260-263]. Notably, in addition to protect ischemic cardiomyocytes, MIF/CD74 axis-mediated AMPK activation is not well characterized but has been shown to have beneficial effect in some cancer

via decreasing cell proliferation and viability [264,265]. Besides MIF, MIF-2 was also shown to activate ERK1/2/MAPK signaling pathway and AMPK pathway via binding to CD74 receptor [161,169]. Therefore, it will be interesting to further study whether these MIF/CD74 axis- or MIF-2/CD74 axis-induced pathways discussed above are also involved in ischemic stroke in the future.

Besides upregulation of CD74, I also found in this thesis that the expression of MIF's classical chemokine receptors is altered in ischemic stroke. Briefly, CXCR2 was strongly enhanced in both primary neuronal cells and BV-2 microglial cells under OGD stress. On the contrary, CXCR4 was downregulated in hypoxia-treated neurons and microglia, but it is upregulated in the ischemic brain in both WT and *Mif*-KO mice. In addition, CXCR7 was also increased in BV-2 microglia under OGD stress.

The difference in CXCR4 expression between the *in vitro* and *in vivo* data could be due to the notion that I checked the whole hemisphere including several cell types *in vivo*, but the cells I used *in vitro* are mainly one single type, suggesting that ischemia-induced alteration of CXCR4 is different in cell types like astrocytes as opposed to neurons or microglia. This could also explain why I did not find the expected upregulation of CXCR2 in the ipsilateral hemisphere after MCAO model like suggested by *in vitro* data. Nevertheless, these hypotheses still need to be further explored in the future.

The potential roles of MIF/CXCR2/4/7 axes in ischemic stroke are still not understood, but these signaling pathways and associated actions are well described in other cardiovascular diseases, which have been linked to chemokine-like functions of MIF to recruit inflammatory cells as mentioned above. Whether MIF-mediated chemotaxis responses via binding to CXCR2/4/7 are also involved in ischemic stroke is currently unclear and should be assessed in further studies.

There are some studies that addressed the role of these MIF receptors and their classical chemokine ligands in ischemic stroke. Although it has not been widely studied and is still partially controversial, CXCR2 was found to be upregulated in brain [266] and peripheral leukocytes [102] in ischemic stroke. The dysregulation of CXCR2 and its cognate ligands, especially CXCL1, CXCL2, and CXCL8 (IL-8), is correlated with worse outcome [102,267,268], mainly through an increased infiltration of neutrophils [268-270]. CXCR4 and its cognate ligand CXCL12 are also involved in ischemic stroke with more complicated effects.

Following ischemic stroke, CXCR4 and CXCL12 were shown to be upregulated in the penumbra and to be associated with infiltration of bone marrow-derived cells (especially monocytes) into the ischemic area in the brain [271,272]. In addition, an upregulated CXCL12/CXCR4 axis was found to regulate the infiltration/migration of neural stem cells [273], neural progenitor cells [274] and endothelial progenitor cells [275-277]. Interestingly, CXCR4 was also shown to regulate microglia migration [278,279]. These chemotaxis functions of different cells indicate that the CXCL12/CXCR4 axis not only plays roles in the inflammatory response and aggravates stroke pathology, but may also has beneficial effects and participate in stroke repair via promoting neurogenesis and angiogenesis [111,280,281]. Similar to CXCR4, CXCR7 was also shown to be upregulated in brain during ischemic stroke [224,282], with a protective effect as it was demonstrated to promote neural progenitor cell survival [283]. Although MIF as an ACK has structural similarity with cognate CXCR ligands and "utilizes" the receptors CXCR2, CXCR4, and CXCR7, it does not mimic all the functions that have been reported for the cognate ligands. In this thesis, I found that the receptors of MIF are altered during ischemic stroke, however the potential effects of these dysregulated receptors and their mediated signaling cascades still need to be further studied, also capitalizing on approaches that can differentiate between the MIF proteins and the cognate ligands. It will be helpful to answer this question by further studying *MIF*-deficient mice *versus* using of pharmacological antagonists of its non-cognate chemokine receptors-CXCR2, CXCR4, and CXCR7 under ischemic conditions.

4.4 The MIF/CD74 axis may promote cell death and aggravate neurologic symptoms after experimental stroke

In this study, both *Mif* deficiency and *Cd74* deficiency showed decreased infarct volume and less neurologic deficits after experimental stroke *in vivo*, which is in line with the *in vitro* results showing the involvement of the MIF/CD74 axis in neuronal death in ischemic stroke.

As described above, several studies reported the relevance of MIF in the pathogenesis of stroke. However, the reported findings are divergent and controversial, claiming a possible two-faced role of MIF in this disease, namely both a protective and detrimental role. Indeed, on one hand upregulation of MIF under ischemic conditions promoted the disruption of the BBB and an increase of the infarct area, indicating a detrimental effect [206,207,213]. On the other hand downregulation or genetic depletion of *Mif* enhanced caspase-3 activation, neuronal cell death,

and led to an increase of infarct size, suggesting a protective effect of MIF in stroke [215]. Remarkably, the common point between these studies consists in the importance of MIF expression that correlates with the infarct size and the prognosis of stroke severity and at the same time controls the fine-tuning of the neurological outcome of ischemic stroke. Noteworthy, the precise mechanisms driven by MIF remain to be explored.

In addition, the impact of *Mif* deficiency in ischemic stroke seems to be gender-dependent, and only in female mice genetic ablation of MIF contributed to worse stroke outcomes after stroke, but this effect was not found in male mice [214]. However, in my MD thesis study, I found that the *Mif*-KO is protective in both genders, although that data sets did not reach statistical significance. Reasons for this discrepancy with previous studies could be due to technical issues as there is no standard protocol for MCAO models. Both rats and mice were found to be used in the various studies, as well as two different kinds of MCAO models, i.e. an intraluminal suture/filament MCAO model and a direct distal MCAO model. Furthermore, the MCA occlusion time and observation window also differed between the studies.

Notably, in this thesis, I analyzed the cerebral vessel anatomy (PcomA anatomy and MCA-territory) of *Mif*$^{-/-}$ compared to WT mice. Of note, after deficiency of *Mif* gene, mice showed a better formed PcomAs on the right side (contralateral side) compared to WT mice. Although no differences were seen in the left PcomAs (ipsilateral side), these results indicated that *Mif*$^{-/-}$ mice could have a better vessel collateralization between posterior cerebral artery (PCA) and basilar artery (BA), and thus increase the CBF of MCA-territory in reperfusion phase after MCAO induction, which is related to a better outcome of ischemic stroke [284,285]. These confounding effects could also be a reason to explain why there was uneven distribution of data points in the infarct volume results. This finding also makes things more challenging to further elucidate the effect of MIF in ischemic stroke. Whether it is due to MIF directly affecting on the brain parenchyma like neurons and microglia or is related to the changing of PcomA is still unclear. Therefore, further *in vivo* experiments that combine distal MCAO model which induces less infarct size and won't be influenced by PcomA as well as pharmacological studies targeting MIF in WT mice would certainly give a better understanding about the role of MIF in ischemic stroke.

Interestingly, besides MIF, I also found that *Cd74* deficiency has a neuronal protective effect during ischemic stroke. Although it's still a tendency due to so far limited mouse numbers in each treatment group, this is the first time to directly reveal the role of CD74 in ischemic stroke

in both male and female mice. Notably, my *in vitro* data shows a protective effect of *Cd74* deficiency that is more pronounced than that of *Mif* deficiency in primary cortical neurons under ODG treatment, suggesting that besides the MIF/CD74 axis, probably the MIF-2/CD74 axis could also be involved in regulating cell viability during ischemia stress; this need to be further confirmed in the future. The underlying mechanism that how CD74 leads to neuronal death in ischemic stroke is still not clear. Whether this is partly because of the signaling pathways mediated via MIF/CD74 axis discussed above in other diseases or whether there are some other ischemic stroke specific pathways need to be further studied.

Besides MIF/CD74 axis, I didn't study if the other receptors (CXCR2/4/7) and the potential cascades discussed above are also involved in cell death in ischemic stroke. These should be studied in the future using specific inhibitors of these receptors.

In addition to these receptors-mediated extracellular roles of MIF, the intracellular role of MIF could be another reason of MIF's exacerbating effect in ischemic stroke. As mentioned in the introduction, the intracellular interaction between MIF with AIF and the potential nuclease effect of MIF could cause neural cell death during ischemic stroke [159]. This finding opens new challenges that raise numerous questions involving the regulatory mechanisms of intracellular and extracellular MIF during ischemic stroke and their interplay and role in the neurological outcome of ischemic stroke.

Last but not least, MIF acts as an ACK that could alter the overall inflammation state in the cerebral microenvironment. Accordingly, *Mif* depletion could lower the overall inflammatory state during ischemic stroke and this could also influence stroke outcome, as discussed later in this discussion section.

4.5 MIF and the inflammatory response after experimental stroke

The inflammatory response is a major driver of ischemic stroke and it participates in all the stages of the pathogenic cascade. A large number of studies have addressed inflammatory mechanisms in ischemic stroke in recent decades and it is well accepted that neuroinflammation plays both detrimental and beneficial effects [111]. During ischemic stroke, cytokines as key mediators of neuroinflammation are upregulated and they are secreted by activated microglia, astrocytes, neurons, endothelial cells, as well as the recruited peripheral immune cells.

MIF, as an ACK, has critical roles in various inflammatory diseases like sepsis, atherosclerosis and rheumatoid arthritis [140,286]. It has been demonstrated that MIF may directly or indirectly regulate the generation of various inflammatory cytokines, such as TNF-α, IFN-γ, IL-1β, IL-2 and so on [140,287-290].

Based on this, I therefore studied the mRNA expression of several selected pro- and anti-inflammatory cytokines in ipsilateral hemisphere of both *Mif* $^{-/-}$ and *Mif* $^{+/+}$ mice and found both pro- and anti-inflammatory cytokine expression was upregulated after the deletion of *Mif* in the injured brain hemisphere 24 h after experimental stroke, including IL-1β, TNF-α, IL-6, IL-10 and TGF-β1. In line with this finding, deficiency of *Mif* gene was pointed out to be associated with higher galetin-3 immunoreactivity in the ischemic brain in previous studies, which suggested MIF could affect the macrophage or microglia response in ischemic stroke [212]. Interestingly, galetin-3 was found could form heterodimers with CXCL12 and can inhibit CXCL12-related leukocyte migration recently [291]. However, no changes in IL-1β expression was observed in brain 7 days after MCAO [212]. Similarly, *Mif* deletion did not affect some other inflammatory cytokines expression, like IL-2, IFN-γ, IL-10 and TNF-α in the brain during 2 days after MCAO [208]. These effects are not consistent with my findings. The lack of a standardized protocol for MCAO experimental models as well as differences in occlusion time, filament size, and observation window could again be explanations for the discrepancy and divergence of my obtained results compared to other studies, making it difficult to compare intensity of infarction and inflammation. To better understand how MIF affects the inflammatory response during ischemic stroke, it would be interesting to further explore the level of inflammatory cytokines using additional and different time windows after stroke and study both mRNA and protein levels.

As key mediators of inflammatory response, inflammatory cytokines can be subtyped to pro-inflammatory cytokines and anti-inflammatory cytokines, which contribute to ischemic damage or favor stroke outcome, respectively [292]. In this study, I analyzed the most commonly studied pro- and anti-inflammatory cytokines involved in ischemic stroke in the ipsilateral hemisphere and surprisingly found that all of them are upregulated in *Mif*-KO mice compared to the WT group after MCAO treatment. Indeed, the overall effect of inflammatory dysregulation caused by the absence of MIF could be a reason for this observation. Notably, although considered a pro-inflammatory cytokine, TNF-α has been demonstrated to have not only detrimental but also beneficial effects in ischemic stroke [293,294]; the same is true for

IL-6 [295,296]. Nevertheless, the necessity of additional studies is needed to further explore the mechanism of MIF- and MIF-2-mediated effects on the regulation of inflammatory responses including cytokine expression and cell survival under physiological and pathophysiological conditions after stroke.

4.6 Conclusion

To conclude, my results demonstrate that MIF works as a key mediator in neuronal death during ischemic stroke in mice of both genders, and the mechanism could be related to the MIF/CD74 signaling pathway. In addition, MIF also seems to be involved in post-stroke neuroinflammation. I show *in vitro* and *in vivo* data which support a role for CD74 receptor in ischemic stroke for the first time. Overall, my study suggests that the MIF/CD74 axis could be served as a promising treatment target and that the application of MIF and/or CD74 inhibitors could be useful for stroke treatment.

5. SUMMARY

5.1 English summary

In addition to classical chemokines, more and more recent studies also found atypical chemokines (ACKs) to have a pivotal effect in neuroinflammation and ischemic stroke. Macrophage migration inhibitory factor (MIF) as a proinflammatory cytokine and ACK, was well characterized in cardiovascular diseases like atherosclerosis and myocardial infarction. However, its role in the brain has remained poorly investigated and its role in ischemic stroke is unclear. MIF effects are mediated through its non-cognate interaction with the CXC chemokine receptors CXCR2, CXCR4, and CXCR7, as well as through CD74, the surface form of MHC class II invariant chain, functioning as a fourth and cognate MIF receptor. In this thesis, I studied the potential role of MIF and its receptors in brain and ischemic stroke. I found that primary neuronal cells showed a significantly enhanced protein expression, secretion and mRNA levels of MIF after oxygen and glucose deprivation (OGD) stress. At the same time, the expression of MIF's receptors was altered under OGD treatment, which led to an upregulation of CXCR2 and a downregulation of CXCR4 in both primary neurons and BV-2 microglial cells. In this thesis, evidence for an involvement of the more recently discovered MIF homolog MIF-2/D-DT in ischemic stroke was obtained for the first time. My data suggested OGD led to a downregulation of MIF-2/D-DT mRNA level in primary neurons but increased its secretion. Interestingly, *Mif* or *Cd74* deficiency was associated with an upregulation of cell viability of primary neuronal cells under the same conditions, suggesting a potential role of MIF/CD74 axis in this process. I also explored the impact of *Mif* deficiency in experimental stroke *in vivo* using middle cerebral artery occlusion (MCAO) model and obtained preliminary data suggestive of a protective phenotype upon *Mif* depletion, which is associated with an enhanced expression of both CD74 and CXCR4 in ipsilateral hemisphere. Surprisingly, deficiency of *Mif* also increased both pro-inflammatory and anti-inflammatory cytokines expression in the ipsilateral hemisphere. A similar potential protective role was also observed in *Cd74* depletion mice, arguing thereby for the involvement of the MIF/CD74 axis in ischemic stroke, which could be promising as a therapeutic target for pharmacological treatment.

5.2 Zusammenfassung

Zusätzlich zu klassischen Chemokinen spielen atypische Chemokine (ACKs) eine zentrale Rolle sowohl in der Neuroinflammation als auch beim ischämischen Schlaganfall. MIF *(Makrophage migration inhibitory factor)* ist ein proinflammatorisches Zytokin mit chemokinähnlichen Funktionen, das bei zahlreichen Herz-Kreislauf-Erkrankungen wie Atherosklerose und Myokardinfarkt bereits gut charakterisiert wurde. Bislang bleibt die Rolle von MIF im zentralen Nervensystem insbesondere im Gehirn und beim ischämischen Schlaganfall jedoch unklar. MIF-vermittelte Effekte werden durch die sogenannte non-cognate-Interaktion mit den CXC-Chemokinrezeptoren CXCR2, CXCR4 und CXCR7 vermittelt. Neben diesen drei CXC-Chemokinrezeptoren bindet MIF affin an die invariante Kette (Ii) der MHC-Klasse II Moleküle, welche nach Oberflächenexpression als CD74 bezeichnet wird und damit als vierter MIF-Rezeptor fungiert. Der Fokus meiner Dissertation liegt auf der Entschlüsselung der potenziellen Rolle von MIF und seiner Rezeptoren im Gehirn und beim ischämischen Schlaganfall. Ich fand heraus, dass primäre neuronale Zellen eine signifikant erhöhte Proteinexpression, Sekretion und mRNA-Spiegel von MIF nach der Depletion von Sauerstoff und Glukose (OGD, *oxygen and glucose deprivation*) zeigten. Gleichzeitig ändert sich die Expression der MIF-Rezeptoren unter denselben Bedingungen. So wurde eine Hochregulierung der CXCR2-Expression sowohl in primären Neuronen als auch in BV-2-Mikrogliazelllinie festgestellt. Hingegen wurde die Expression von CXCR4 in denselben Zellen runterreguliert. Außerdem wurden in dieser Arbeit erste Hinweise auf eine mögliche Beteiligung des kürzlich entdeckten MIF-Homologen MIF-2/D-DT am ischämischen Schlaganfall erhalten. So deuten meine Daten darauf hin, dass OGD-Konditionen zu einer Herunterregulierung der MIF-2/D-DT-mRNA-Expression in primären Neuronen führte, aber deren Sekretion erhöhte. Interessanterweise führte ein Defizit des *Mif*- beziehungsweise des *Cd74*-Gens zu einer Erhöhung der Viabilität der primären neuronalen Zellen unter OGD, was auf eine neue potentielle Rolle der MIF/CD74-Achse in diesem Prozess hinweist. Zusätzlich habe ich den Einfluss der der Deletion des *Mif*-Gens auf den ischämischen Schlaganfall *in vivo* durch Verwendung des MCAO-Modells (*middle cerebral artery occlusion*) untersucht und fand heraus, dass MIF-Mangel einen schützenden Effekt auf die Entwicklung des Schlaganfalls ausübt, und dass die Expression von CD74 und CXCR4 in der ipsilateralen Hemisphäre verstärkt sind. Überraschenderweise führte die Depletion des *Mif*-Gens zu einer Hochregulierung sowohl der proinflammatorischen als auch der antiinflammatorischen Zytokine Expression in der ipsilateralen Hemisphäre. Bemerkenswerterweise wurde ein

ähnlich schützender Effekt auch in *Cd74* $^{-/-}$ Mäusen nach experimentellem Schlaganfall beobachtet, was auf eine Rolle der MIF/CD74-Achse in der Pathogenese des ischämischen Schlaganfalls hinweist und gleichzeitig auf CD74 als mögliches Zielmolekül für Strategien in der Prävention und Therapie hinweist.

6. REFERENCES

1. Grysiewicz RA, Thomas K, Pandey DK. Epidemiology of ischemic and hemorrhagic stroke: incidence, prevalence, mortality, and risk factors. Neurol Clin. 2008 Nov;26(4):871-95, vii.
2. Makris K, Haliassos A, Chondrogianni M, et al. Blood biomarkers in ischemic stroke: potential role and challenges in clinical practice and research. Crit Rev Clin Lab Sci. 2018 Aug;55(5):294-328.
3. Adams Jr HP, Bendixen BH, Kappelle LJ, et al. Classification of subtype of acute ischemic stroke. Definitions for use in a multicenter clinical trial. TOAST. Trial of Org 10172 in Acute Stroke Treatment. stroke. 1993;24(1):35-41.
4. Hart RG, Diener HC, Coutts SB, et al. Embolic strokes of undetermined source: the case for a new clinical construct. Lancet Neurol. 2014 Apr;13(4):429-38.
5. Hisham NF, Bayraktutan U. Epidemiology, pathophysiology, and treatment of hypertension in ischaemic stroke patients. J Stroke Cerebrovasc Dis. 2013 Oct;22(7):e4-14.
6. Weir NU, Dennis MS. Meeting the challenge of stroke. Scott Med J. 1997 Oct;42(5):145-7.
7. Bejot Y, Bailly H, Durier J, et al. Epidemiology of stroke in Europe and trends for the 21st century. Presse Med. 2016 Dec;45(12 Pt 2):e391-e398.
8. Strong K, Mathers C, Bonita R. Preventing stroke: saving lives around the world. Lancet Neurol. 2007 Feb;6(2):182-7.
9. Feigin VL, Norrving B, Mensah GA. Global Burden of Stroke. Circ Res. 2017 Feb 3;120(3):439-448.
10. Marini C, Russo T, Felzani G. Incidence of stroke in young adults: a review. Stroke research and treatment. 2011;2011.
11. Hacke W, Kaste M, Bluhmki E, et al. Thrombolysis with alteplase 3 to 4.5 hours after acute ischemic stroke. N Engl J Med. 2008 Sep 25;359(13):1317-29.
12. Brzica H, Abdullahi W, Ibbotson K, et al. Role of Transporters in Central Nervous System Drug Delivery and Blood-Brain Barrier Protection: Relevance to Treatment of Stroke. J Cent Nerv Syst Dis. 2017;9:1179573517693802.
13. Nogueira RG, Jadhav AP, Haussen DC, et al. Thrombectomy 6 to 24 hours after stroke with a mismatch between deficit and infarct. New England Journal of Medicine. 2018;378(1):11-21.
14. Thomalla G, Gerloff C. Acute imaging for evidence-based treatment of ischemic stroke. Curr Opin Neurol. 2019 Aug;32(4):521-529.
15. Sutherland BA, Minnerup J, Balami JS, et al. Neuroprotection for ischaemic stroke: translation from the bench to the bedside. Int J Stroke. 2012 Jul;7(5):407-18.
16. Evans MA, Lim R, Kim HA, et al. Acute or Delayed Systemic Administration of Human Amnion Epithelial Cells Improves Outcomes in Experimental Stroke. Stroke. 2018 Mar;49(3):700-709.
17. Chelluboina B, Nalamolu KR, Mendez GG, et al. Mesenchymal Stem Cell Treatment Prevents Post-Stroke Dysregulation of Matrix Metalloproteinases and Tissue Inhibitors of Metalloproteinases. Cell Physiol Biochem. 2017;44(4):1360-1369.
18. Garbuzova-Davis S, Haller E, Lin R, et al. Intravenously transplanted human bone marrow endothelial progenitor cells engraft within brain capillaries, preserve mitochondrial morphology, and display pinocytotic activity toward blood-brain barrier repair in ischemic stroke rats. Stem cells. 2017;35(5):1246-1258.

19. Yang Q, Huang Q, Hu Z, et al. Potential Neuroprotective Treatment of Stroke: Targeting Excitotoxicity, Oxidative Stress, and Inflammation. Front Neurosci. 2019;13:1036.
20. Srivastava MP, Bhasin A, Bhatia R, et al. Efficacy of minocycline in acute ischemic stroke: a single-blinded, placebo-controlled trial. Neurology India. 2012;60(1):23.
21. Joy MT, Ben Assayag E, Shabashov-Stone D, et al. CCR5 Is a Therapeutic Target for Recovery after Stroke and Traumatic Brain Injury. Cell. 2019 Feb 21;176(5):1143-1157 e13.
22. Luo Y, Yang H, Zhou YF, et al. Dual and multi-targeted nanoparticles for site-specific brain drug delivery. J Control Release. 2020 Jan 10;317:195-215.
23. Nozohouri S, Sifat AE, Vaidya B, et al. Novel approaches for the delivery of therapeutics in ischemic stroke. Drug Discov Today. 2020 Mar;25(3):535-551.
24. Astrup J, Siesjö BK, Symon L. Thresholds in cerebral ischemia-the ischemic penumbra. Stroke. 1981;12(6):723-725.
25. Bandera E, Botteri M, Minelli C, et al. Cerebral blood flow threshold of ischemic penumbra and infarct core in acute ischemic stroke: a systematic review. Stroke. 2006 May;37(5):1334-9.
26. Jung S, Gilgen M, Slotboom J, et al. Factors that determine penumbral tissue loss in acute ischaemic stroke. Brain. 2013;136(12):3554-3560.
27. Lo EH. A new penumbra: transitioning from injury into repair after stroke. Nature medicine. 2008;14(5):497-500.
28. Martin RL, Lloyd HG, Cowan AI. The early events of oxygen and glucose deprivation: setting the scene for neuronal death? Trends Neurosci. 1994 Jun;17(6):251-7.
29. Smith G, Hesketh K, Metcalfe J, et al. Energy metabolism, ion homeostasis, and cell damage in the brain. Biochem Soc Trans. 1994;22(4):991-996.
30. Nishizawa Y. Glutamate release and neuronal damage in ischemia. Life Sci. 2001 Jun 15;69(4):369-81.
31. Takahashi M, Billups B, Rossi D, et al. The role of glutamate transporters in glutamate homeostasis in the brain. J Exp Biol. 1997 Jan;200(Pt 2):401-9.
32. Vaarmann A, Kovac S, Holmstrom KM, et al. Dopamine protects neurons against glutamate-induced excitotoxicity. Cell Death Dis. 2013 Jan 10;4(1):e455.
33. Furukawa K, Fu W, Li Y, et al. The actin-severing protein gelsolin modulates calcium channel and NMDA receptor activities and vulnerability to excitotoxicity in hippocampal neurons. J Neurosci. 1997 Nov 1;17(21):8178-86.
34. Lipton P. Ischemic cell death in brain neurons. Physiol Rev. 1999 Oct;79(4):1431-568.
35. Bano D, Munarriz E, Chen H, et al. The plasma membrane Na+/Ca2+ exchanger is cleaved by distinct protease families in neuronal cell death. Annals of the New York Academy of Sciences. 2007;1099(1):451-455.
36. Kimelberg HK, Macvicar BA, Sontheimer H. Anion channels in astrocytes: biophysics, pharmacology, and function. Glia. 2006 Nov 15;54(7):747-57.
37. Kiselyov K, Muallem S. ROS and intracellular ion channels. Cell Calcium. 2016 Aug;60(2):108-14.
38. De Silva TM, Miller AA. Cerebral small vessel disease: targeting oxidative stress as a novel therapeutic strategy? Frontiers in pharmacology. 2016;7:61.
39. Abramov AY, Scorziello A, Duchen MR. Three distinct mechanisms generate oxygen free radicals in neurons and contribute to cell death during anoxia and reoxygenation. J Neurosci. 2007 Jan 31;27(5):1129-38.
40. Forstermann U. Nitric oxide and oxidative stress in vascular disease. Pflugers Arch. 2010 May;459(6):923-39.

41. Iadecola C, Zhang F, Casey R, et al. Delayed reduction of ischemic brain injury and neurological deficits in mice lacking the inducible nitric oxide synthase gene. J Neurosci. 1997 Dec 1;17(23):9157-64.
42. Fujimura M, Morita-Fujimura Y, Kawase M, et al. Manganese superoxide dismutase mediates the early release of mitochondrial cytochrome C and subsequent DNA fragmentation after permanent focal cerebral ischemia in mice. J Neurosci. 1999 May 1;19(9):3414-22.
43. Kondo T, Reaume AG, Huang TT, et al. Reduction of CuZn-superoxide dismutase activity exacerbates neuronal cell injury and edema formation after transient focal cerebral ischemia. J Neurosci. 1997 Jun 1;17(11):4180-9.
44. Pacher P, Beckman JS, Liaudet L. Nitric oxide and peroxynitrite in health and disease. Physiol Rev. 2007 Jan;87(1):315-424.
45. Lo EH, Dalkara T, Moskowitz MA. Mechanisms, challenges and opportunities in stroke. Nat Rev Neurosci. 2003 May;4(5):399-415.
46. Gouriou Y, Demaurex N, Bijlenga P, et al. Mitochondrial calcium handling during ischemia-induced cell death in neurons. Biochimie. 2011 Dec;93(12):2060-7.
47. Green DR, Kroemer G. The pathophysiology of mitochondrial cell death. Science. 2004 Jul 30;305(5684):626-9.
48. Kontos HA. Oxygen radicals in cerebral ischemia: the 2001 Willis lecture. Stroke. 2001 Nov;32(11):2712-6.
49. Iadecola C, Anrather J. The immunology of stroke: from mechanisms to translation. Nat Med. 2011 Jul;17(7):796-808.
50. Guruswamy R, ElAli A. Complex Roles of Microglial Cells in Ischemic Stroke Pathobiology: New Insights and Future Directions. Int J Mol Sci. 2017 Feb 25;18(3):496.
51. Yenari MA, Kauppinen TM, Swanson RA. Microglial activation in stroke: therapeutic targets. Neurotherapeutics. 2010 Oct;7(4):378-91.
52. Gülke E, Gelderblom M, Magnus T. Danger signals in stroke and their role on microglia activation after ischemia. Therapeutic advances in neurological disorders. 2018;11:1756286418774254.
53. Taylor RA, Chang CF, Goods BA, et al. TGF-beta1 modulates microglial phenotype and promotes recovery after intracerebral hemorrhage. J Clin Invest. 2017 Jan 3;127(1):280-292.
54. Schilling M, Strecker JK, Schabitz WR, et al. Effects of monocyte chemoattractant protein 1 on blood-borne cell recruitment after transient focal cerebral ischemia in mice. Neuroscience. 2009 Jul 7;161(3):806-12.
55. Dong Y, Benveniste EN. Immune function of astrocytes. Glia. 2001 Nov;36(2):180-90.
56. Barreto G, White RE, Ouyang Y, et al. Astrocytes: targets for neuroprotection in stroke. Cent Nerv Syst Agents Med Chem. 2011 Jun 1;11(2):164-73.
57. Wang H, Song G, Chuang H, et al. Portrait of glial scar in neurological diseases. Int J Immunopathol Pharmacol. 2018 Jan-Dec;31:2058738418801406.
58. Hayakawa K, Nakano T, Irie K, et al. Inhibition of reactive astrocytes with fluorocitrate retards neurovascular remodeling and recovery after focal cerebral ischemia in mice. J Cereb Blood Flow Metab. 2010 Apr;30(4):871-82.
59. Danton GH, Dietrich WD. Inflammatory mechanisms after ischemia and stroke. J Neuropathol Exp Neurol. 2003 Feb;62(2):127-36.
60. Wang Q, Tang XN, Yenari MA. The inflammatory response in stroke. J Neuroimmunol. 2007 Mar;184(1-2):53-68.

61. Hallenbeck JM. Significance of the inflammatory response in brain ischemia. Mechanisms of Secondary Brain Damage in Cerebral Ischemia and Trauma: Springer; 1996. p. 27-31.
62. Perez-de-Puig I, Miro-Mur F, Ferrer-Ferrer M, et al. Neutrophil recruitment to the brain in mouse and human ischemic stroke. Acta Neuropathol. 2015 Feb;129(2):239-57.
63. Lattanzi S, Brigo F, Trinka E, et al. Neutrophil-to-Lymphocyte Ratio in Acute Cerebral Hemorrhage: a System Review. Transl Stroke Res. 2019 Apr;10(2):137-145.
64. Jickling GC, Liu D, Ander BP, et al. Targeting neutrophils in ischemic stroke: translational insights from experimental studies. J Cereb Blood Flow Metab. 2015 Jun;35(6):888-901.
65. Zlokovic BV. Remodeling after stroke. Nat Med. 2006 Apr;12(4):390-1.
66. McDonald B, Pittman K, Menezes GB, et al. Intravascular danger signals guide neutrophils to sites of sterile inflammation. Science. 2010 Oct 15;330(6002):362-6.
67. Feng Y, Liao S, Wei C, et al. Infiltration and persistence of lymphocytes during late-stage cerebral ischemia in middle cerebral artery occlusion and photothrombotic stroke models. J Neuroinflammation. 2017 Dec 15;14(1):248.
68. Yilmaz G, Arumugam TV, Stokes KY, et al. Role of T lymphocytes and interferon-in ischemic stroke. Circulation. 2006;113(17):2105-2112.
69. Gelderblom M, Leypoldt F, Steinbach K, et al. Temporal and spatial dynamics of cerebral immune cell accumulation in stroke. Stroke. 2009 May;40(5):1849-57.
70. Kleinschnitz C, Schwab N, Kraft P, et al. Early detrimental T-cell effects in experimental cerebral ischemia are neither related to adaptive immunity nor thrombus formation. Blood, The Journal of the American Society of Hematology. 2010;115(18):3835-3842.
71. Shichita T, Sugiyama Y, Ooboshi H, et al. Pivotal role of cerebral interleukin-17-producing gammadeltaT cells in the delayed phase of ischemic brain injury. Nat Med. 2009 Aug;15(8):946-50.
72. Filiano AJ, Gadani SP, Kipnis J. How and why do T cells and their derived cytokines affect the injured and healthy brain? Nature Reviews Neuroscience. 2017;18(6):375.
73. Liew FY. TH 1 and TH 2 cells: a historical perspective. Nature Reviews Immunology. 2002;2(1):55-60.
74. Xiong X, Fang W, Zhu X, et al. The Involvement and Therapy Target of Immune Cells After Ischemic Stroke. Frontiers in immunology. 2019;10:2167.
75. Liesz A, Hu X, Kleinschnitz C, et al. Functional role of regulatory lymphocytes in stroke: facts and controversies. Stroke. 2015 May;46(5):1422-30.
76. Liesz A, Suri-Payer E, Veltkamp C, et al. Regulatory T cells are key cerebroprotective immunomodulators in acute experimental stroke. Nat Med. 2009 Feb;15(2):192-9.
77. Mracsko E, Liesz A, Stojanovic A, et al. Antigen dependently activated cluster of differentiation 8-positive T cells cause perforin-mediated neurotoxicity in experimental stroke. J Neurosci. 2014 Dec 10;34(50):16784-95.
78. Offner H, Hurn PD. A novel hypothesis: regulatory B lymphocytes shape outcome from experimental stroke. Transl Stroke Res. 2012 Sep;3(3):324-30.
79. Schuhmann MK, Langhauser F, Kraft P, et al. B cells do not have a major pathophysiologic role in acute ischemic stroke in mice. Journal of neuroinflammation. 2017;14(1):112.
80. Ren X, Akiyoshi K, Dziennis S, et al. Regulatory B cells limit CNS inflammation and neurologic deficits in murine experimental stroke. J Neurosci. 2011 Jun 8;31(23):8556-63.
81. Chen Y, Bodhankar S, Murphy SJ, et al. Intrastriatal B-cell administration limits infarct size after stroke in B-cell deficient mice. Metabolic brain disease. 2012;27(4):487-493.

82. Ren X, Akiyoshi K, Dziennis S, et al. Regulatory B cells limit CNS inflammation and neurologic deficits in murine experimental stroke. Journal of Neuroscience. 2011;31(23):8556-8563.
83. Kostulas N, Li HL, Xiao BG, et al. Dendritic cells are present in ischemic brain after permanent middle cerebral artery occlusion in the rat. Stroke. 2002 Apr;33(4):1129-34.
84. Gan Y, Liu Q, Wu W, et al. Ischemic neurons recruit natural killer cells that accelerate brain infarction. Proceedings of the National Academy of Sciences. 2014;111(7):2704-2709.
85. Lünemann A, Lünemann JD, Roberts S, et al. Human NK cells kill resting but not activated microglia via NKG2D-and NKp46-mediated recognition. The Journal of Immunology. 2008;181(9):6170-6177.
86. Vosshenrich CA, Ranson T, Samson SI, et al. Roles for common cytokine receptor gamma-chain-dependent cytokines in the generation, differentiation, and maturation of NK cell precursors and peripheral NK cells in vivo. J Immunol. 2005 Feb 1;174(3):1213-21.
87. Stolp HB. Neuropoietic cytokines in normal brain development and neurodevelopmental disorders. Mol Cell Neurosci. 2013 Mar;53:63-8.
88. Baldo BA. Side effects of cytokines approved for therapy. Drug Saf. 2014 Nov;37(11):921-43.
89. Sairanen T, Carpén O, Karjalainen-Lindsberg M-L, et al. Evolution of cerebral tumor necrosis factor-production during human ischemic stroke. Stroke. 2001;32(8):1750-1758.
90. Liu T, Clark RK, McDonnell PC, et al. Tumor necrosis factor-alpha expression in ischemic neurons. Stroke. 1994 Jul;25(7):1481-8.
91. Lakhan SE, Kirchgessner A, Hofer M. Inflammatory mechanisms in ischemic stroke: therapeutic approaches. J Transl Med. 2009 Nov 17;7(1):97.
92. Allan SM, Rothwell NJ. Cytokines and acute neurodegeneration. Nat Rev Neurosci. 2001 Oct;2(10):734-44.
93. Ramiro L, Simats A, García-Berrocoso T, et al. Inflammatory molecules might become both biomarkers and therapeutic targets for stroke management. Therapeutic advances in neurological disorders. 2018;11:1756286418789340.
94. Doll DN, Barr TL, Simpkins JW. Cytokines: their role in stroke and potential use as biomarkers and therapeutic targets. Aging and disease. 2014;5(5):294.
95. Vitkovic L, Maeda S, Sternberg E. Anti-inflammatory cytokines: expression and action in the brain. Neuroimmunomodulation. 2001;9(6):295-312.
96. Deb P, Sharma S, Hassan KM. Pathophysiologic mechanisms of acute ischemic stroke: An overview with emphasis on therapeutic significance beyond thrombolysis. Pathophysiology. 2010 Jun;17(3):197-218.
97. Lively S, Hutchings S, Schlichter LC. Molecular and Cellular Responses to Interleukin-4 Treatment in a Rat Model of Transient Ischemia. J Neuropathol Exp Neurol. 2016 Nov 1;75(11):1058-1071.
98. Steinman L. A brief history of Th 17, the first major revision in the Th 1/Th 2 hypothesis of T cell–mediated tissue damage. Nature medicine. 2007;13(2):139-145.
99. Raman D, Sobolik-Delmaire T, Richmond A. Chemokines in health and disease. Exp Cell Res. 2011 Mar 10;317(5):575-89.
100. Ransohoff RM, Trettel F. Editorial Research Topic "Chemokines and chemokine receptors in brain homeostasis". Frontiers in Cellular Neuroscience. 2015;9:132.
101. Bajetto A, Bonavia R, Barbero S, et al. Chemokines and their receptors in the central nervous system. Frontiers in neuroendocrinology. 2001;22(3):147-184.

102. Hughes CE, Nibbs RJ. A guide to chemokines and their receptors. The FEBS journal. 2018;285(16):2944-2971.
103. Dimitrijevic OB, Stamatovic SM, Keep RF, et al. Absence of the chemokine receptor CCR2 protects against cerebral ischemia/reperfusion injury in mice. Stroke. 2007 Apr;38(4):1345-53.
104. Fang W, Zhai X, Han D, et al. CCR2-dependent monocytes/macrophages exacerbate acute brain injury but promote functional recovery after ischemic stroke in mice. Theranostics. 2018;8(13):3530-3543.
105. Guo YQ, Zheng LN, Wei JF, et al. Expression of CCL2 and CCR2 in the hippocampus and the interventional roles of propofol in rat cerebral ischemia/reperfusion. Exp Ther Med. 2014 Aug;8(2):657-661.
106. Shichinohe H, Kuroda S, Yano S, et al. Role of SDF-1/CXCR4 system in survival and migration of bone marrow stromal cells after transplantation into mice cerebral infarct. Brain research. 2007;1183:138-147.
107. Tang Z, Gan Y, Liu Q, et al. CX3CR1 deficiency suppresses activation and neurotoxicity of microglia/macrophage in experimental ischemic stroke. J Neuroinflammation. 2014 Feb 3;11(1):26.
108. Tarozzo G, Campanella M, Ghiani M, et al. Expression of fractalkine and its receptor, CX3CR1, in response to ischaemia-reperfusion brain injury in the rat. Eur J Neurosci. 2002 May;15(10):1663-8.
109. Vidale S, Consoli A, Arnaboldi M, et al. Postischemic Inflammation in Acute Stroke. J Clin Neurol. 2017 Jan;13(1):1-9.
110. Dimitrijevic OB, Stamatovic SM, Keep RF, et al. Effects of the chemokine CCL2 on blood-brain barrier permeability during ischemia-reperfusion injury. J Cereb Blood Flow Metab. 2006 Jun;26(6):797-810.
111. Le Thuc O, Blondeau N, Nahon JL, et al. The complex contribution of chemokines to neuroinflammation: switching from beneficial to detrimental effects. Ann N Y Acad Sci. 2015 Sep;1351(1):127-40.
112. Abbott NJ, Rönnbäck L, Hansson E. Astrocyte–endothelial interactions at the blood–brain barrier. Nature reviews neuroscience. 2006;7(1):41.
113. Liebner S, Dijkhuizen RM, Reiss Y, et al. Functional morphology of the blood-brain barrier in health and disease. Acta Neuropathol. 2018 Mar;135(3):311-336.
114. Petty MA, Lo EH. Junctional complexes of the blood-brain barrier: permeability changes in neuroinflammation. Prog Neurobiol. 2002 Dec;68(5):311-23.
115. del Zoppo GJ. Inflammation and the neurovascular unit in the setting of focal cerebral ischemia. Neuroscience. 2009 Feb 6;158(3):972-82.
116. Brouns R, De Deyn PP. The complexity of neurobiological processes in acute ischemic stroke. Clin Neurol Neurosurg. 2009 Jul;111(6):483-95.
117. ElAli A, Theriault P, Rivest S. The role of pericytes in neurovascular unit remodeling in brain disorders. Int J Mol Sci. 2014 Apr 16;15(4):6453-74.
118. Fernandez-Klett F, Priller J. Diverse functions of pericytes in cerebral blood flow regulation and ischemia. J Cereb Blood Flow Metab. 2015 Jun;35(6):883-7.
119. Stanimirovic D, Satoh K. Inflammatory mediators of cerebral endothelium: a role in ischemic brain inflammation. Brain Pathol. 2000 Jan;10(1):113-26.
120. Lakhan SE, Kirchgessner A, Tepper D, et al. Matrix metalloproteinases and blood-brain barrier disruption in acute ischemic stroke. Front Neurol. 2013;4:32.
121. Serlin Y, Shelef I, Knyazer B, et al., editors. Anatomy and physiology of the blood–brain barrier. Seminars in cell & developmental biology; 2015: Elsevier.
122. del Zoppo GJ, Hallenbeck JM. Advances in the vascular pathophysiology of ischemic stroke. Thromb Res. 2000 May 1;98(3):73-81.

123. Ceulemans AG, Zgavc T, Kooijman R, et al. The dual role of the neuroinflammatory response after ischemic stroke: modulatory effects of hypothermia. J Neuroinflammation. 2010 Nov 1;7(1):74.
124. Pardridge WM. Drug transport across the blood-brain barrier. J Cereb Blood Flow Metab. 2012 Nov;32(11):1959-72.
125. Ginsberg MD, Busto R. Rodent models of cerebral ischemia. Stroke. 1989 Dec;20(12):1627-42.
126. Traystman RJ. Animal models of focal and global cerebral ischemia. ILAR J. 2003;44(2):85-95.
127. Sicard KM, Fisher M. Animal models of focal brain ischemia. Exp Transl Stroke Med. 2009 Nov 13;1(1):7.
128. Yamaguchi M, Calvert JW, Kusaka G, et al. One-stage anterior approach for four-vessel occlusion in rat. Stroke. 2005 Oct;36(10):2212-4.
129. Braeuninger S, Kleinschnitz C. Rodent models of focal cerebral ischemia: procedural pitfalls and translational problems. Exp Transl Stroke Med. 2009 Nov 25;1(1):8.
130. Howells DW, Porritt MJ, Rewell SS, et al. Different strokes for different folks: the rich diversity of animal models of focal cerebral ischemia. J Cereb Blood Flow Metab. 2010 Aug;30(8):1412-31.
131. Yan T, Chopp M, Chen J. Experimental animal models and inflammatory cellular changes in cerebral ischemic and hemorrhagic stroke. Neurosci Bull. 2015 Dec;31(6):717-34.
132. Fluri F, Schuhmann MK, Kleinschnitz C. Animal models of ischemic stroke and their application in clinical research. Drug design, development and therapy. 2015;9:3445.
133. Woodruff TM, Thundyil J, Tang SC, et al. Pathophysiology, treatment, and animal and cellular models of human ischemic stroke. Mol Neurodegener. 2011 Jan 25;6(1):11.
134. Sommer CJ. Ischemic stroke: experimental models and reality. Acta Neuropathol. 2017 Feb;133(2):245-261.
135. Stroke Therapy Academic Industry R. Recommendations for standards regarding preclinical neuroprotective and restorative drug development. Stroke. 1999 Dec;30(12):2752-8.
136. Skelding KA, Arellano JM, Powis DA, et al. Excitotoxic stimulation of brain microslices as an in vitro model of stroke. J Vis Exp. 2014 Feb 4(84):e51291.
137. Roque C, Baltazar G. Impact of Astrocytes on the Injury Induced by In Vitro Ischemia. Cell Mol Neurobiol. 2017 Nov;37(8):1521-1528.
138. Mischke R, Kleemann R, Brunner H, et al. Cross-linking and mutational analysis of the oligomerization state of the cytokine macrophage migration inhibitory factor (MIF). FEBS Lett. 1998 May 1;427(1):85-90.
139. David JR. Delayed hypersensitivity in vitro: its mediation by cell-free substances formed by lymphoid cell-antigen interaction. Proc Natl Acad Sci U S A. 1966 Jul;56(1):72-7.
140. Calandra T, Roger T. Macrophage migration inhibitory factor: a regulator of innate immunity. Nat Rev Immunol. 2003 Oct;3(10):791-800.
141. Yoshida T, Sonozaki H, Cohen S. The production of migration inhibition factor by B and T cells of the guinea pig. J Exp Med. 1973 Oct 1;138(4):784-97.
142. Asare Y, Schmitt M, Bernhagen J. The vascular biology of macrophage migration inhibitory factor (MIF). Expression and effects in inflammation, atherogenesis and angiogenesis. Thromb Haemost. 2013 Mar;109(3):391-8.
143. Choi SS, Lee HJ, Lim I, et al. Human astrocytes: secretome profiles of cytokines and chemokines. PLoS One. 2014;9(4):e92325.

144. Koda M, Nishio Y, Hashimoto M, et al. Up-regulation of macrophage migration-inhibitory factor expression after compression-induced spinal cord injury in rats. Acta Neuropathol. 2004 Jul;108(1):31-6.
145. O'Reilly C, Doroudian M, Mawhinney L, et al. Targeting MIF in Cancer: Therapeutic Strategies, Current Developments, and Future Opportunities. Med Res Rev. 2016 May;36(3):440-60.
146. Suzuki T, Ogata A, Tashiro K, et al. Augmented expression of macrophage migration inhibitory factor (MIF) in the telencephalon of the developing rat brain. Brain Res. 1999 Jan 23;816(2):457-62.
147. Bernhagen J, Calandra T, Mitchell R, et al. MIF is a pituitary-derived cytokine that potentiates lethal endotoxaemia. Nature. 1993;365(6448):756-759.
148. Alampour-Rajabi S, El Bounkari O, Rot A, et al. MIF interacts with CXCR7 to promote receptor internalization, ERK1/2 and ZAP-70 signaling, and lymphocyte chemotaxis. Faseb J. 2015 Nov;29(11):4497-511.
149. Bachelerie F, Ben-Baruch A, Burkhardt AM, et al. International Union of Basic and Clinical Pharmacology. [corrected]. LXXXIX. Update on the extended family of chemokine receptors and introducing a new nomenclature for atypical chemokine receptors. Pharmacol Rev. 2014;66(1):1-79.
150. Bernhagen J, Krohn R, Lue H, et al. MIF is a noncognate ligand of CXC chemokine receptors in inflammatory and atherogenic cell recruitment. Nature medicine. 2007 May;13(5):587-96.
151. Assis DN, Takahashi H, Leng L, et al. A macrophage migration inhibitory factor polymorphism is associated with autoimmune hepatitis severity in US and Japanese patients. Digestive diseases and sciences. 2016;61(12):3506-3512.
152. Morand EF, Leech M, Bernhagen J. MIF: a new cytokine link between rheumatoid arthritis and atherosclerosis. Nature reviews Drug discovery. 2006;5(5):399-411.
153. Zernecke A, Bernhagen J, Weber C. Macrophage migration inhibitory factor in cardiovascular disease. Circulation. 2008 Mar 25;117(12):1594-602.
154. Chatterjee M, Borst O, Walker B, et al. Macrophage migration inhibitory factor limits activation-induced apoptosis of platelets via CXCR7-dependent Akt signaling. Circ Res. 2014 Nov 07;115(11):939-49.
155. Leng L, Metz CN, Fang Y, et al. MIF signal transduction initiated by binding to CD74. J Exp Med. 2003 Jun 2;197(11):1467-76.
156. Luedike P, Hendgen-Cotta UB, Sobierajski J, et al. Cardioprotection through S-nitros (yl) ation of macrophage migration inhibitory factor. Circulation. 2012;125(15):1880-1889.
157. Miller EJ, Li J, Leng L, et al. Macrophage migration inhibitory factor stimulates AMP-activated protein kinase in the ischaemic heart. Nature. 2008 Jan 31;451(7178):578-82.
158. Shi X, Leng L, Wang T, et al. CD44 is the signaling component of the macrophage migration inhibitory factor-CD74 receptor complex. Immunity. 2006;25(4):595-606.
159. Wang Y, An R, Umanah GK, et al. A nuclease that mediates cell death induced by DNA damage and poly (ADP-ribose) polymerase-1. Science. 2016;354(6308):aad6872.
160. Zhang M, Aman P, Grubb A, et al. Cloning and sequencing of a cDNA encoding rat D-dopachrome tautomerase. FEBS Lett. 1995 Oct 16;373(3):203-6.
161. Merk M, Zierow S, Leng L, et al. The D-dopachrome tautomerase (DDT) gene product is a cytokine and functional homolog of macrophage migration inhibitory factor (MIF). Proc Natl Acad Sci U S A. 2011 Aug 23;108(34):E577-85.
162. Merk M, Mitchell RA, Endres S, et al. D-dopachrome tautomerase (D-DT or MIF-2): doubling the MIF cytokine family. Cytokine. 2012 Jul;59(1):10-7.

163. Kim BS, Pallua N, Bernhagen J, et al. The macrophage migration inhibitory factor protein superfamily in obesity and wound repair. Exp Mol Med. 2015 May 1;47(5):e161.
164. Kim BS, Tilstam PV, Hwang SS, et al. D-dopachrome tautomerase in adipose tissue inflammation and wound repair. J Cell Mol Med. 2017 Jan;21(1):35-45.
165. Kim BS, Stoppe C, Grieb G, et al. The clinical significance of the MIF homolog d-dopachrome tautomerase (MIF-2) and its circulating receptor (sCD74) in burn. Burns. 2016 Sep;42(6):1265-76.
166. Stoppe C, Rex S, Goetzenich A, et al. Interaction of MIF family proteins in myocardial ischemia/reperfusion damage and their influence on clinical outcome of cardiac surgery patients. Antioxidants & redox signaling. 2015;23(11):865-879.
167. Voss S, Kruger S, Scherschel K, et al. Macrophage Migration Inhibitory Factor (MIF) Expression Increases during Myocardial Infarction and Supports Pro-Inflammatory Signaling in Cardiac Fibroblasts. Biomolecules. 2019 Jan 23;9(2):38.
168. Kim BS, Tilstam PV, Arnke K, et al. Differential regulation of macrophage activation by the MIF cytokine superfamily members MIF and MIF-2 in adipose tissue during endotoxemia. FASEB journal : official publication of the Federation of American Societies for Experimental Biology. 2020 Mar;34(3):4219-4233.
169. Qi D, Atsina K, Qu L, et al. The vestigial enzyme D-dopachrome tautomerase protects the heart against ischemic injury. J Clin Invest. 2014 Aug;124(8):3540-50.
170. Ma Y, Su KN, Pfau D, et al. Cardiomyocyte d-dopachrome tautomerase protects against heart failure. JCI Insight. 2019 Sep 5;4(17).
171. Burger-Kentischer A, Gobel H, Kleemann R, et al. Reduction of the aortic inflammatory response in spontaneous atherosclerosis by blockade of macrophage migration inhibitory factor (MIF). Atherosclerosis. 2006 Jan;184(1):28-38.
172. Chen Z, Sakuma M, Zago AC, et al. Evidence for a role of macrophage migration inhibitory factor in vascular disease. Arterioscler Thromb Vasc Biol. 2004 Apr;24(4):709-14.
173. Sinitski D, Kontos C, Krammer C, et al. Macrophage Migration Inhibitory Factor (MIF)-Based Therapeutic Concepts in Atherosclerosis and Inflammation. Thromb Haemost. 2019 Apr;119(4):553-566.
174. Burger-Kentischer A, Goebel H, Seiler R, et al. Expression of macrophage migration inhibitory factor in different stages of human atherosclerosis. Circulation. 2002 Apr 2;105(13):1561-6.
175. Wirtz TH, Tillmann S, Strussmann T, et al. Platelet-derived MIF: a novel platelet chemokine with distinct recruitment properties. Atherosclerosis. 2015 Mar;239(1):1-10.
176. Lin SG, Yu XY, Chen YX, et al. De novo expression of macrophage migration inhibitory factor in atherogenesis in rabbits. Circ Res. 2000 Dec 8;87(12):1202-8.
177. Schober A, Bernhagen J, Thiele M, et al. Stabilization of atherosclerotic plaques by blockade of macrophage migration inhibitory factor after vascular injury in apolipoprotein E-deficient mice. Circulation. 2004 Jan 27;109(3):380-5.
178. Weber C, Kraemer S, Drechsler M, et al. Structural determinants of MIF functions in CXCR2-mediated inflammatory and atherogenic leukocyte recruitment. Proc Natl Acad Sci U S A. 2008 Oct 21;105(42):16278-83.
179. Klasen C, Ohl K, Sternkopf M, et al. MIF promotes B cell chemotaxis through the receptors CXCR4 and CD74 and ZAP-70 signaling. J Immunol. 2014 Jun 01;192(11):5273-84.
180. Schwartz V, Lue H, Kraemer S, et al. A functional heteromeric MIF receptor formed by CD74 and CXCR4. FEBS Lett. 2009 Sep 3;583(17):2749-57.

181. Qi D, Hu X, Wu X, et al. Cardiac macrophage migration inhibitory factor inhibits JNK pathway activation and injury during ischemia/reperfusion. J Clin Invest. 2009 Dec;119(12):3807-16.
182. Dayawansa NH, Gao XM, White DA, et al. Role of MIF in myocardial ischaemia and infarction: insight from recent clinical and experimental findings. Clin Sci (Lond). 2014 Aug;127(3):149-61.
183. Gao XM, Liu Y, White D, et al. Deletion of macrophage migration inhibitory factor protects the heart from severe ischemia-reperfusion injury: a predominant role of anti-inflammation. Journal of molecular and cellular cardiology. 2011 Jun;50(6):991-9.
184. Bacher M, Meinhardt A, Lan HY, et al. MIF expression in the rat brain: implications for neuronal function. Mol Med. 1998 Apr;4(4):217-30.
185. Ogata A, Nishihira J, Suzuki T, et al. Identification of macrophage migration inhibitory factor mRNA expression in neural cells of the rat brain by in situ hybridization. Neurosci Lett. 1998 May 1;246(3):173-7.
186. Conboy L, Varea E, Castro JE, et al. Macrophage migration inhibitory factor is critically involved in basal and fluoxetine-stimulated adult hippocampal cell proliferation and in anxiety, depression, and memory-related behaviors. Molecular psychiatry. 2011;16(5):533-547.
187. Ohta S, Misawa A, Fukaya R, et al. Macrophage migration inhibitory factor (MIF) promotes cell survival and proliferation of neural stem/progenitor cells. J Cell Sci. 2012 Jul 1;125(Pt 13):3210-20.
188. Nicoletti A, Fagone P, Donzuso G, et al. Parkinson's disease is associated with increased serum levels of macrophage migration inhibitory factor. Cytokine. 2011 Aug;55(2):165-7.
189. Shvil N, Banerjee V, Zoltsman G, et al. MIF inhibits the formation and toxicity of misfolded SOD1 amyloid aggregates: implications for familial ALS. Cell Death Dis. 2018 Jan 25;9(2):107.
190. Li S, Nie K, Zhang Q, et al. Macrophage Migration Inhibitory Factor Mediates Neuroprotective Effects by Regulating Inflammation, Apoptosis and Autophagy in Parkinson's Disease. Neuroscience. 2019 Sep 15;416:50-62.
191. Israelson A, Ditsworth D, Sun S, et al. Macrophage migration inhibitory factor as a chaperone inhibiting accumulation of misfolded SOD1. Neuron. 2015 Apr 08;86(1):218-32.
192. Bacher M, Deuster O, Aljabari B, et al. The role of macrophage migration inhibitory factor in Alzheimer's disease. Mol Med. 2010 Mar;16(3-4):116-21.
193. Popp J, Bacher M, Kolsch H, et al. Macrophage migration inhibitory factor in mild cognitive impairment and Alzheimer's disease. J Psychiatr Res. 2009 May;43(8):749-53.
194. Bryan KJ, Zhu X, Harris PL, et al. Expression of CD74 is increased in neurofibrillary tangles in Alzheimer's disease. Mol Neurodegener. 2008 Sep 11;3:13.
195. Hagman S, Raunio M, Rossi M, et al. Disease-associated inflammatory biomarker profiles in blood in different subtypes of multiple sclerosis: prospective clinical and MRI follow-up study. J Neuroimmunol. 2011 May;234(1-2):141-7.
196. Rinta S, Kuusisto H, Raunio M, et al. Apoptosis-related molecules in blood in multiple sclerosis. J Neuroimmunol. 2008 Dec 15;205(1-2):135-41.
197. Yang DB, Yu WH, Dong XQ, et al. Serum macrophage migration inhibitory factor concentrations correlate with prognosis of traumatic brain injury. Clin Chim Acta. 2017 Jun;469:99-104.

198. Mattugini N, Merl-Pham J, Petrozziello E, et al. Influence of white matter injury on gray matter reactive gliosis upon stab wound in the adult murine cerebral cortex. Glia. 2018 Aug;66(8):1644-1662.
199. Nishio Y, Koda M, Hashimoto M, et al. Deletion of macrophage migration inhibitory factor attenuates neuronal death and promotes functional recovery after compression-induced spinal cord injury in mice. Acta Neuropathol. 2009 Mar;117(3):321-8.
200. Chesney JA, Mitchell RA. 25 Years On: A Retrospective on Migration Inhibitory Factor in Tumor Angiogenesis. Mol Med. 2015 Oct 27;21 Suppl 1(1):S19-24.
201. Baron N, Deuster O, Noelker C, et al. Role of macrophage migration inhibitory factor in primary glioblastoma multiforme cells. J Neurosci Res. 2011 May;89(5):711-7.
202. Piette C, Deprez M, Roger T, et al. The dexamethasone-induced inhibition of proliferation, migration, and invasion in glioma cell lines is antagonized by macrophage migration inhibitory factor (MIF) and can be enhanced by specific MIF inhibitors. J Biol Chem. 2009 Nov 20;284(47):32483-92.
203. Mittelbronn M, Platten M, Zeiner P, et al. Macrophage migration inhibitory factor (MIF) expression in human malignant gliomas contributes to immune escape and tumour progression. Acta Neuropathol. 2011 Sep;122(3):353-65.
204. Zeiner PS, Preusse C, Blank AE, et al. MIF Receptor CD74 is Restricted to Microglia/Macrophages, Associated with a M1-Polarized Immune Milieu and Prolonged Patient Survival in Gliomas. Brain Pathol. 2015 Jul;25(4):491-504.
205. Ghoochani A, Schwarz MA, Yakubov E, et al. MIF-CD74 signaling impedes microglial M1 polarization and facilitates brain tumorigenesis. Oncogene. 2016 Dec 01;35(48):6246-6261.
206. Li Q, He Q, Baral S, et al. MicroRNA-493 regulates angiogenesis in a rat model of ischemic stroke by targeting MIF. FEBS J. 2016 May;283(9):1720-33.
207. Wang L, Zis O, Ma G, et al. Upregulation of macrophage migration inhibitory factor gene expression in stroke. Stroke. 2009 Mar;40(3):973-6.
208. Inacio AR, Bucala R, Deierborg T. Lack of macrophage migration inhibitory factor in mice does not affect hallmarks of the inflammatory/immune response during the first week after stroke. J Neuroinflammation. 2011 Jun 29;8:75.
209. Inacio AR, Ruscher K, Wieloch T. Enriched environment downregulates macrophage migration inhibitory factor and increases parvalbumin in the brain following experimental stroke. Neurobiol Dis. 2011 Feb;41(2):270-8.
210. Baugh JA, Gantier M, Li L, et al. Dual regulation of macrophage migration inhibitory factor (MIF) expression in hypoxia by CREB and HIF-1. Biochem Biophys Res Commun. 2006 Sep 8;347(4):895-903.
211. Welford SM, Bedogni B, Gradin K, et al. HIF1α delays premature senescence through the activation of MIF. Genes & development. 2006;20(24):3366-3371.
212. Inacio AR, Ruscher K, Leng L, et al. Macrophage migration inhibitory factor promotes cell death and aggravates neurologic deficits after experimental stroke. J Cereb Blood Flow Metab. 2011 Apr;31(4):1093-106.
213. Liu YC, Tsai YH, Tang SC, et al. Cytokine MIF Enhances Blood-Brain Barrier Permeability: Impact for Therapy in Ischemic Stroke. Sci Rep. 2018 Jan 15;8(1):743.
214. Turtzo LC, Li J, Persky R, et al. Deletion of macrophage migration inhibitory factor worsens stroke outcome in female mice. Neurobiol Dis. 2013 Jun;54:421-31.
215. Zhang S, Zis O, Ly PT, et al. Down-regulation of MIF by NFkappaB under hypoxia accelerated neuronal loss during stroke. FASEB J. 2014 Oct;28(10):4394-407.
216. Culmsee C, Zhu C, Landshamer S, et al. Apoptosis-inducing factor triggered by poly(ADP-ribose) polymerase and Bid mediates neuronal cell death after oxygen-

glucose deprivation and focal cerebral ischemia. J Neurosci. 2005 Nov 2;25(44):10262-72.
217. Plesnila N, Zhu C, Culmsee C, et al. Nuclear translocation of apoptosis-inducing factor after focal cerebral ischemia. J Cereb Blood Flow Metab. 2004 Apr;24(4):458-66.
218. Hwang IK, Park JH, Lee TK, et al. CD74-immunoreactive activated M1 microglia are shown late in the gerbil hippocampal CA1 region following transient cerebral ischemia. Mol Med Rep. 2017 Jun;15(6):4148-4154.
219. Benedek G, Zhu W, Libal N, et al. A novel HLA-DRalpha1-MOG-35-55 construct treats experimental stroke. Metab Brain Dis. 2014 Mar;29(1):37-45.
220. Wang J, Ye Q, Xu J, et al. DRalpha1-MOG-35-55 Reduces Permanent Ischemic Brain Injury. Transl Stroke Res. 2017 Jun;8(3):284-293.
221. Connell BJ, Gordon JR, Saleh TM. ELR-CXC chemokine antagonism is neuroprotective in a rat model of ischemic stroke. Neurosci Lett. 2015 Oct 8;606:117-22.
222. Hill JW, Nemoto EM. Matrix-derived inflammatory mediator N-acetyl proline-glycine-proline is neurotoxic and upregulated in brain after ischemic stroke. J Neuroinflammation. 2015 Nov 21;12:214.
223. Schioppa T, Uranchimeg B, Saccani A, et al. Regulation of the chemokine receptor CXCR4 by hypoxia. J Exp Med. 2003 Nov 3;198(9):1391-402.
224. Schonemeier B, Schulz S, Hoellt V, et al. Enhanced expression of the CXCl12/SDF-1 chemokine receptor CXCR7 after cerebral ischemia in the rat brain. J Neuroimmunol. 2008 Jul 31;198(1-2):39-45.
225. Timasheva YR, Nasibullin TR, Mustafina OE. The CXCR2 Gene Polymorphism Is Associated with Stroke in Patients with Essential Hypertension. Cerebrovasc Dis Extra. 2015 Sep-Dec;5(3):124-31.
226. Li YS, Chen W, Liu S, et al. Serum macrophage migration inhibitory factor levels are associated with infarct volumes and long-term outcomes in patients with acute ischemic stroke. Int J Neurosci. 2017 Jun;127(6):539-546.
227. Wang CW, Ma PJ, Wang YY, et al. Serum level of macrophage migration inhibitory factor predicts severity and prognosis in patients with ischemic stroke. Cytokine. 2019 Mar;115:8-12.
228. Yang L, Kong Y, Ren H, et al. Upregulation of CD74 and its potential association with disease severity in subjects with ischemic stroke. Neurochem Int. 2017 Jul;107:148-155.
229. Xu T, Pu S, Ni Y, et al. Elevated plasma macrophage migration inhibitor factor as a risk factor for the development of post-stroke depression in ischemic stroke. J Neuroimmunol. 2018 Jul 15;320:58-63.
230. Zis O, Zhang S, Dorovini-Zis K, et al. Hypoxia signaling regulates macrophage migration inhibitory factor (MIF) expression in stroke. Mol Neurobiol. 2015 Feb;51(1):155-67.
231. Fingerle-Rowson G, Petrenko O, Metz CN, et al. The p53-dependent effects of macrophage migration inhibitory factor revealed by gene targeting. Proc Natl Acad Sci U S A. 2003 Aug 5;100(16):9354-9.
232. Heinrichs D, Knauel M, Offermanns C, et al. Macrophage migration inhibitory factor (MIF) exerts antifibrotic effects in experimental liver fibrosis via CD74. Proc Natl Acad Sci U S A. 2011 Oct 18;108(42):17444-9.
233. Groger M, Lebesgue D, Pruneau D, et al. Release of bradykinin and expression of kinin B2 receptors in the brain: role for cell death and brain edema formation after focal cerebral ischemia in mice. J Cereb Blood Flow Metab. 2005 Aug;25(8):978-89.

234. Kataoka H, Kim SW, Plesnila N. Leukocyte-endothelium interactions during permanent focal cerebral ischemia in mice. J Cereb Blood Flow Metab. 2004 Jun;24(6):668-76.
235. Lourbopoulos A, Mamrak U, Roth S, et al. Inadequate food and water intake determine mortality following stroke in mice. J Cereb Blood Flow Metab. 2017 Jun;37(6):2084-2097.
236. Lunardi Baccetto S, Lehmann C. Microcirculatory Changes in Experimental Models of Stroke and CNS-Injury Induced Immunodepression. Int J Mol Sci. 2019 Oct 19;20(20).
237. Plesnila N, Zinkel S, Le DA, et al. BID mediates neuronal cell death after oxygen/ glucose deprivation and focal cerebral ischemia. Proc Natl Acad Sci U S A. 2001 Dec 18;98(26):15318-23.
238. Zweckberger K, Stoffel M, Baethmann A, et al. Effect of decompression craniotomy on increase of contusion volume and functional outcome after controlled cortical impact in mice. J Neurotrauma. 2003 Dec;20(12):1307-14.
239. Zhao L, Mulligan MK, Nowak TS, Jr. Substrain- and sex-dependent differences in stroke vulnerability in C57BL/6 mice. J Cereb Blood Flow Metab. 2019 Mar;39(3):426-438.
240. Beaudoin GM, 3rd, Lee SH, Singh D, et al. Culturing pyramidal neurons from the early postnatal mouse hippocampus and cortex. Nat Protoc. 2012 Sep;7(9):1741-54.
241. Blasi E, Barluzzi R, Bocchini V, et al. Immortalization of murine microglial cells by a v-raf/v-myc carrying retrovirus. J Neuroimmunol. 1990 May;27(2-3):229-37.
242. Heid CA, Stevens J, Livak KJ, et al. Real time quantitative PCR. Genome Res. 1996 Oct;6(10):986-94.
243. Kim BS, Rongisch R, Hager S, et al. Macrophage Migration Inhibitory Factor in Acute Adipose Tissue Inflammation. PLoS One. 2015;10(9):e0137366.
244. Strussmann T, Tillmann S, Wirtz T, et al. Platelets are a previously unrecognised source of MIF. Thromb Haemost. 2013 Nov;110(5):1004-13.
245. Brewer GJ, Torricelli JR, Evege EK, et al. Optimized survival of hippocampal neurons in B27-supplemented Neurobasal, a new serum-free medium combination. J Neurosci Res. 1993 Aug 1;35(5):567-76.
246. Ahlemeyer B, Baumgart-Vogt E. Optimized protocols for the simultaneous preparation of primary neuronal cultures of the neocortex, hippocampus and cerebellum from individual newborn (P0.5) C57Bl/6J mice. J Neurosci Methods. 2005 Dec 15;149(2):110-20.
247. Wright AA, Todorovic M, Murtaza M, et al. Macrophage migration inhibitory factor and its binding partner HTRA1 are expressed by olfactory ensheathing cells. Mol Cell Neurosci. 2020 Jan;102:103450.
248. Svenningsen ÅF, Löring S, Sørensen AL, et al. Macrophage migration inhibitory factor (MIF) modulates trophic signaling through interaction with serine protease HTRA1. Cellular and molecular life sciences. 2017;74(24):4561-4572.
249. Poepsel S, Sprengel A, Sacca B, et al. Determinants of amyloid fibril degradation by the PDZ protease HTRA1. Nat Chem Biol. 2015 Nov;11(11):862-9.
250. Bacher M, Schrader J, Thompson N, et al. Up-regulation of macrophage migration inhibitory factor gene and protein expression in glial tumor cells during hypoxic and hypoglycemic stress indicates a critical role for angiogenesis in glioblastoma multiforme. Am J Pathol. 2003 Jan;162(1):11-7.
251. Lee KS, Chung JH, Lee KH, et al. Bioplex analysis of plasma cytokines in Alzheimer's disease and mild cognitive impairment. Immunol Lett. 2008 Dec 22;121(2):105-9.

252. Rodrigo R, Fernandez-Gajardo R, Gutierrez R, et al. Oxidative stress and pathophysiology of ischemic stroke: novel therapeutic opportunities. CNS Neurol Disord Drug Targets. 2013 Aug;12(5):698-714.
253. Webb A, Bond R, McLean P, et al. Reduction of nitrite to nitric oxide during ischemia protects against myocardial ischemia-reperfusion damage. Proc Natl Acad Sci U S A. 2004 Sep 14;101(37):13683-8.
254. Pohl J, Hendgen-Cotta UB, Rammos C, et al. Targeted intracellular accumulation of macrophage migration inhibitory factor in the reperfused heart mediates cardioprotection. Thromb Haemost. 2016 Jan;115(1):200-12.
255. Schindler L, Dickerhof N, Hampton MB, et al. Post-translational regulation of macrophage migration inhibitory factor: Basis for functional fine-tuning. Redox Biol. 2018 May;15:135-142.
256. Tilstam PV, Pantouris G, Corman M, et al. A selective small-molecule inhibitor of macrophage migration inhibitory factor-2 (MIF-2), a MIF cytokine superfamily member, inhibits MIF-2 biological activity. The Journal of biological chemistry. 2019;294(49):18522-18531.
257. Bernhagen J. Separating cytokine twins with a small molecule. J Biol Chem. 2019 Dec 6;294(49):18532-18533.
258. Yoshiyama Y, Arai K, Oki T, et al. Expression of invariant chain and pro-cathepsin L in Alzheimer's brain. Neurosci Lett. 2000 Aug 25;290(2):125-8.
259. Teo BH, Wong SH. MHC class II-associated invariant chain (Ii) modulates dendritic cells-derived microvesicles (DCMV)-mediated activation of microglia. Biochem Biophys Res Commun. 2010 Oct 1;400(4):673-8.
260. Gore Y, Starlets D, Maharshak N, et al. Macrophage migration inhibitory factor induces B cell survival by activation of a CD74-CD44 receptor complex. J Biol Chem. 2008 Feb 1;283(5):2784-92.
261. Amin MA, Haas CS, Zhu K, et al. Migration inhibitory factor up-regulates vascular cell adhesion molecule-1 and intercellular adhesion molecule-1 via Src, PI3 kinase, and NFkappaB. Blood. 2006 Mar 15;107(6):2252-61.
262. Choudhary S, Hegde P, Pruitt JR, et al. Macrophage migratory inhibitory factor promotes bladder cancer progression via increasing proliferation and angiogenesis. Carcinogenesis. 2013 Dec;34(12):2891-9.
263. Naujokas MF, Morin M, Anderson MS, et al. The chondroitin sulfate form of invariant chain can enhance stimulation of T cell responses through interaction with CD44. Cell. 1993 Jul 30;74(2):257-68.
264. Kim HS, Kim MJ, Kim EJ, et al. Berberine-induced AMPK activation inhibits the metastatic potential of melanoma cells via reduction of ERK activity and COX-2 protein expression. Biochem Pharmacol. 2012 Feb 1;83(3):385-94.
265. Lee CW, Wong LL, Tse EY, et al. AMPK promotes p53 acetylation via phosphorylation and inactivation of SIRT1 in liver cancer cells. Cancer Res. 2012 Sep 1;72(17):4394-404.
266. Brait VH, Rivera J, Broughton BR, et al. Chemokine-related gene expression in the brain following ischemic stroke: no role for CXCR2 in outcome. Brain Res. 2011 Feb 4;1372:169-79.
267. Losy J, Zaremba J, Skrobanski P. CXCL1 (GRO-alpha) chemokine in acute ischaemic stroke patients. Folia Neuropathol. 2005;43(2):97-102.
268. Mirabelli-Badenier M, Braunersreuther V, Viviani GL, et al. CC and CXC chemokines are pivotal mediators of cerebral injury in ischaemic stroke. Thromb Haemost. 2011 Mar;105(3):409-20.

269. Herz J, Sabellek P, Lane TE, et al. Role of Neutrophils in Exacerbation of Brain Injury After Focal Cerebral Ischemia in Hyperlipidemic Mice. Stroke. 2015 Oct;46(10):2916-25.
270. Villa P, Triulzi S, Cavalieri B, et al. The interleukin-8 (IL-8/CXCL8) receptor inhibitor reparixin improves neurological deficits and reduces long-term inflammation in permanent and transient cerebral ischemia in rats. Mol Med. 2007 Mar-Apr;13(3-4):125-33.
271. Hill WD, Hess DC, Martin-Studdard A, et al. SDF-1 (CXCL12) is upregulated in the ischemic penumbra following stroke: association with bone marrow cell homing to injury. J Neuropathol Exp Neurol. 2004 Jan;63(1):84-96.
272. Werner Y, Mass E, Ashok Kumar P, et al. Cxcr4 distinguishes HSC-derived monocytes from microglia and reveals monocyte immune responses to experimental stroke. Nat Neurosci. 2020 Mar;23(3):351-362.
273. Imitola J, Raddassi K, Park KI, et al. Directed migration of neural stem cells to sites of CNS injury by the stromal cell-derived factor 1alpha/CXC chemokine receptor 4 pathway. Proc Natl Acad Sci U S A. 2004 Dec 28;101(52):18117-22.
274. Robin AM, Zhang ZG, Wang L, et al. Stromal cell-derived factor 1alpha mediates neural progenitor cell motility after focal cerebral ischemia. J Cereb Blood Flow Metab. 2006 Jan;26(1):125-34.
275. Bogoslovsky T, Spatz M, Chaudhry A, et al. Stromal-derived factor-1α correlates with circulating endothelial progenitor cells and with acute lesion volume in stroke patients. Stroke. 2011;42(3):618-625.
276. Chen J, Chen J, Chen S, et al. Transfusion of CXCR4-primed endothelial progenitor cells reduces cerebral ischemic damage and promotes repair in db/db diabetic mice. PLoS One. 2012;7(11):e50105.
277. Mao L, Huang M, Chen SC, et al. Endogenous Endothelial Progenitor Cells Participate in Neovascularization via CXCR 4/SDF-1 axis and Improve Outcome After Stroke. CNS neuroscience & therapeutics. 2014;20(5):460-468.
278. Lipfert J, Ödemis V, Wagner DC, et al. CXCR 4 and CXCR 7 form a functional receptor unit for SDF-1/CXCL 12 in primary rodent microglia. Neuropathology and applied neurobiology. 2013;39(6):667-680.
279. Tanabe S, Heesen M, Yoshizawa I, et al. Functional expression of the CXC-chemokine receptor-4/fusin on mouse microglial cells and astrocytes. J Immunol. 1997 Jul 15;159(2):905-11.
280. Chen C, Chu SF, Liu DD, et al. Chemokines play complex roles in cerebral ischemia. Neurochem Int. 2018 Jan;112:146-158.
281. Li Y, Huang J, He X, et al. Postacute stromal cell-derived factor-1alpha expression promotes neurovascular recovery in ischemic mice. Stroke. 2014 Jun;45(6):1822-9.
282. Zhang Y, Zhang H, Lin S, et al. SDF-1/CXCR7 chemokine signaling is induced in the peri-infarct regions in patients with ischemic stroke. Aging and disease. 2018;9(2):287.
283. Bakondi B, Shimada IS, Peterson BM, et al. SDF-1α secreted by human CD133-derived multipotent stromal cells promotes neural progenitor cell survival through CXCR7. Stem cells and development. 2011;20(6):1021-1029.
284. Kitagawa K, Matsumoto M, Yang G, et al. Cerebral ischemia after bilateral carotid artery occlusion and intraluminal suture occlusion in mice: evaluation of the patency of the posterior communicating artery. J Cereb Blood Flow Metab. 1998 May;18(5):570-9.
285. Ozdemir YG, Bolay H, Erdem E, et al. Occlusion of the MCA by an intraluminal filament may cause disturbances in the hippocampal blood flow due to anomalies of circle of Willis and filament thickness. Brain Res. 1999 Mar 20;822(1-2):260-4.

286. Harris J, VanPatten S, Deen NS, et al. Rediscovering MIF: New Tricks for an Old Cytokine. Trends Immunol. 2019 May;40(5):447-462.
287. Calandra T, Bernhagen J, Metz CN, et al. MIF as a glucocorticoid-induced modulator of cytokine production. Nature. 1995;377(6544):68-71.
288. Flores M, Saavedra R, Bautista R, et al. Macrophage migration inhibitory factor (MIF) is critical for the host resistance against Toxoplasma gondii. The FASEB Journal. 2008;22(10):3661-3671.
289. Stojanovic I, Mirkov I, Kataranovski M, et al. A role for macrophage migration inhibitory factor in protective immunity against Aspergillus fumigatus. Immunobiology. 2011 Sep;216(9):1018-27.
290. Moonah SN, Abhyankar MM, Haque R, et al. The macrophage migration inhibitory factor homolog of Entamoeba histolytica binds to and immunomodulates host macrophages. Infect Immun. 2014 Sep;82(9):3523-30.
291. Eckardt V, Miller MC, Blanchet X, et al. Chemokines and galectins form heterodimers to modulate inflammation. EMBO Rep. 2020 Apr 3;21(4):e47852.
292. Lambertsen KL, Biber K, Finsen B. Inflammatory cytokines in experimental and human stroke. J Cereb Blood Flow Metab. 2012 Sep;32(9):1677-98.
293. Hallenbeck JM. The many faces of tumor necrosis factor in stroke. Nat Med. 2002 Dec;8(12):1363-8.
294. Bruce AJ, Boling W, Kindy MS, et al. Altered neuronal and microglial responses to excitotoxic and ischemic brain injury in mice lacking TNF receptors. Nat Med. 1996 Jul;2(7):788-94.
295. Herrmann O, Tarabin V, Suzuki S, et al. Regulation of body temperature and neuroprotection by endogenous interleukin-6 in cerebral ischemia. J Cereb Blood Flow Metab. 2003 Apr;23(4):406-15.
296. Clark WM, Rinker LG, Lessov NS, et al. Lack of interleukin-6 expression is not protective against focal central nervous system ischemia. Stroke. 2000 Jul;31(7):1715-20.

7. LIST OF FIGURES

8. LIST OF ABBREVIATIONS

ACKs	Atypical chemokines
AD	Alzheimer's disease
AIF	Apoptosis-inducing factor
ALS	Amyotrophic lateral sclerosis
AMPK	Adenosine monophosphate kinase
CBF	Cerebral blood flow
CD74	Cluster of differentiation 74
CNS	Central nervous system
CSF	Cerebrospinal fluid
CVDs	Cardiovascular diseases
D-DT	D-dopachrome tautomerase
ELISA	Enzyme-linked immunosorbent assay
ERK	Extracellular signal regulated kinase
FACS	Fluorescence-active cell sorting
FBS	Fetal bovine serum
GST	Glutathione S-transferase
HIF-1α	Hypoxia-inducible factor 1-alpha
HREs	Hypoxia responsive elements
HTRA1	High temperature requirement serine protease A1
ICD	Intracellular domain
IFN- γ	Interferon gamma
IL-10	Interleukin-10
IL-1β	Interleukin-1 beta
IL-6	Interleukin-6
IPTG	Isopropyl-1-thio-β-D-galactopyranoside
KO	Knock out
MAPK	Mitogen-activated protein kinase
MCA	Middle cerebral artery

MCAO	Middle cerebral artery occlusion
MFI	Median fluorescence intensity
MHC II	Major histocompatibility complex II
MIF	Macrophage migration inhibitory factor
MIF-2	Macrophage migration inhibitory factor-2
MMP	Matrix metalloproteinases
MS	Multiple sclerosis
N2a	Neuro-2a
NF-κB	Nuclear factor kappa-light-chain-enhancer of activated B cells
OGD	Oxygen and glucose deprivation
PBMC	Peripheral blood mononuclear cells
PBS	Phosphate buffered saline
PcomA	Posterior communicating artery.
PD	Parkinson´s disease (PD)
PI3K	Phosphatidylinositol-4,5-bisphosphate3- kinase
ROS	Reactive oxygen species
SDF-1	Stromal cell derived factor 1
SDS-PAGE	Sodium dodecyl sulfate-polyacrylamide gel electrophoresis
TBS	Tris buffered saline
TBST	Tris buffered saline with 0.1% Tween
TGF-β	Transforming growth factor beta
TNF-α	Tumor necrosis factor-alpha
WT	Wild type

9. ACKNOWLEDGEMENTS

First, I would like to thank my supervisor Prof. Dr. Jürgen Bernhagen for giving me the opportunity to perform my doctoral thesis in his lab, for the continuous support, help and encouragement. Many thanks to my technical supervisor Dr. Omar El Bounkari for being patient with me, for his great guidance, for sharing his knowledge and expertise with me, and for being helpful all the time.

I acknowledge our collaborators Prof. Dr. med. Nikolaus Plesnila and Ms. Uta Mamrak for testing the *Mif*$^{-/-}$ and *Cd74* $^{-/-}$ mice in their established MCAO stroke model. I am also very thankful to Prof. Plesnila for his guidance and faithful discussions. Big thanks to Ms. Mamrak for her supervision and her valuable advice. Many thanks also to Prof. Dr. med. Arthur Liesz for his collaborative help on various challenges regarding the experimental stroke models. Thank you to Dr. Ozgun Gokce and Prof. Plesnila for advice on the AIF work in this thesis. *Cd74* $^{-/-}$ mice were initially kindly provided by the Prof. Richard Bucala, MD/PhD, Yale University School of Medicine, New Haven, CT, USA.

I would also like to thank all my colleagues in the lab. I really enjoyed the lovely atmosphere and had the chance to have an unforgettable time. Special thanks to Ms. Priscila Bourilhón and Simona Gerra for their support in the lab. Big thanks to Dr. Dzmitry Sinitski for the discussions and his advice on my project. I also want to gladly thank Ms. Chunfang Zan for supporting me during my experiments on various ends. Also, many thanks to our team assistant Sabrina Lukanovic for her great patience and kind help with the numerous administrative challenges, and to always have an open ear.

My sincere thanks to the Chinese scholarship council for the valuable chance to join the very exciting CSC program as well as for the financial support.

I also want to thank all my friends I know in Munich, especially Liting Shang and Yue Hu. Thanks for all the great travels and happy time we had together.

Great thanks to my parents who always support me unconditionally in pursuing my career and making my dreams real. Thanks a lot for offering me emotional and financial help. Thanks for the caring of my friend in China. Finally, I want to say thank you to my dear friend Qingluan Hu, my classmate during our Bachelor and Master study. She encouraged me to apply and

perform my doctoral thesis in Germany. Her comfort and encouragement always keep me moving forward despite the distance between our cities to study.

Affidavit

Affidavit

Wang Sijia

Surname, first name

Feodor-Lynen-Straße 17

Street

81377, Munich, Germany

Zip code, town, country

I hereby declare, that the submitted thesis entitled:

The role of MIF proteins in ischemic stroke

is my own work. I have only used the sources indicated and have not made unauthorized use of services of a third party. Where the work of others has been quoted or reproduced, the source is always given.

I further declare that the submitted thesis or parts thereof have not been presented as part of an examination degree to any other university.

Munich, 01.05.2021 — Sijia Wang

place, date — Signature doctoral candidate

11. LIST OF PUBLICATIONS

WANG Si-Jia, Li Lian-Hong. PTEN and gastric cancer. *Journal of International Oncology*, 2013,40(9): 689-692.

WANG Tao, WANG Xiao-hong, WANG Su-ping, DU Yun-xia, ZHAO Shu-fang, WANG Si-jia. Research of Bone Marrow Mesenchymal Stem Cell Transplantation for Rat Cerebral Infarction Recovery of Neurological Function. *Progress in Modern Biomedicine*, 2017,17(22):4227-4231.

Xiaohong Wang, Lin Zhang, Sijia Wang, Cui Wang. The effect of deep brain stimulation on the non-motor symptoms of Parkinson's disease. *Journal of Clinical Neurology*, 2018,31(02):147-151.